

International Baltic Earth Secretariat Publication No. 7, October 2015

HyMex-Baltic Earth Workshop

Joint regional climate system modelling for the European sea regions

ENEA, Rome, Italy, 5- 6 November 2015

Programme, Abstracts, Participants



Impressum

International Baltic Earth Secretariat Publications

ISSN 2198-4247

International Baltic Earth Secretariat
Helmholtz-Zentrum Geesthacht GmbH
Max-Planck-Str. 1
D-21502 Geesthacht, Germany

www.baltic-earth.eu

balticearth@hzg.de

Font cover, upper plot: Sea surface height in the Mediterranean Sea as reproduced by a hindcast simulation 1958-2004 (Sannino et al. 2014, Proceedings of the MedClivar Conference 2014 in Ankara, Turkey). Lower plot: Projected change in spring mean ensemble average sea surface height in the Baltic Sea by the end of the century (Meier et al. 2012, SMHI Report Oceanografi No112). Photo: The Colloseum at dusk (photo by David Iliff.; license CC-BY-SA 3.0)

Inside plot: Map of SST warming at the end of the 21st century: minimum and maximum warming expected from an ensemble of scenario simulations (Adloff et al. 2015, Clim Dyn).

Inside photo: The LION buoy, measuring air-sea exchanges in the Gulf of Lions, one of the deep water formation areas in the Mediterranean Sea (photo: Meteo-France)

Table of Contents

Introduction	1
Programme	3
Abstracts	9
Participants	99
International Baltic Earth Secretariat Publication Series	103

A HyMex-Baltic Earth Workshop
Joint regional climate system modelling
for the European sea regions

ENEA, Rome, Italy

5-6 November 2015

Co-Organized by



Scientific Committee

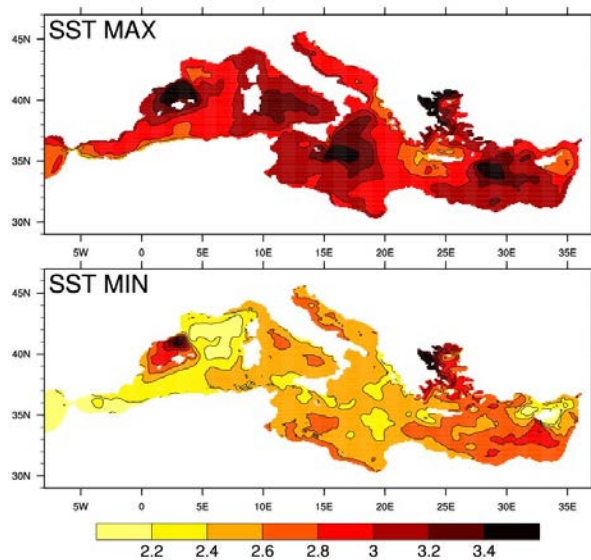
Bodo Ahrens (GUF, Germany)
Ole Bøssing Christensen (DMI, Denmark)
Marilaure Gregoire (ULG, Belgium)
Daniela Jacob (HZG, Germany)
Gabriel Jordà (UIB, Spain)
Uwe Mikolajewicz (MPI Hamburg, Germany)
Gianmaria Sannino (ENEA, Italy)
Anna Rutgersson (University of Uppsala, Sweden)
Samuel Somot (CNRM, France)
Markus Meier (SMHI, Sweden)

Organizing Committee

Gianmaria Sannino (ENEA, Italy)
Markus Meier (SMHI, Sweden)
Samuel Somot (CNRM, France)
Marcus Reckermann (IBES, HZG, Germany)
Silke Köppen (IBES, HZG, Germany)

Find up-to date information on the Baltic Earth website: www.baltic-earth.eu/rome2015

Objectives and expected outcome



This workshop aims to contribute to the understanding of regional energy, momentum, water, and matter fluxes and their effects on the regional climate using observations and Regional Climate System Models (RCSMs), encompassing processes in the atmosphere, land, sea, and anthroposphere. In this workshop, we will focus on European seas and their catchment areas like the Mediterranean Sea, Black Sea, North Sea, Baltic Sea and Arctic Ocean - highly sensitive areas where global models fail to give reliable information about changing climate because key processes are not properly resolved.

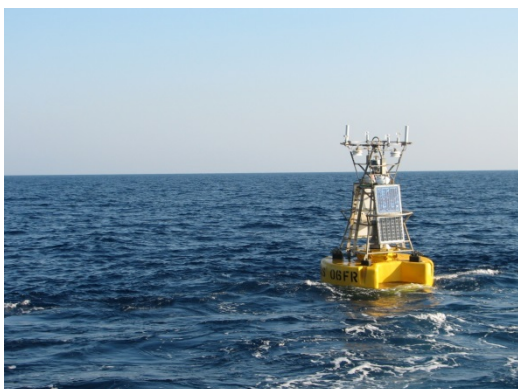
In recent years, coupled atmosphere – sea ice – ocean models have been elaborated further by using a hierarchy of sub-models for the Earth system, combining regional climate models with sub-models for surface waves, land vegetation, hydrology, land and marine biogeochemistry, the marine carbon cycle as well as marine biology and food webs. Hence, there is a tendency to develop so-called regional Earth system models with the aim to investigate the impact of climate change on the entire terrestrial and marine environment.

Studies on any of the session topics described below will be presented at the workshop. Discussions on progress in the field and challenges will complement the oral and poster presentations.

Sessions

Session 1: Development and evaluation of regional climate system models. New coupled atmosphere – ice – ocean – land surface/vegetation – biogeochemical/carbon – food web models are presented and the results of hindcast simulations are compared to observations. Furthermore, model improvement, new data sets for model evaluation and bias correction methods are discussed.

Session 2: Regional process studies and studies on the added value of coupled models with high resolution. A special focus on land-atmosphere, ocean-atmosphere and land-ocean (rivers) interactions is given. In particular, discussions of advantages and disadvantages of regional climate system models are encouraged.



Session 3: Extreme and high impact events. The focus of the session is on the basic scientific understanding of high impact events, and on assessing impacts on key areas with different adaptation potential.

Session 4: Climate change impact studies and uncertainty assessments of projections using coupled model simulations. Dynamical downscaling of Earth System Models, multi-model ensemble studies, and multi-stressor approaches will be discussed.

Programme

Day 1: Thursday 5 November	
9:00	Registration
10:00	Welcome and Opening
10:15	Regional climate system modelling for European sea regions – Aims of the workshop Meier H.E.M., Reckermann M., Rutgersson A., Sannino G. and Somot S.

<i>Topic 1: Development and evaluation of regional climate system models</i>	
10:30 – 10:50	Evaluation of simulated decadal variability over the Euro-Mediterranean region from ENSEMBLES to Med-CORDEX Dell'Aquila A. and Mariotti A.
10:50 – 11:10	Improved Regional Climate Model Simulation of Precipitation by a Dynamical Coupling to a Hydrology Model Larsen M. A. D., Drews M., Christensen J. H., Butts M. B. and Refsgaard J.C.
11:10 - 11:40	Coffee break
11:40 - 12:00	Which complexity of regional climate system models is essential for downscaling of anthropogenic climate change for the North Sea? Mikolajewicz U., Mathis M. and Elizalde A.
12:00 - 12:20	On the resolution of inter-basin exchanges in numerical models: The example of Black Sea and Baltic Sea straits Stanev E. V., Grashorn S., Grayek S. and Zhang Y.L.
12:20 - 12:40	Mediterranean cyclone climatology: Assessment of an ensemble of coupled and uncoupled atmosphere-ocean regional climate models applying six cyclone tracking methods Flaounas E., Gaertner M., Kelemen F., Lionello P., Sanchez E., Wernli H., Naveed A., Calmanti S., Conte D., Podrascanin Z., Reale M., Romera R. and Somot S.
12:40 - 13:10	Topic 1 Open discussion
13:10 – 14:10	Lunch

<i>Topic 2: Regional process studies and studies on the added value of coupled models with high resolution</i>	
14:10 – 14:30	Low frequency salinity variations in the Baltic Sea Schimanke S. and Meier H.E.M.
14:30 – 14:50	Carbon and total alkalinity budgets for the Baltic Sea Gustafsson G., Deutsch B., Gustafsson B.G., Humborg C., Mörth C.-M., Omstedt A. and Wällstedt T.
14:50 – 15:10	A study of the heat budget of the Mediterranean Sea from MedCORDEX forced and coupled simulations Harzallah A., Jordà G., Dubois C., Sannino G., Carillo A., Li L., Arsouze T., Cavicchia L., Beuvier J. and Akhtar N.
15:10 – 15:40	Coffee break
15:40 – 16:00	The role of the ocean in the European climate dynamical downscaling Sein D., Cabos W., Sidorenko D., Wang Q. and Jacob D.
16:00 – 16:20	Impact of resolution and ocean-coupling on regional climate model simulations over the Mediterranean Sea Akhtar N., Brauch J. and Ahrens B.
16:20 - 16.40	Interannual variability of the deep water formation in the North-West Mediterranean Sea using a fully-coupled regional climate system model Somot S., Houpert L., Sevault F., Testor P., Bosse A., Taupier-Letage I., Bouin M.-N., Waldman R., Cassou C., Durrieu de Madron X., Adloff F. and Herrmann M.

16:40 – 18:00	Poster Discussions
18:30	Ice Breaker and End of Day 1

Day 2: Friday 6. November	
9:00 – 9:20	Results from simulations with a coupled regional atmospheric-ocean-ice model over the Baltic Sea Christensen O. B., Tian T. and Boberg F.
9:20 – 9:40	Direct and semi-direct aerosol radiative effect on the Mediterranean climate variability using a coupled regional climate system model Nabat P., Somot S., Mallet M., Sevault F., Chiacchio M. and Wild M.
9:40 – 10:00	Added value of interactive air-sea coupling assessed from hindcast simulations for the North and Baltic seas Gröger M., Dieterich C., Schimanke S. and Meier H.E.M.
10:00 – 10:30	Topic 2 Open Discussion
10:30 – 11:00	Coffee break

<i>Topic 3: Extreme and high impact events</i>	
11:00 – 11:20	Temperature-precipitation extremes relationship in the Mediterranean: past climate assessment and projection in anthropogenic scenarios Drobinski P., Da Silva N., Panthou G., Bastin S., Muller C., Ahrens B., Borga M., Conte D., Fosser G., Giorgi F., Güttler I., Kotroni V., Li L., Morin E., Onol B., Quintana-Segui P., Romera R. and Zsolt T. C.
11:20 – 11:40	Spatiotemporal characterization of very long dry spells in the Mediterranean region Raymond F., Ullman A., Camberlin P. and Drobinski P.
11:40 – 12:10	Analysis of atmospheric and coupled ocean-atmosphere regional climate models capability to simulate tropical-like cyclones over the Mediterranean Sea from MedCORDEX and EUROCORDEX multimodel simulations Gaertner M. Á., Sánchez E., Domínguez M., Romera R., Gil V., Gallardo C., Miglietta M.M. and the Med-CORDEX and EURO-CORDEX teams
12:10 – 12:40	Spatiotemporal characterization of Mediterranean extreme precipitation events: a multi-model assessment Cavicchia L., Scoccimarro E., Gualdi S., Ahrens B., Berthou S., Conte D., Dell’Aquila A., Drobinski P., Djurdjevic V., Dubois C., Gallardo C., Sanna A. and Torma C.
12:40 – 13:10	Topic 3 Open Discussion
13:10 – 14:10	Lunch

<i>Topic 4: Climate change impact studies and uncertainty assessments of projections using coupled model simulations</i>	
14:10 – 14:30	Climate change and anthropogenic impacts on Mediterranean Sea ecosystems for the end of the 21st century Macias Moy D., Stips A. and Garcia-Gorritz E.
14:30 – 14:50	Surface heat budget over the North Sea in climate change simulations Dieterich C., Wang S., Schimanke S., Gröger M., Klein B., Hordoir R., Samuelsson P., Liu Y., Axell L., Höglund A. and Meier H.E.M.
14:50 – 15:10	Three ocean scenarios of the 2006-2100 period for the Mediterranean Sea with the regional climate system model CNRM-RCSM4 Sevault F., Somot S., Alias A. and Dubois C.
15:10 – 15:30	Projected acidification of the Mediterranean Sea Le Vu B., Orr J. C., Palmier J., Dutay J.-C., Sevault F. and Somot S.
15:30 – 16:00	Topic 4 Open Discussion
16:00 – 16:30	Coffee break

16:30 – 18:30	Overall workshop discussion and wrap-up
18:30	End of workshop and discovering Rome at night...

Poster presentations

<i>Topic 1: Development and evaluation of regional climate system models</i>
On the representation of Mediterranean sea level in regional climate models Adloff F., Jorda G., Somot S., Sevault F., Meyssignac B., Arzouse T., Li L. and Planton S.
Heat and freshwater budgets over the Mediterranean area from a new 34-year MED-CORDEX hindcast Béranger, K., Anquetin S., Arsouze T., Bastin S., Bouin M-N., Berthou S., Boudevillain B., Claud C., Lebeau-pin Brossier C., Delrieu G., Dubois C., Drobinski P., Froidurot S., Molinié G., Polcher J., Rysman J-F., Sevault F., Somot S. and Stéfanon M.
Coupling of COSMO-CLM and NEMO in two regions Brauch J., Früh B., Lenhardt J., Van Pham T., Akhtar N. and Ahrens B.
High-resolution downscaling of ERA40 for region of South East Europe with NMMB model Djurdjevic D. and Krzic A.
Application of the Weather Generator to Bias-correct the Regional Climate Model Output Dubrovsky M. and Duce P.
Arctic regional atmosphere-ocean-sea ice coupling, sensitivity to the domain geographical location Koldunov N.V., Sein D.V., Pinto J.G. and Cabos W.
Very High Resolution Observations of Regional Climate from Offshore Platforms near the German Coast Leiding T., Tinz B. and Gates L.
Heat and salt redistribution in the Mediterranean Sea. Insights from the MedCORDEX model ensemble Llasses J., Jordà G., Gomis D., Adloff F., Macías-Moy D., Harzallah A., Arzouse T., Ahrens B., Li L., Elizalde A. and Sannino G.
The Regional Earth System Model (RegESM) using RegCM4 coupled with the MITgcm ocean model: First assessments over the MED-CORDEX domain Mariotti L., Turuncoglu U., Farneti R., Sannino G., Dell'Aquila A., Sitz L., Fuentes RF. and Di Santi F.
Modeling of the marine ecosystem and the carbon cycle in the Barents Sea Martyanov S.
Mistral and Tramontane time series in (un)coupled regional climate simulations Obermann A. and Ahrens B.
Modeling the heat and the water balances including sea levels in the Mediterranean Sea Omstedt A. and Shaltout M.

Modelling the impacts of atmospheric dust deposition on the biogeochemical cycles in the Mediterranean Sea

Richon C., Dutay J-C., Dulac F., Vincent J., Laurent B., Desboeufs K., Mallet M., Nabat P. and Palmieri J.

Impact of land surface coupling on the Mediterranean continental water cycle

Stéfanon M. and Polcher J.

Flood zone modeling for a river system relying on the water spread over a terrain

Volchek A., Kostjuk D. and Petrov D.

Topic 2: Regional process studies and studies on the added value of coupled models with high resolution

Quasi-biennial oscillation effect on Baltic Sea region climate indicators: Lithuania's case

Bukantis A. and Akstinas V.

Response of the Black Sea's benthos ecological functions to an environmental gradient

Grégoire A., Drion R., Gomoiu M., Todorova V., Velikova V. and Capet A.

Coupling of regional atmospheric-ocean models (WRF-ROMS) for climate applications in the Mediterranean basin

Jiménez-Guerrero P. and Montávez J.P.

Feedback of Coastal Upwelling on the Near-Surface Wind Speed at the Baltic Sea

Raub T., Lehmann A. and Jacob D.

Comparing on centennial time scale the deviation of sea level from the global mean of two marginal seas: Baltic and Adriatic Sea

Scarascia L. and Lionello P.

Multimodel for sea level forecast by artificial neural network

Sztobryn M.

The influence of vegetation feedbacks on recent sea ice dynamics – results from a regional Earth system model

Zhang W., Döscher R., Koenigk T., Miller P.A., Smith B., Jansson C. and Samuelsson P.

Seasonality in Intraseasonal and Interannual Variability of Mediterranean SST and its Links to Regional Atmospheric Dynamics

Zveryaev I.I.

Topic 3: Extreme and high impact events

Modulation of heavy precipitation in the region of Valencia (Spain) by Mistral-induced sea-surface cooling in the previous days

Berthou S., Mailler S., Drobinski P., Arsouze T., Bastin S., Béranger K. and Brossier C.L.

Generation of heavy rainfall during the Oder flood event in July 1997: On the role of soil moisture

Ho-Hagemann H.T.M., Hagemann S. and Rockel B.

The role of the atmospheric coupling in the ability of ORCHIDEE to simulate droughts

Polcher J. and Stéfanon M.

Topic 4: Climate change impact studies and uncertainty assessments of projections using coupled model simulations

A downscaling investigation of multi-model uncertainty of hindcasted and projected regional temperatures

MacKenzie B. and Meier H.E.M.

Evaluating the utility of dynamical regionalization of climate for predicting climate impacts on forests

Martin-St. Paul N., Stéfanon M., Guillemot J., Ruffault J., Francois C., Somot P., Dufrene E. and Leadley P.

Modelling climate change impact on hydroecological conditions of the Tyligulskyi Liman lagoon (north-western coast of the Black Sea)

Tuchkovenko Y. and Khokhlov V.

Abstracts in first author alphabetical order

On the representation of Mediterranean sea level in regional climate models

Fanny Adloff¹, Gabriel Jorda², Samuel Somot¹, Florence Sevault¹, Benoit Meyssignac³, Thomas Arzouse⁴,
Laurent Li⁵ and Serge Planton¹

¹ CNRM-GAME, Météo-France, CNRS, Toulouse, France (fanny.adloff@meteo.fr)

² IMEDEA, UIB, Palma de Mallorca, Spain

³ LEGOS, UMR5566, CNRS-CNES-IRD-Université de Toulouse, Toulouse, France

⁴ ParisTech, ENSTA, UME, Palaiseau, France

⁵ Univ Paris 6, LMD, Paris, France

1. Introduction

So far, the question about future sea level change in the Mediterranean remains open. Climate modelling attempts to assess future sea level change in the Mediterranean were unsuccessful. On one hand, global models (e.g. CMIP-type models) have a rather low resolution which prevents an accurate representation of important small scales processes acting over the Mediterranean region - a basic pre-requisite to achieve a good representation of water masses and sea level in this region. Additionally, global models often parameterize the water exchange at the narrow Strait of Gibraltar, which strongly influences the circulation and the changes in sea level in the Mediterranean Sea. There is thus a need to use high resolution regional ocean modelling to answer the question of ongoing and future Mediterranean sea level change. However, up to now, long term regional Mediterranean ocean models do not integrate the full sea level information from the Atlantic even if it has been shown that sea level variability in the east Atlantic drives the Mediterranean variability at interannual and interdecadal scales (Calafat et al, 2012; Tsimplis et al., 2013).

2. Modelling approach

In the present study, we aim to improve the representation of sea level in the regional ocean model NEMOMED12. This new ocean simulation, called MED12, covers the hindcast period 1980-2013. At the Atlantic buffer zone, we apply a restoring to the temperature, salinity and sea surface height from the reanalysis ORAS4 (Balmaseda et al., 2014). The seasonal cycle of the sea surface height is corrected with the altimetry (CCI-ECV sea level data, Ablain et al. 2015). We evaluate the quality of the simulated Mediterranean sea level through the comparison with altimetry and reconstructed sea level fields for the pre-altimetric period (Calafat et al. 2011 ; Meyssignac et al. 2009). We assess the added value of this new dataset of Atlantic boundary forcing comparing our new simulation with former hindcast simulations from 3 different regional coupled climate models : CNRM-RCSM4 (Sevault et al, 2014), MORCE-MED (Lebeaupin et al. 2015) and LMDZ-MED (L'Hévéder et al. 2012), all part of the MedCORDEX framework (www.medcordex.eu). This validation procedure of sea level representation in regional ocean simulations is a crucial step before planning climate change scenario simulations with regional models.

3. Methodology on how to calculate Mediterranean sea level from baroclinic models

Sea level is usually represented as the dynamic sea surface height (SSH) in the NEMO ocean model. This corresponds to the dynamic layer located above the first vertical layer of the ocean model, at the surface. The dynamic SSH is influenced winds, density gradients, air-sea fluxes, currents and lateral boundary conditions.

Later, a steric component has been included as part of the sea level signal (Marcos et al., 2008, Calafat et al. 2012, Carillo et al. 2012). This steric component represents the density changes of the Mediterranean water. The steric component can be split into two components : the thermosteric contribution resulting from the temperature changes of the water and the halosteric contribution corresponding to the salinity changes.

A recent study by Jorda et al. (2013) underlined the relevance to include the mass addition related to salinity changes in the basin. Because most of ocean models have a constant volume, the volume related to the changes of basin salt content should be considered as an additional contributor to sea level change.

In the frame of this study, we propose a new hindcast simulation (MED12) with sea level Atlantic boundary conditions including the complete signal from the Atlantic: steric trend, changes in land water storage, ice sheet melting etc. With such a simulation, there is no need to compute steric variations since their signal is included in the boundary conditions. Thus the dynamic SSH contains the full signal.

3. First results

The treatment of boundary conditions differs in each simulation. Fig. 1 represents interannual sea level variations averaged for the Atlantic zone of the models, west from Gibraltar. The absence of trend is noted for the three coupled models which do not include steric sea level and mass variations from the Atlantic. Considering CCI-ECV as the reference, MED12-BC represents best the interannual variations with a correlation of 0.91 with the CCI-ECV dataset. Among the coupled models, CNRM-RCSM4 performs best until 2003, when MORCE-MED takes the lead, because they practice a sea level relaxation toward the interannual signal of the GLORYS reanalysis (Ferry et al. 2010) from 2002 on. The interannual variability of MORCE-MED before 2002 is very poor due to their experimental setup.

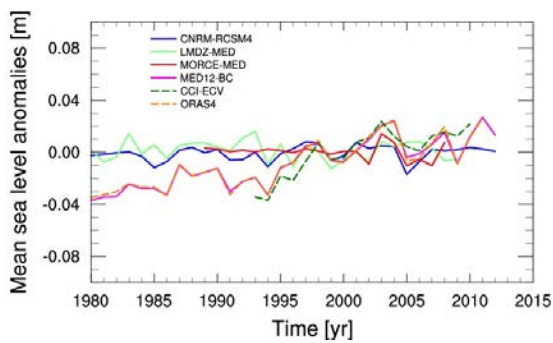


Figure 1. Interannual variability of SSH averaged over the Atlantic box. The different simulations are compared to satellite-derived data (CCI-ECV) and the ORAS4 reanalysis.

Each panel in Fig. 2 represents the interannual variations of Mediterranean sea level calculated with one of the different methodologies detailed in section 2. Simulations from the different models are compared to reconstructions and satellite-derived product. The new method with the implementation of correct Atlantic sea level boundary conditions simulates the best the Mediterranean SSH interannual variability.

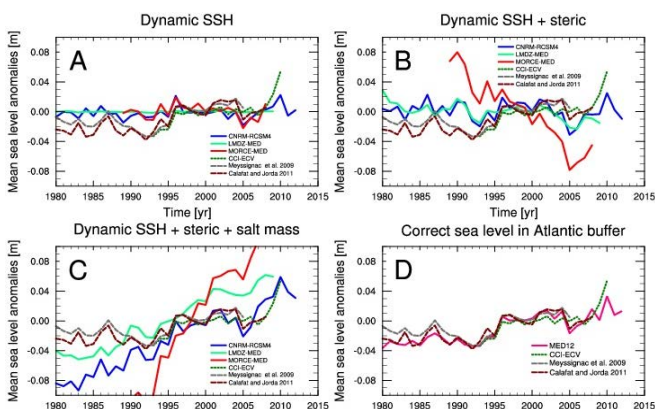


Figure 2. Interannual variability of SSH averaged over the Mediterranean for different methods of calculation for the sea level signal. Hindcast simulations from different models are compared to satellite-derived data (CCI-ECV) and sea level reconstructions (Calafat et al. 2011; Meysignac et al. 2009).

4. Conclusions

Our study shows the relevance to integrate a full Atlantic sea level signal at the western boundary of Mediterranean ocean models to account for the global trend which considerably influences Mediterranean sea level signal. This approach should be adopted in future scenario simulations aiming at investigating the impact of climate change on Mediterranean sea level.

References

Ablain M, Cazenave A, Larnicol G, Balmaseda M, Cipollini P, Fauge`re Y, Fernandes MJ, Henry O, Johannessen JA, Knudsen P, Andersen O, Legeais J, Meysignac B, Picot N, Roca M, Rudenko S, Scharffenberg MG, Stammer D, Timms G, Benveniste J (2015) Improved sea level record over the satellite altimetry era (1993–2010) from the climate change initiative project. *Ocean Science* 11(1):67–82, DOI 10.5194/os-11-67-2015, URL <http://www.ocean-sci.net/11/67/2015/>

Balmaseda MA, Mogens K, Weaver AT (2013) Evaluation of the ecmwf ocean reanalysis system oras4. *Quarterly Journal of the Royal Meteorological Society* 139(674):1132–1161, DOI 10.1002/qj.2063

Calafat FM, Gomis D, Marcos M (2009) Comparison of Mediterranean sea level fields for the period 1961–2000 as given by a data reconstruction and a 3D model. *Global And Planetary Change* 68(3):175–184

Calafat FM, Jord G, Marcos M, Gomis D (2012) Comparison of mediterranean sea level variability as given by three baroclinic models. *J Geophys Res*, URL <http://dx.doi.org/10.1029/2011JC007277>

Ferry N, Parent L, Garric G, Barnier B, Jourdain N, the Mercator Ocean team (2010) Mercator global eddy permitting ocean reanalysis glorys1v1: Description and results. Tech. 201 rep., Mercator Ocean Q. Newsl., 36, 15–28.

IPCC (2013) *Climate Change 2013: The Physical Science Basis*. 205 Working Group I Contribution to the Fifth Assessment Report of the Intergovernmental Panel on Climate Change. Cambridge University Press, Cambridge, U.K.

Jorda G, Gomis D (2013) On the interpretation of the steric and mass components of sea level variability: The case of the mediterranean basin. *Journal of Geophysical Research oceans* 118(2):953–963, DOI 10.1002/jgrc.20060

Marcos M, Tsimplis MN (2008) Comparison of results of AOGCMs in the Mediterranean Sea during the 21st century. *Journal Of Geophysical Research-Oceans* 113(C12):C12,028

Meysignac B, Calafat FM, Somot S, Rupolo V, Stocchi P, Llovel W, Cazenave A (2011) Two-dimensional reconstruction of the mediterranean sea level over 1970–2006 from tide gage data and regional ocean circulation model outputs. *Global and Planetary Change* 77(1-2):49–61, DOI 10.1016/j.gloplacha.2011.03.002

Lebeaupin-Brossier C, Bastin S, Béranger K, Drobinski P (2015) Regional mesoscale air–sea coupling impacts and extreme meteorological events role on the Mediterranean Sea water budget. *Clim. Dyn.* DOI 10.1007/s00382-014-2252-z

L'Hévéder B, Li L, Sevault F, Somot, S. 2013. Interannual variability of deep convection in the Northwestern Mediterranean simulated with a coupled AORCM. *Clim. Dyn.* 41(34), 937960.

Sevault F, S. Somot, A. Alias, C. Dubois, C. Lebeaupin-Brossier, P. Nabat, F. Adloff, M. Déqué and B. Decharme (2014) A fully coupled Mediterranean regional climate system model: design and evaluation of the ocean component for the 1980–2012 period, *Tellus A*, 66, 23967.

Tsimplis MN, Shaw AGP (2010) Seasonal sea level extremes in the Mediterranean Sea and at the Atlantic European coasts. *Natural Hazards And Earth System Sciences* 10(7):1457– 1475

Impact of resolution and ocean-coupling on regional climate model simulations over the Mediterranean Sea

Naveed Akhtar¹, Jennifer Brauch² and Bodo Ahrens¹

¹ Institute of Atmospheric and Environmental Science, Goethe University Frankfurt am Main, Germany (naveed.akhtar@iau.uni-frankfurt.de)

² German Weather Service, Offenbach am Main, Germany

1. Introduction

The semi-enclosed Mediterranean Sea has a strong impact on the local and even remote climate system as a source of moisture and a heat reservoir. To study the Mediterranean climate and weather it is important to consider the effects of mesoscale features, complex orography, strong air-sea interaction, and the regional mechanisms that characterizing it. Global models with coarse resolution cannot fully resolve the local and mesoscale processes that characterized the Mediterranean region and results in underestimation the air-sea fluxes of heat and momentum (Elguindi et al., 2009). Studies show that high-resolution regional ocean-atmosphere coupled models produced more accurate estimates of the SST and air-sea fluxes of heat and momentum (Artale et al., 2010; Somot et al., 2008).

2. Experiment Set-up

In this study we employed a newly developed ocean-atmosphere regional coupled model (COSMO-CLM/NEMO-MED12) and atmosphere-only (COSMO-CLM) to study the affects of coupling on the atmosphere and ocean and air-sea fluxes of heat and momentum on sub-daily and seasonal timescale over the Mediterranean basin. To study the impact of resolution we used two different horizontal atmospheric grid spacings 0.44° (~ 50 km) and 0.08° (~ 9 km) in the atmosphere-only and coupled regional models. The atmospheric model uses the ERA-Interim data from ECWMF for both the coupled and atmosphere-only runs. However, in the coupled runs, SST over the Mediterranean Sea is calculated by NEMO-MED12 and elsewhere prescribed and derived from the reanalysis data.

The NEMO-MED12 is a regional configuration of OGCM (Ocean General Circulation Model) NEMO (Madec et al., 2008) for the Mediterranean Sea (Lebeaupin Brossier et al., 2011). The resolution of ocean grid is $1/12^\circ$ (~ 6.5 – 8 km in latitude and ~ 5.5 – 7.5 km in longitude, 567×264 and 50 vertical levels). The ocean model is initialized using MEDATLAS-II (Rixen, 2012) monthly mean seasonal climatology (1945-2002) in the Mediterranean Sea. The climatological average of Ludwig et al., (2009) inter-annual data is used to compute monthly runoff values for river discharge of freshwater into the Mediterranean Sea (Beuvier et al., 2012). The ocean model NEMO-MED12 is coupled via the OASIS3-MCT coupler (Valcke, 2013) to the atmospheric model COSMO-CLM (Akhtar et al., 2014). Hereafter, we used the abbreviations for the coupled "CPLxx" and atmosphere-only "CCLMxx", where "xx" refers to resolution 44 for 0.44° and 08 for 0.08° . The air-sea fluxes are compared with the OAFflux dataset (<http://oaf flux.who i.edu/>).

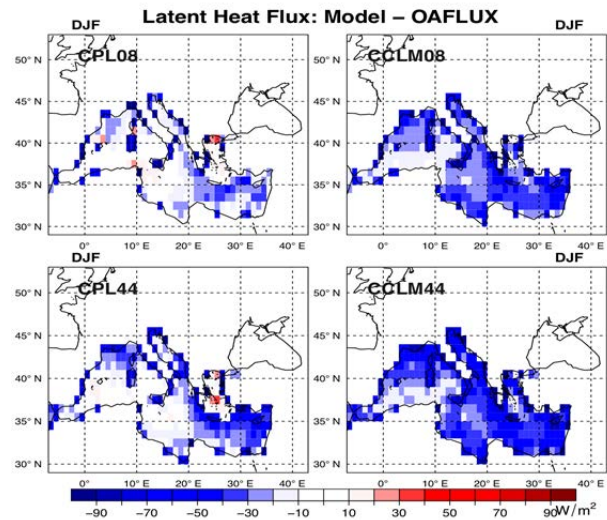


Figure 1. Latent heat flux: Mean difference of winter season between OAFflux and the coupled and atmosphere-only runs at 0.44° and 0.08° (2000-2003)

3. Results

Figure 1 shows the mean difference of latent heat flux during the winter season between OAFflux and simulations (coupled and atmosphere-only at 0.44° and 0.08°). The results show that differences in CPL44 and OAFflux are smaller compared to the differences in CCLM44 and OAFflux. However, in both 0.44° runs latent heat flux is underestimated during winter season. These differences are smaller during the spring and summer seasons and start increasing again during the autumn season. The higher latent heat flux in CPL44 compared to CCLM44 is caused by higher 10-m wind speed during the winter season (~ 0.4 – 0.7 m/s; not shown here). In higher resolution 0.08° runs the estimates of latent heat flux are improved in both the CPL08 and CCLM08 runs compared to CPL44 and CCLM44 runs. The differences in CCLM08 and OAFflux are higher compared to the differences in CPL08 and OAFflux. The CPL08 shows more realistic estimates of the latent heat in the winter season and also in other the seasons. The CPL08 also shows higher 10-m wind speed (~ 0.6 – 1.2 m/s; not shown here) particularly in the Aegean Sea, Gulf of Lion and in most of the coastal areas during autumn, winter and spring season. The results show that high-resolution ocean-atmosphere coupled model improves the latent heat flux and hence air-sea fluxes of heat and momentum.

4. Conclusion

The results show that estimates of air-sea fluxes are significantly improved in the ocean-atmosphere coupled runs compared to the atmosphere-only runs. The higher atmospheric grid resolution (0.08°) also improves the air-sea fluxes in both the coupled and atmosphere-only runs compared to the coarse grid (0.44°). However, compared to the atmosphere-only runs, the air-sea fluxes are more realistic in the high-resolution coupled runs. The coupled runs have higher 10-m wind speed compared to atmosphere-only runs at both the resolutions 0.44° and 0.08° . At lower resolution (0.44°) the 10-m wind speed in the coupled runs is higher than atmosphere-only runs. However, these differences in 10-m wind speed are larger between coupled and atmosphere-only runs at higher resolution (0.08°). The results show that high-resolution ocean-atmospheric coupled model is necessary to fully resolve the mesoscale and intense local process for more realistic estimates of air-sea fluxes of heat and momentum.

References

- Akhtar, N., J. Brauch, A. Dobler, K. Berenger, B. Ahrens (2014). Medicanes in an ocean-atmosphere coupled regional climate model. *Nat. Hazards Earth Syst. Sci.*, 14, 2189–2201
- Artale, V., Calmanti, S., Carillo, A., Dell'Aquila, A., Herrmann, M., Pisacane, G., Ruti, P. M., Sannino, G., Struglia, M. V., Giorgi, F., Bi, X., Pal, J. S., Rauscher, S. and The PROTHEUS Group (2010). An atmosphere-ocean regional climate model for the Mediterranean area: assessment of a present climate simulation, *Clim. Dynam.*, 35, 721–740.
- Beuville J, B'eranger K, Lebeauvin Brossier C, Somot S, Sevault F, Drillet Y, Bourdall'e-Badie R, Ferry N, Lyard F (2012). Spreading of the Western Mediterranean Deep Water after winter 2005: time-scales and deep cyclone transport. *J. Geophys. Res.* 117: C07022, DOI: 10.1029/2011JC007679.
- Elguindi, N., Somot, S., Déqué, M., and Ludwig, W. (2009). Climate change evolution of the hydrological balance of the Mediterranean, Black and Caspian Seas: impact of climate model resolution, *Clim. Dynam.*, 36, 205–228.
- Lebeauvin Brossier, C., K. B'eranger, C. Deltel, and P. Drobinski (2011). The Mediterranean response to different space-time resolution atmospheric forcings using perpetual mode sensitivity simulations, *Ocean Modell.*, 36, 1–25, doi:10.1016/j.ocemod.2010.10.008.
- Ludwig, W., Dumont, E., Meybeck, M. and Heussner, S. (2009). River discharges of water and nutrients to the Mediterranean and Black Sea: Major drivers for ecosystem changes during past and future decades? *Prog. Oceanogr.* 80, 199–217.
- Madec, G., and the NEMO Team (2008). NEMO Ocean Engine, Note Pôle Modél. 27, Inst. Pierre-Simon Laplace, Paris.
- Rixen, M. (2012). MEDAR/MEDATLAS-II, GAME/CNRM, doi:10.6096/HyMeX.MEDAR/MEDATLAS-II.20120112.
- Somot, S., Sevault, F., Déqué, M., and Crépon, M. (2008). 21st century climate change scenario for the Mediterranean using a coupled atmosphere-ocean regional climate model, *Glob. Planet Change*, 63, 112–126.
- Sverdrup, H. U., Johnson, M. W. and Fleming, R. H. (1942). *The Oceans: Their Physics, Chemistry and General Biology*. Prentice-Hall, Englewood Cliffs, New York, 1087 pp.
- Valcke, S. (2013). The OASIS3 coupler: a European climate modelling community software, *Geosci. Model Dev.*, 6, 373–388, doi:10.5194/gmd-6-373-2013.
- Weller, R. A. and Anderson S. P. (1996). Surface meteorology and air-sea fluxes in the western equatorial Pacific warm pool during the TOGA Coupled Ocean-Atmosphere Response Experiment. *J. Clim.*, 9, 1959–1990.

Heat and freshwater budgets over the Mediterranean area from a new 34-year MED-CORDEX hindcast

Karine Béranger^{1,2}, S. Anquetin², T. Arsouze^{1,3}, S. Bastin⁴, M-N. Bouin⁵, S. Berthou¹, B. Boudevillain²,
C. Claud¹, C. Lebeaupin Brossier⁷, G. Delrieu², C. Dubois⁶, P. Drobinski¹, S. Froidurot², G. Molinié², J. Polcher¹,
J-F. Rysman¹, F. Sevault⁷, S. Somot⁷, M. Stéfanon¹

¹ LMD, Palaiseau, France (karine.beranger@ujf-grenoble.fr)

² LTHE, Grenoble, France

³ ENSTA-ParisTech, Palaiseau, France

⁴ LATMOS, Paris, France

⁵ Météo-France, Brest, France

⁶ Mercator Océan, Toulouse, France

⁷ CNRM/Météo-France, Toulouse, France

1. Abstract

A dynamical downscaling of the ERA-Interim reanalysis has been run over the 1979-2012 period using the WRF model in a new MORCE-MED (Drobinski et al. 2012) configuration covering the MED-CORDEX domain. The model results are analysed through budgets over the Mediterranean Sea and sub-regional land areas. The Mediterranean Sea Heat budget (QNET) and the Mediterranean Sea freshwater budget (EMP) are good indicators of the energy and water balances in this area because they can be controlled at the Gibraltar strait. In fact, climatological values are around -5 W.m^{-2} for the heat budget and 0.7 m yr^{-1} for the freshwater flux. The comparisons with recent climatologies derived from in situ observations, satellite datasets and other modelling studies, suggest a slight warm bias mainly due to a too large shortwave flux contribution to QNET. In the perspective of being coupled to the ocean and land models, we try to reduce this bias that may decrease the thermohaline circulation and change the continental precipitation and river runoff. Preliminary validations of the simulation are presented for QNET, for EMP and for the Mediterranean Sea net shortwave heat budget (QSOL). Then a special outlook is done on 2-m temperature (T2M) and precipitation (P).

2. Model and reference simulation CTL

The atmospheric model is the non-hydrostatic Weather Research and Forecasting (WRF, version 3.6.1) model of the National Center for Atmospheric Research (NCAR) (Skamarock et al. 2007). The WRF domain covers the Europe-Mediterranean basin with a horizontal resolution of 20km. It has 44 sigma-levels in the vertical. A complete set of physics parameterizations is used with the WRF Single-Moment 5-class microphysical scheme (Hong et al. 2004), the Kain-Fritsch convection scheme (Kain 2004), the planetary boundary layer (PBL) scheme and a 2.5 level TKE scheme for the turbulent fluxes (MYNN; Nakanishi and Niino 2006). P and evaporation are solved thanks to these parameterizations. The radiative scheme is based on the Rapid Radiative Transfer Model (RRTM) (Mlawer et al., 1997) and the Dudhia (1989) parameterization for the longwave and shortwave radiation, respectively. The aerosols feedbacks from the parameterization of Alapathy et al. (2012) was applied. In our case, this allowed a relatively low QSOL decrease of about 3 W.m^{-2} and consequently for QNET.

For the land surface, the RUC scheme with 6 layers is used. The model time-step is 60s.

A dynamical downscaling of the ERA-Interim reanalysis (Simmons et al. 2007) is done with this model for which a spectral nudging is applied for temperature, humidity and velocity components above the PBL to keep the chronology of the large scale atmospheric circulation. Outputs are stored every 3-hours. The 34-year reference simulation CTL started in January 1979 and run until December 2012.

3. CTL Results

In average over the sea surface, the CTL results show a good agreement with observations for the sensible, latent, and net longwave heat fluxes, as well as for the EMP. The QSOL warm shift is of the order of 15 W.m^{-2} . The 34-year CTL climatological values are $\text{QNET}=+2.9 \text{ W.m}^{-2}$ and $\text{EMP}=+0.85 \text{ m.yr}^{-1}$.

Over the continental sub-regional areas, T2M is slightly higher than the EOBS observations. Nevertheless, correlation coefficients from monthly time-series are above 0.97. For P, uncorrelated results are noticed between agreements on P budgets and on its seasonal variability according to correlation coefficients (CC). For example, for Tunisia, agreements are relatively low for the seasonal variations ($\text{CC}=0.42$) and for the P budget which is half the EOBS budget. For Israel, although $\text{CC}=0.77$, the P budget is less than half of the EOBS budget. The agreements for Alps is lower than for Pyrenees. The budget for Alps (Pyrenees) is twice ($+0.25\%$) the EOBS budget and $\text{CC}=0.26$ (0.50).

4. Conclusions and perspectives

A 34-year atmospheric simulation of the Europe-Mediterranean area has been done for the 1979-2012 period. The use of the climatology of Nabat et al. (2014) is planned to conclude if in our MORCE-MED configuration the QSOL can be reduced and the QNET decreased to climatological values. Then, the integration of this model in the new MORCE-MED platform with the ocean NEMO-MED12, as previously done by Lebeaupin Brossier et al. (2014), and, the land ORCHIDEE components (Stéfanon et al., this issue), will be achieved.

References

- Alapathy K., Herwehe J. A., Otte T. L. (2012) Introducing subgrid-scale cloud feedbacks to radiation for regional meteorological and climate modeling , *Geophysical Res. Letters*, Vol. 39, L24809, 5pp.
- Duhia J. (1989) Numerical study of convection observed during the winter mooson experiment using a mesoscale two dimensional mode, *J. Atmos. Sci.*, Vol.46, pp. 3077-3107.
- Drobinski P., Anav A., Lebeaupin Brossier C. et al. (2013) Model of the Regional Coupled Earth system (MORCE): application to process and climate studies in vulnerable regions , *Environmental Modelling and Software* , doi:10.1016/j.envsoft.2012.01.017.
- Hong S. Y., Dudhia J., Chen S-H. (2004) A revised approach to ice microphysical processes for the bulk parameterization of clouds and precipitation. *Mon. Wea. Rev.*, Vol.132, pp. 103–120.
- Kain, J.S. (2004) The Kain-Fritsch convective parameterization: An update, *J. Appl. Meteor.*, Vol.43, pp. 170-181.
- Lebeaupin Brossier C., Bastin S., Béranger K. et al. (2014) Regional mesoscale air-sea coupling impacts and extreme meteorological events role on the Mediterranean Sea water budget , *Climate Dynamics*, doi:10.1007/s00382-014-2252-z .
- Mlawer E. J., Taubnam S. J., Brown P. D. et al. (1997) A validated correlated k-model for the longwave, *J. Geophys. Res.*, Vol.102, pp. 16663-16682.
- Nabat P., Somot S., Mallet M. et al. (2013) A 4-D climatology (1979-2009) of the monthly tropospheric aerosol optical depth distribution over the Mediterranean region from a comparative evaluation and blending of remote sensing and model products , *Atmos. Meas. Tech.* , Vol.6, pp. 1287-1314.
- Nakanishi M., Niino H. (2004) An Improved MellorYamada Level-3 Model with Condensation Physics: Its Design and Verification. *Boundary-Layer Meteorology*, Vol. 112(1), pp. 1-31.
- Simons A., Uppala S., Dee D., Kobayashi S. (2007) ERA-interim: New ECMWF re- analysis products from 1989 onwards, *ECMWF Newsletter*, Vol. 110, pp. 25-35.
- Skamarock W.C., Klemp J. B., Dudhia J. et al. (2008) A description of the Advanced Research WRF Version 3, 125pp, NCAR Tech. Note NCAR/TN-475+STR.

Modulation of heavy precipitation in the region of Valencia (Spain) by Mistral-induced sea-surface cooling in the previous days

Ségolène Berthou¹, Sylvain Mailler¹, Philippe Drobinski¹, Thomas Arsouze², Sophie Bastin³,
Karine Béranger⁴ and Cindy Lebeau-pin Brossier⁵

¹ IPSL/Laboratoire de Météorologie Dynamique, CNRS, ENPC, Palaiseau, France (segolene.berthou@lmd.polytechnique.fr)

² ENSTA-ParisTech, Unité de Mécanique, Palaiseau, France

³ IPSL/Laboratoire Atmosphères, Milieux, Observations Spatiales, Guyancourt, France

⁴ LTHE, Grenoble and IPSL/LMD, Palaiseau, France

⁵ GAME-CNRM, Météo France, Toulouse, France

1. Introduction

The region of Valencia in Spain is regularly affected by heavy precipitation events (HPEs), some of which cumulated more than 800mm in less than two days (Peñarrocha et al. (2002)). Pastor et al. (2001) and Pastor et al. (2015) show the importance of the sea surface temperature (SST) upstream the precipitation system in the moisture uptake and destabilisation of the air masses. Furthermore, Berthou et al. (2015) show that this region is one of the regions most sensitive to changes in SST among 6 other Mediterranean region. They further show that important changes in SST at the submonthly timescale occur in the Balearic Sea.

We examine the time relation between events of strong northerly winds from Southern France which cool the Balearic sea and HPEs in the region of Valencia with the help of regional climate modeling.

2. Method

Three nudged RCM hindcast simulations of the Mediterranean region over the period 1989-2008 are used with the platform MORCE :

- CTL: one atmosphere-only simulation with ERA-interim SST
- CPL: one atmosphere-ocean coupled simulation
- SMO: one atmosphere-only simulation forced by the 30 day-averaged SST of the coupled simulation.

The resolution is 25km for the atmosphere and 6-7km for the ocean (see Berthou et al. (2015) for further details on the set-up).

3. Selection of HPEs

The 26 strongest HPEs in the CPL simulation are selected for the study. This corresponds to a threshold of 86mm of rain in this region. 88% of these events are among the 100 largest events in the gridded precipitation product of Herrera et al. (2012).

4. Rossby wave breaking: succession of Mistral and HPE

Among these 26 events, 19 show a cold anomaly of SST between the CPL and SMO simulations, revealing that an episode of SST cooling occurred before the HPE.

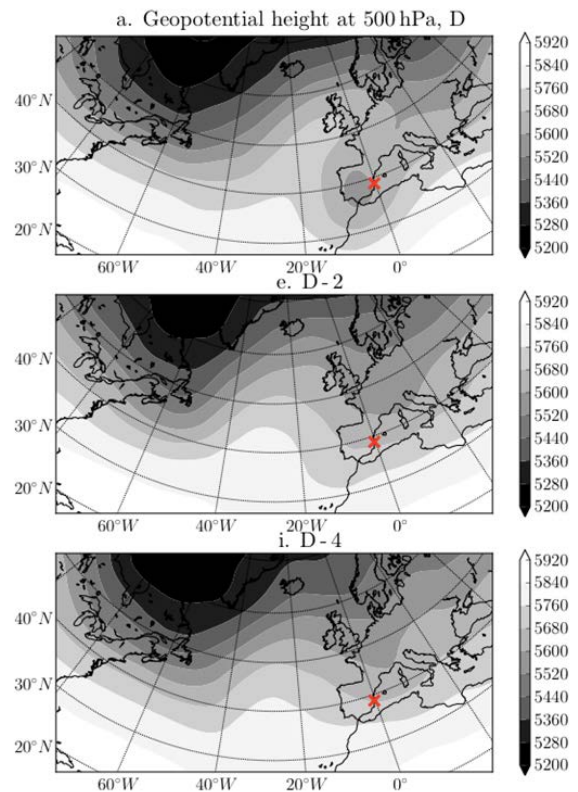


Figure 1: Composite of the 500hPa geopotential height for the 19 selected HPE days (top), 2 days before the HPEs (middle) and 4 days before them (bottom)

The composite for the 19 events of the 500hPa geopotential height are given in figure 1. The top picture illustrates a typical situation of HPE in this region: a cut-off low located above the Iberian peninsula together with a surface low which sustains a north-easterly low-level jet towards the region of Valencia (not shown).

The middle figure and the bottom figure show the composite situation 2 and 4 days before the HPE. This clearly shows a propagating Rossby wave that breaks on the HPE day.

The succession ridge/trough located over eastern France 2 to 5 days before the HPE leads to Mistral conditions. This is characterized by a northerly flow channeled by the French orography (not shown), which cools down the SST, by 0.3°C in the upstream zone in average (Figure 2).

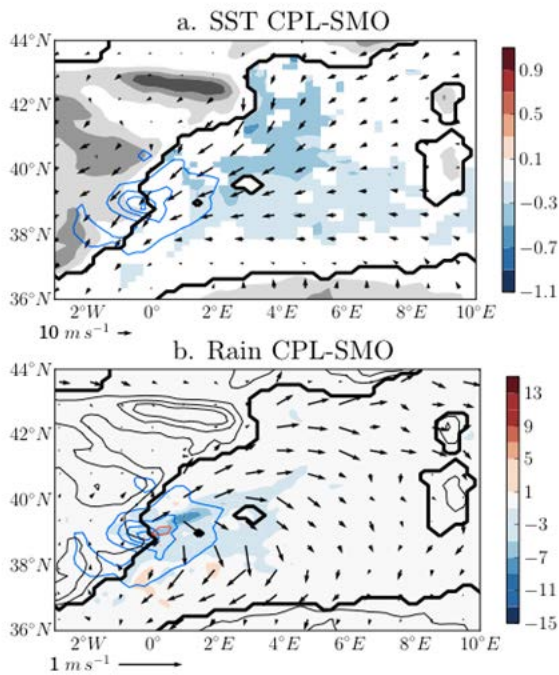


Figure 2: Composite for the 19 events. a: colours: SST differences (only significant values above 99% probability of rejecting a zero average difference with a Student t-test are shown), arrows: CPL wind, blue contours: CPL rain (contour every 50\,mm). b: colours: Rain differences, red contours: significant rain difference values above 99%, arrows: wind differences, blue contours: CPL rain

5. The cooling from the Mistral impacts the following HPE.

Figure 2 shows the composite of SST and rain differences between two simulations. The decrease in SST of 0.3°C induces a decrease in rain of about 3mm in average over all events. This decrease occurs mainly upstream of the rain maximum. Further study of larger differences given by CPL-CTL show that this decrease mainly affects the precipitation generated by the convective scheme of the model in this region. The decrease of precipitation in this region is most probably linked with a decrease in CAPE due both to a decrease in surface fluxes and a decrease in moisture convergence because of the build-up of a pressure anomaly where the weaker CAPE is consumed.

6. Conclusion

In 70% of the strongest HPEs represented by the RCM, a SST cooling occurs before the HPE. In these cases, a ridge-trough complex evolves slowly towards the east within the 5 to 2 days preceding the HPE before the Rossby wave breaks and generates a cut-off low. The cooling of about 0.3°C in average which occurs before the HPE decreases the intensity of the precipitation. Limits to this study are that the decrease in precipitation intensity mostly affects the parameterised precipitation in RCM with 25km resolution. Therefore, similar studies with a higher resolution RCM would complete this study: Pastor et al. (2015) show a larger sensitivity of rain to the SST with a higher resolution in this region for a few cases.

References

- Berthou, S., Mailler, S., Drobinski, P., Arsouze, T., Bastin, S., Béranger, K., Flaouas, E., Lebeaupin Brossier, C., Somot, S., Stéfanon, M. (subm.) Where does submonthly air-sea coupling influence heavy precipitation events in the Northwestern Mediterranean?, QJRM
- Herrera, S., Gutierrez, J., Ancell, R., M.R., P., Frias, M., Fernandez, J. (2012). Development and analysis of a 50 year high-resolution daily gridded precipitation dataset over Spain (spain02). *Int. J. Climatol.*, 32, pp. 74-85.
- Pastor, F., Estrela, M. J., Peñarrocha, D., Millán, M. M. (2001) Torrential rains on the Spanish Mediterranean coast: Modeling the effects of the sea surface temperature, *J. Appl. Meteorol.*, 40, 7, pp. 1180-1195.
- Pastor, F., Valiente, J. A., Estrela, M. J. (2015) Sea surface temperature and torrential rains in the Valencia region : modelling the role of recharge areas. *NHESS Discussions*, 3, 2, pp. 1357-1396.
- Peñarrocha, D., Estrela, M. J., Millán, M. (2002) Classification of daily rainfall patterns in a Mediterranean area with extreme intensity levels : the Valencia region, *International Journal of Climatology*, 22, 6, pp. 677-695.

Coupling of COSMO-CLM and NEMO in two regions

Jennifer Brauch¹, Barbara Fröh¹, Jennifer Lenhardt¹, Trang Van Pham², Naveed Akhtar^{2,3},
Bodo Ahrens^{2,3}

¹ Deutscher Wetterdienst, Offenbach am Main, Germany (jennifer.brauch@dwd.de)

² Biodiversity and Climate Research Center, Frankfurt am Main, Germany

³ Institute of Atmospheric and Environmental Science, Goethe University, Frankfurt am Main, Germany

1. Abstract

We have established two coupled regional atmosphere ocean models, one for the Mediterranean Sea and the other for the North and Baltic Seas. The atmosphere model chosen is COSMO-CLM, for the ocean, it is NEMO, which includes the sea ice model LIM3. Both models are coupled via the OASIS3-MCT coupler. This coupler interpolates heat, fresh water, momentum fluxes, sea level pressure and the fraction of sea ice at the interface in space and time.

We will present the individual setups for the two regions and show results of our hindcast experiments. Additionally, we have investigated how well the model components scale and what the optimal processor configuration for the components is, so the waiting time is reduced.

2. Introduction

The Mediterranean region and the region to east of the Baltic Sea have been identified as the two main hot-spots of climate change by Giorgi, 2006, on the base of temperature and precipitation variability. So, our main areas of interest are the Mediterranean Sea with its diverse wind patterns in the atmosphere and deep convection in the ocean and the North- and Baltic Seas with the complex water exchange between them. The development of a regional coupled climate model is a logical step to understand the local interactions between atmosphere and ocean. The complex processes on the interface between atmosphere and ocean are realized with direct flux exchange in a high frequency so the models could react to changes in the other component immediately.

3. Experimental Setup

In the present study, a regional COSMO-CLM (Rockel 2008), atmosphere model is coupled to the ocean model NEMO.

We use the EURO-CORDEX setup for COSMO-CLM (Giorgi 2006) which covers the whole of Europe, North Africa, the Atlantic Ocean and the Mediterranean Sea. It is coupled to NEMO-Nordic adapted to the North and Baltic Sea region as described in a technical report by Hordoir 2013. The flux correction for the ocean surface was not applied in our experiments. The coupling mechanism is handled by OASIS3. The coupled model is forced by the ERA-Interim reanalysis (Dee 2011), with a spin up from 1979 to 1984, and evaluation 1985 - 1994.

For the representation of the Mediterranean Sea, COSMO-CLM is coupled to NEMO-MED12 (Lebeaupin 2011)

with the help of OASIS3-MCT (Akhtar 2014). As a first evaluation of the system, we look at the sea surface temperature in the coupled versus the uncoupled system.

4. Results and Conclusion

For the North- and Baltic seas, the coupled run has large biases compared with the E-OBS reference data (Figure 1). However, these biases are in the usual range of biases found in other COSMO-CLM studies. Compared with observations, the coupled model in this study has, most of the time, smaller biases than the uncoupled atmospheric model.

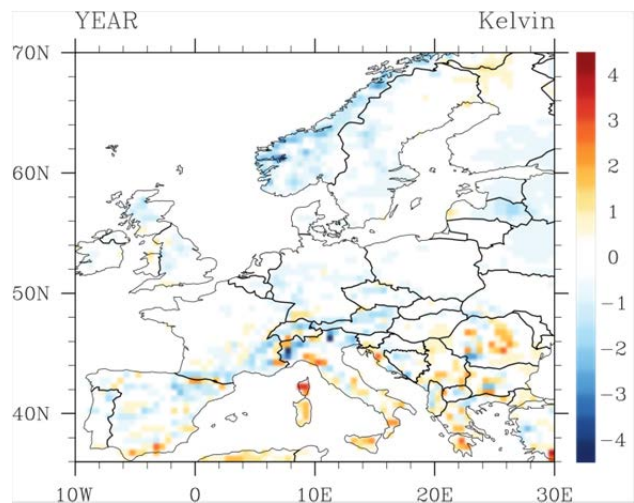


Figure 1. Yearly mean of the differences in 2-m temperature over land between the coupled run and E-OBS data, averaged over the period 1985-1994 ($T2MCOUP - T2ME-OBS$).

The spatial distribution of temperature biases in spring, summer and autumn (not shown here) resemble the yearly mean distribution; however, the bias magnitudes vary among those three seasons, with summer showing the largest warm bias among the three seasons, up to 3 K in southern Europe.

For the Mediterranean Sea, the coupled system produces here warmer SSTs in summer and in winter a slight reduction of temperature (Figure 2).

The results about the scaling analysis will be presented at the meeting.

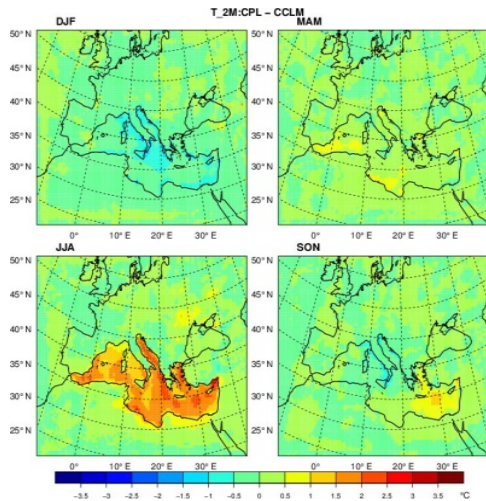


Figure 2. Seasonal mean of the differences in 2-m temperature between the coupled and uncoupled run, averaged over the period 1994-1999.

References

- Akhtar N., Ahrens B., and J. Brauch (2014), "Simulation of medicanes in a regional atmospheric model coupled with one dimensional ocean model", *Nat. Hazards Earth Syst. Sci.*, in revision.
- Dee, D.P. et al., (2011), "ERA-Interim reanalysis configuration and performance of the data assimilation system", *Quart. J. Roy. Met. Soc.* 137(656).
- Giorgi, F. (2006), "Climate change hot-spots", *Geophys.Res.Lett.* 33(8).
- Hordoir R., An B. W., Haapala J., Dieterich C., Schimanke S., Hoeglund A., and H.E.M. Meier, 2013, "A 3D Ocean Modelling Configuration for Baltic & North Sea Exchange Analysis", Report Oceanography No. 48, ISSN: 0283-1112, SMHI.
- Lebeaupin, B. C., Béranger, K., Deltel, C., and Drobinski, P. (2011), "The Mediterranean response to different space-time resolution atmospheric forcings using perpetual mode sensitivity simulations", *Ocean Model.*, 36, 1–25.
- Pham, Trang Van, Brauch, J., Dieterich, C., Frueh, B. and B. Ahrens (2014), "New coupled atmosphere-ocean-ice system COSMO-CLM/NEMO: assessing air temperature sensitivity over the North and Baltic Seas", *Oceano. Acta*, accepted.

Quasi-biennial oscillation effect on Baltic Sea region climate indicators: Lithuania's case

Arunas BUKANTIS¹, Vytautas AKSTINAS²

¹ Department of Hydrology and Climatology, Vilnius University, Lithuania (arunas.bukantis@gf.vu.lt)

² Lithuanian Energy Institute, Kaunas, Lithuania, (vytautas.akstinas@lei.lt)

1. Introduction

The quasi-biennial oscillation (QBO) of the winds in the equatorial stratosphere was detected in the 1950s due to the establishment of a global, regularly measuring radiosonde network. Analysing the data transmitted by radiosondes was found that equatorial stratosphere winds are characterised by periodically recurring easterly and westerly phases (Graystone 1959; Ebdon 1960; Reed *et al.* 1961). These air flows are generated 30 km (13 hPa) above sea level and descend through the stratosphere at 1 km month⁻¹. The wind direction is changing every 13–14 months simultaneously over the entire equatorial zone. The complete cycle of the oscillation embraces 26–29 months.

QBO may not only affect the equatorial atmospheric circulation but also the atmospheric circulation of higher latitudes and formation of long-lasting weather anomalies. Investigations of the influence of the easterly and westerly QBO phases on the precipitation amounts in different European regions showed a strong signal in the region of the British Isles, Central Europe and Belarus (Brazdil, Zolotokrylin 1995).

The possibility of the QBO influence on the Arctic Polar Vortex has been considered since long ago (Holton, Tan 1980). It has been determined that the Arctic Polar Vortex is weaker during the easterly QBO phase than during the westerly phase (Garfinkel *et al.* 2012; Watson, Gray 2014), furthermore, other authors have found that the Arctic Oscillation (AO) index in cold season (November–April) tends to positive values during the westerly QBO phase whereas negative AO values are dominant during the easterly QBO phase. In both cases, the pattern has been established for QBO at 30 hPa yet in warm season (May–October) in the Northern Hemisphere this link discontinues (Lu, Pandolfo 2011). In recent years, the aspects of QBO seasonal variations and their effects on the stratosphere chemistry have been increasingly investigated using digital climate models (Hurvitz *et al.* 2013; Krismer *et al.* 2013).

The last hundred years in the East Baltic countries was marked by many long-lasting droughts related to the strong anticyclonic circulation (Jaagus *et al.* 2010; Rimkus *et al.* 2013). It has been established that droughts in warm seasons can be generated by the Arctic and Azores anticyclones as well as the distribution of atmospheric activity centers and damping processes whereas precipitation anomalies of cold season may be predetermined by intensifying or damping of the westerly flow and other advective factors (Akstinas, Bukantis 2015; Bukantis, Bartkeviciene 2005; Trigo *et al.* 2008).

The effects of QBO on the climate indices in Baltic Sea region have been scantily investigated. The aim of this study was to analyse if there exists in Lithuania a relationship of precipitation anomalies and long-lasting periods without precipitation (PWP) with QBO and whether

the damping of the westerly transport and intensity of cyclonic processes in the Scandinavian–Baltic Sea region are affected by the QBO. The knowledge of the link between the precipitation amount anomalies and QBO would contribute to improvement of the methods for prediction of long-lasting precipitation anomalies (droughts or high rainfall spans).

2. Study area, data and methods

The QBO data were taken from the database of the Institute of Meteorology, Freie Universität Berlin (Freie Universität Berlin 2013). The data of the stratospheric winds (direction and velocity, m s⁻¹) for 1953–2009 are analysed.

The present study represents an analysis of mean monthly wind parameters in the 30 hPa isobaric surface where the oscillation amplitude of wind velocities is highest. For the relationship between the amount of precipitation and QBO, the monthly and daily precipitation data for 01 01 1953 to 30 12 2009 from three Lithuanian meteorological stations (Lazdijai, Vilnius and Šiauliai) were analysed. The chosen meteorological stations represent the greater part of Lithuania's territory and are located in different physical geographical regions (Fig. 1).

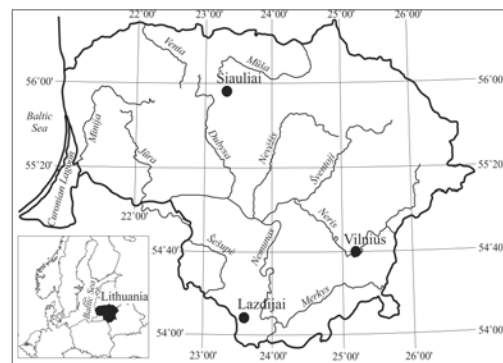


Figure 1. Locations of meteorological stations from which the amount of precipitation were used in the present study.

A time limit of 10 days was chosen for identification of periods without precipitation (PWP). This means that PWP is a time span of no less than 10 days without precipitation in at least two meteorological stations. The empirical PWP recurrence probability for respective QBO phases was calculated, i.e. the number of PWP during the westerly QBO phase was counted and then subtracted by the sum of westerly QBO months. The same principle was applied in calculating the probability of recurrence during the easterly phase. The deviation of precipitation from the mean value for the entire period is then calculated for

the both phases. In total, 20 easterly and westerly QBO events for each month were analysed. For evaluation of the statistical validity of conclusions, the Wilcoxon rank-sum test (WRST) was used.

The compositional maps of precipitation and sea level pressure during the westerly and easterly QBO phases were compiled using the interactive website *Monthly/Seasonal Climate Composites* based on the reanalysis data from NCEP and developed by NOAA Earth System Research Laboratory (NOAA, 2014).

3. Results

In the analysed time frame 1953–2009, the average recurrence of periods without precipitation (PWP) amounted to 2.46–2.92 events per year. Usually, the PWP lasted for 10–14 days (1.93–2.26 events per year on the average). The longer periods only occurred in some years.

Analysis of the relationship between the recurrence of PWP in Lithuania and QBO showed that higher recurrence of PWP was characteristic of the easterly QBO phase at 30 hPa and that namely during this phase, the events of PWP occurred even 4–5 times per year. The QBO at 50 hPa had no palpable effect on PWP in the territory of Lithuania.

The statistically valid (according to WRST) QBO effect on the precipitation amount in Lithuania was established in May, September and November. During the easterly QBO phase in cold season (November–March), the average amount of precipitation in Lithuania is by 15.5 mm (7.9%) lower, whereas during the westerly phase in warm season (April–October), it is by 19.4 mm (4.5%) lower than the climate normal.

During the different QBO phases at 30 hPa, the patterns of atmospheric circulation vary considerably: during the westerly QBO phase in May, the Baltic Sea region is predominated by the high-pressure area, damping the western transport of air masses, whereas during the easterly phase, it is predominated by the low-pressure area (Fig. 2). This is why during the westerly QBO phase in May, the negative precipitation anomalies occur not only in Lithuania but also in other parts of the Baltic Sea region and during the easterly phase the precipitation amount exceeds the long-term average.

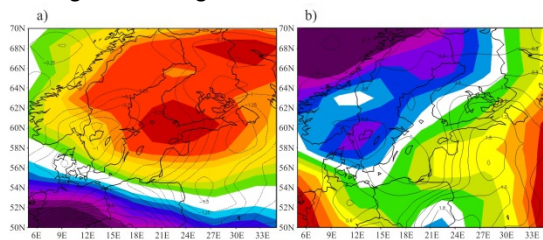


Figure 2. Sea level pressure (red/green – high pressure, purple/blue – low pressure) and precipitation anomalies (isolines mm/day) in May during the westerly (a) and easterly (b) quasi-biennial oscillation (QBO) phases.

In September and November, the low-pressure area in the territory under consideration expands during the westerly QBO phase and is responsible for the positive precipitation anomalies whereas during the easterly phase, the Baltic Sea regions finds itself in the northern part of the high-pressure area and is subject to the negative precipitation anomalies.

The analysed investigations stated that during the easterly QBO phase the AO index gets negative values. This coincides with the results of this research, where in

September and November during the easterly QBO phase over the Baltic Sea region high pressure field together with negative anomalies of precipitation was formed. This explains the higher rate and frequency of periods without precipitation (PWP) during the easterly QBO phase. Thus it can be assumed that the effect of QBO on the pressure and precipitation anomalies in Lithuania and the Baltic Sea Region reveals itself by interaction between QBO and AO.

References

- Akstinas V., Bukantis A. (2015) Quasi-biennial oscillation effect on climate indicators: Lithuania's case. *Baltica* 28 (1), pp. 19–28.
- Brazdil R., Zolotokrylin A. N. (1995) The QBO signal in monthly precipitation field over Europe. *Theoretical and Applied Climatology* 51 (1), pp. 3–12.
- Bukantis A., Bartkevičienė G. (2005) Thermal effects of the North Atlantic Oscillation on the cold period of the year in Lithuania. *Climate Research* 25 (3), pp. 221–228.
- Ebdon R. A. (1960). Notes on the wind flow at 50 mb in tropical and sub-tropical regions in January 1957 and January 1958. *Quarterly Journal of the Royal Meteorological Society* 86, 540–542.
- Freie Universität Berlin Meteorological Institute (2013) The Quasi-Biennial-Oscillation (QBO) Data Serie. Source: www.geo.fu-berlin.de/en/met/ag/strat/produkte/qbo/
- Garfinkel C. I., Shaw T. A., Hartmann D. L., Waugh D. W. (2012) Does the Holton-Tan mechanism explain how the quasi-biennial oscillation modulates the Arctic Polar vortex? *Journal of the Atmospheric Sciences* 69 (5), 1713–1733.
- Graystone P. (1959) Meteorological office discussion on tropical meteorology. *Meteorological Magazine* 88, pp. 117.
- Holton J. R., Tan H. C. (1980) The influence of the equatorial quasi-biennial oscillation on the global circulation at 50 mb. *Journal of the Atmospheric Science* 37, pp. 2200–2208.
- Hurwitz M. M., Oman L. D., Newman P. A., Song L. S. (2013) Net influence of an internally generated quasi-biennial oscillation on modelled stratospheric climate and chemistry. *Atmospheric Chemistry and Physics* 13 (5), pp. 12187–12197.
- Jaagus J., Briede A., Rimkus E., Remm K. (2010) Precipitation pattern in the Baltic countries under the influence of large-scale atmospheric circulation and local landscape factors. *International Journal of Climatology* 30 (5), pp. 705–720.
- Krismer T. R., Giorgetta M. A., Esch M. (2013) Seasonal aspects of the quasi-biennial oscillation in the Max Planck Institute Earth System Model and ERA-40. *Journal of Advances in Modeling Earth Systems* 5 (2), pp. 406–421.
- Lu B. W., Pandolfo L. (2011) Nonlinear relation of the Arctic oscillation with the quasi-biennial oscillation. *Climate Dynamics* 36 (8), pp. 1491–1504.
- NOAA Earth System Research Laboratory Physical Sciences Division (2014) Monthly/Seasonal Climate Composites. Source: <http://www.esrl.noaa.gov/psd/cgi-bin/data/composites/printpage.pl>
- Reed R. J., Campbell W. J., Rasmussen L. A., Rogers R. G. (1961) Evidence of a downward propagating annual wind reversal in the equatorial stratosphere. *Journal Geophysical Research* 66 (3), 813–818.
- Rimkus E., Stonevičius E., Korneev V., Kažys J., Valiuškevičius G., Pakhomau A., 2013. Dynamics of meteorological and hydrological droughts in the Neman river basin. *Environmental Research Letters* 8 (4), 5014, 10 pp.
- Trigo R. M., Valente M. A., Trigo I. F., Miranda P., Ramos A. M., Paredes D., Garcia-Herrera R. (2008) The impact of North Atlantic wind and cyclone trends and their impact in the European precipitation and Atlantic significant wave height. *Annals of the New York Academy of Sciences* 1146, pp. 212–234.
- Watson P. A. G., Gray L. J. (2014) How does the quasi-biennial oscillation affect the stratospheric polar vortex? *Journal of the Atmospheric Sciences* 71 (1), pp. 391–409.

Spatio-temporal characterization of Mediterranean extreme precipitation events: a multi-model assessment

Leone Cavicchia¹, Enrico Scoccimarro^{1,2}, Silvio Gualdi^{1,2}, Bodo Ahrens³, Ségolène Berthou⁴, Dario Conte¹, Alessandro Dell'Aquila⁵, Philippe Drobinski⁴, Vladimir Djurdjevic⁶, Clotilde Dubois⁷, Clemente Gallardo⁸, Antonella Sanna¹ and Csaba Torma⁹

¹ CMCC-Centro Euro-Mediterraneo sui Cambiamenti Climatici, Bologna, Italy (leone.cavicchia@cmcc.it)

² Istituto Nazionale di Geofisica e Vulcanologia (INGV), Bologna, Italy

³ Institute for Atmospheric and Environmental Sciences, Goethe University Frankfurt am Main, Germany

⁴ IPSL/Laboratoire de Meteorologie Dynamique, Ecole Polytechnique, ENS, UPMC, ENPC, CNRS, Palaiseau, France

⁵ ENEA Climate Modeling and Impacts, Rome, Italy

⁶ Institute of Meteorology, Faculty of Physics, University of Belgrade, Serbia

⁷ Météo France, Toulouse, France

⁸ Departamento de Ciencias Ambientales Universidad de Castilla-La Mancha, Toledo, Spain

⁹ Abdus Salam International Centre for Theoretical Physics, Trieste, Italy

1. Introduction

The Mediterranean region, due to the complex topography and land-ocean interactions, is known to be an area severely affected by extreme precipitation events (Scoccimarro et al. 2014). Exploiting the added value of the ensemble of high-resolution model simulations –including several ocean-atmosphere coupled regional model systems– provided by the Med-CORDEX coordinated initiative, an updated assessment of Mediterranean extreme precipitation events as represented in different observational, reanalysis and modelling datasets is presented. The aim of the present work is twofold. On one hand, an updated spatiotemporal characterisation of the long-term statistics of extreme precipitation events is provided in a multi-model approach. On the other hand, we aim to evaluate the respective impact of a number of model features on the models skill in reproducing the observed statistics of Mediterranean extreme precipitation events, including: a high resolution of the atmosphere, different physical parameterisations employed in atmospheric models, and the coupling with high resolution models of the Mediterranean Sea ocean circulation.

2. Data and methods

Modeling data used in the present study is provided by the simulations performed in the coordinated Med-CORDEX initiative (Ruti et al. 2015), the Mediterranean contribution to the regional climate downscaling project CORDEX. We use data from several different simulations performed with both atmosphere-only regional models and coupled atmosphere-ocean regional models at different resolutions. All the simulations are driven from the same lateral boundary conditions derived from the ERA-Interim reanalysis. For the uncoupled simulations, the bottom boundary condition (sea surface temperature) are also taken from ERA-Interim. The horizontal resolution of the atmospheric model of the analyzed simulations ranges between 50 km and 10 km. In addition to modeling data, the analysis of Mediterranean extreme precipitation events includes three reanalysis datasets (ERA-Interim, MERRA and JRA-55). The observational reference dataset is the ECA&D E-OBS gridded dataset.

The spatio-temporal characterisation of the long-term statistics of extreme precipitation is performed using a

number of different diagnostic indices, including the 99th percentile of daily precipitation (P99). Employing a novel approach based on the timing of extreme precipitation events (i.e. the maximum in the twelve months histogram of events exceeding the precipitation 99th percentile) a number of physically consistent subregions are defined.

The comparison of different diagnostics over the Mediterranean domain and physically homogeneous subdomains is presented and discussed, focussing on the relative impact of several model configuration features (resolution, coupling and physical parameterisations) on the performance in reproducing extreme precipitation events.

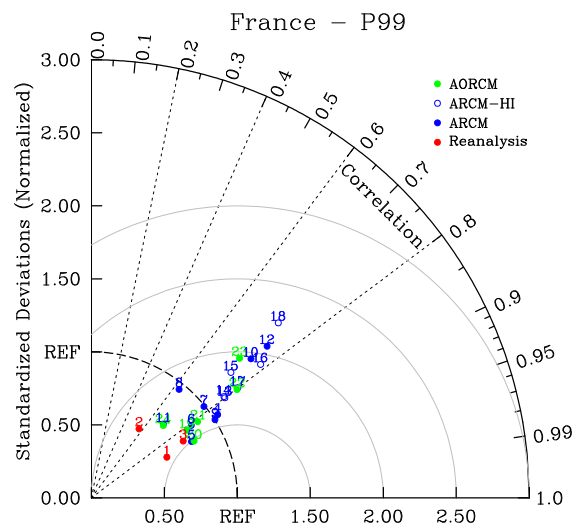


Figure 1. Taylor plots of 99th percentile of daily precipitation in different datasets, for the France sub-region. Red dots: reanalysis datasets; blue dots: atmosphere-only RCMs; blue circles: high resolution atmosphere-only RCMs; green dots: coupled ocean-atmosphere RCMs. Numerical labels identify different datasets. The label REF indicates the reference dataset (E-OBS).

3. Results

Considering the spatial correlation between modeled and observed extreme precipitation, a number of regions emerges, where most of the datasets

appear to be more skilled in reproducing the observed patterns: Iberia, France (as shown in Fig. 1), the great alpine region and Anatolia. The largest deviations from observations are found, on the other hand, in the eastern Balkans and north-west Africa regions. Moreover, within the same region, the different types of dataset analyzed (reanalysis, high/low resolution coupled/uncoupled models) exhibit generally a correlation with observations comparable to each other, independently on the overall performance in the specific region. On the other hand, focusing on spatial variability, reanalyses tend on average to show a smaller standard deviation compared to observations, while high-resolution models show standard deviation generally larger than observations. Finally, we find that, for models for which paired coupled/uncoupled runs are available, the two simulations produce generally values of both correlation and spatial variability very close to each other.

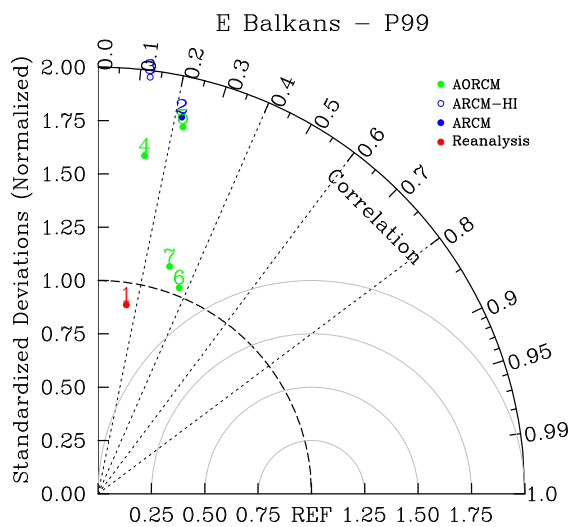


Figure 2. Taylor plots of 99th percentile of daily precipitation for different versions of the CMCC model, for the East Balkans sub-region. Red dots: ERA-Interim datasets; blue dot: atmosphere-only RCMs; blue circle: high resolution atmosphere-only RCMs; green dots: coupled ocean-atmosphere RCMs, with different physical parameterizations. The label REF indicates the reference dataset (E-OBS).

We find that the regions where extreme precipitation agrees better with the observations (Iberia, great alpine region, Anatolia, France) are the ones where large scale precipitation gives a significant contribution to extreme precipitation. Exploiting one particular model (the CMCC model, Cavicchia et al 2015), of which several realizations of the hindcast simulation are available, we focus on the areas where extreme precipitation is poorly represented. We find (see Fig. 2) that neither switching on the coupling nor increasing the horizontal resolution seems to improve the spatial correlation with respect to the driving ERA-Interim reanalysis. Changing the convective parameterization results instead in a larger impact on the increase of correlation, and on the reduction of mean error between modeled and observed extreme events.

4. Conclusions

The present analysis provides two main achievements. First, a novel approach for the subsetting of the domain

based on the timing of precipitation is provided. Such approach allows to divide the domain in several subregions by clustering areas characterised by coherent timing behaviours; the resulting areas are thus defined in a way that relies on the physical properties of precipitation rather than on merely geographical criteria, providing a more meaningful insight on the typical variability patterns of the considered diagnostics.

Furthermore, it was shown that increasing resolution and adding coupling has a mild impact on the long-term statistics of extreme precipitation. Changes of the convective parameterisation on the other hand, turn out to have a relatively larger impact on the correlation between modeled and observed extreme precipitation.

References

- Cavicchia L, Gualdi S, Sanna A, Oddo P (2015) The regional ocean-atmosphere coupled model COSMO-NEMO_MFS. CMCC Research Paper RP0254
- Ruti PM, Somot S, Giorgi F, Dubois C, Flaounas E, Obermann A, Dell'Aquila A, Pisacane G, Harzallah A, Lombardi E, Ahrens B, Akhtar N, Alias A, Arsouze T, Aznar R, Bastin S, Bartholy J, Béranger K, Beuvier J, Bouffies-Cloch e S, Brauch J, Cabos W, Calmanti S, Calvet J-C, Carillo A, Conte D, Coppola E, Djurdjevic V, Drobinski P, Elizalde-Arellano A, Gaertner M, Gal n P, Gallardo C, Gualdi S, Goncalves M, Jorba O, Jord  G, L'Heveder B, Lebeaupin-Brossier C, Li L, Liguori G, Lionello P, Maci s D, Nabat P, Onol B, Raikovic B, Ramage K, Sevault F, Sannino G, MV Struglia, Sanna A, Torma C, Vervatis V (2015) MED-CORDEX initiative for Mediterranean Climate studies, *BAMS*, in revision
- Scoccimarro E, Gualdi S, Bellucci A, Zampieri M, Navarra A (2014) Heavy precipitation events over the Euro-Mediterranean region in a warmer climate: results from CMIP5 models. *Regional Environmental Change* pp 1–8

Results from simulations with a coupled regional atmospheric-ocean-ice model over the Baltic Sea

Ole B. Christensen, Tian Tian and Fredrik Boberg

Danish Meteorological Institute, Copenhagen, Denmark (obc@dmi.dk)

1. Background

Sea surface fields in small ocean basins from global circulation models (GCMs) are often greatly biased, to a high extent due to the coarse resolution. A high-resolution coupled model system has been configured, comprising the HIRHAM5 atmospheric regional climate model (RCM) and the HBM regional ocean model for the North Sea and Baltic Sea regions. Here, we assess the bias in the air-sea interface in the Baltic Sea induced by the GCM boundary forcing in the uncoupled simulation, and improvements in sea surface temperatures and ice cover resulting from the coupling. Also, preliminary analyses of climate change calculations are presented, where this system has been driven with the EC-Earth GCM.

2. Validation

The first experiment is forced by ERA-Interim (ERA-I) reanalysis for the period 1990-2010. ERA-I overestimates the Baltic sea ice extent (Fig. 1) by about 72% in winter. The coupled run has resulted in a 33% lower value than the uncoupled one, showing better agreement in daily sea ice extent with observations. The second experiment is forced by EC-Earth CMIP5 climate simulations, with a focus on the historical period 1986-2005 for assessment. The EC-Earth forcing shows a significant warm bias in winter surface air temperature and hence very low sea ice cover. This bias results in an unrealistic amplitude of the seasonal cycle in surface air temperature and an underestimation of the sea ice cover in the uncoupled run. A large improvement is found in the coupled run. In both experiments, the coupled simulation tends to mitigate the effects of bias induced by the forcing.

The validation in the ERA-I driven experiment has been described in detail in Tian et al. (2013).

3. Climate Change

With lateral boundaries from EC-Earth, transient experiments have been performed in both coupled and uncoupled mode according to the standard RCP4.5 and RCP8.5 scenarios. Analyses of the effect of coupling on climate change signal will be presented.

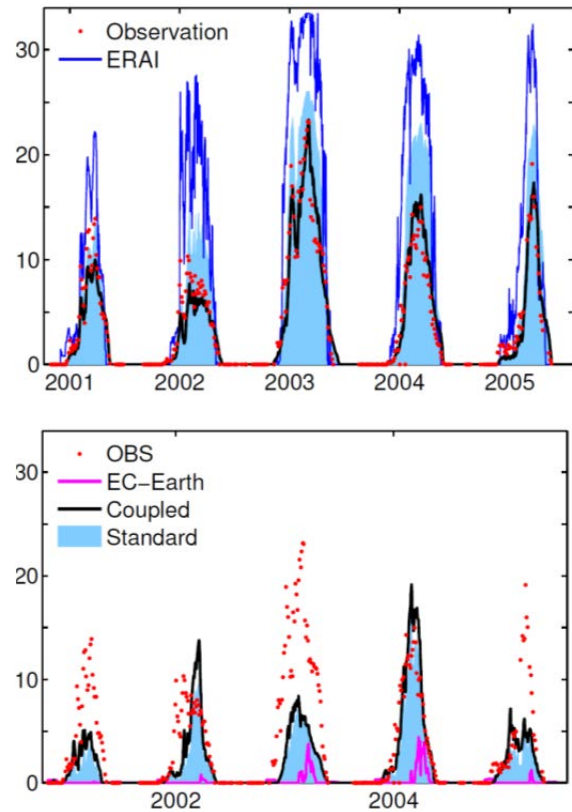


Figure 1. Time series of sea ice extent in the Baltic Sea from observation (dots) and from un-coupled (blue shading) and coupled (black lines) regional simulations. GCM results in blue (top panel, ERA-INTERIM) and red (bottom panel, EC-Earth), respectively.

References

Tian, T., F. Boberg, O. B. Christensen, J. H. Christensen, J. She and T. Vihma (2013) Resolved complex coastlines and land-sea contrasts in a high-resolution regional climate model: a comparative study using prescribed and modelled SSTs, *Tellus A*, **65**, 19951, doi:10.3402/tellusa.v65i0.19951

Evaluation of simulated decadal variability over the Euro-Mediterranean region from ENSEMBLES to Med-CORDEX

Alessandro Dell'Aquila¹, Annarita Mariotti²

¹ ENEA, Rome, Italy (alessandro.dellaquila@enea.it)

² NOAA MAPP/Climate Program Office, Silver Spring, MD USA

1. Introduction

The Med-Cordex simulations over the period 1970-2010 are here evaluated with regard to their capability to represent observed decadal variability over the Euro-Mediterranean region and improve upon previous generation simulations from the ENSEMBLES project in their various experimental set-ups. Such an evaluation is needed to inform the use of these simulations and also future model development.

2. Data & methodology

We analyze the Med-Cordex evaluation runs available from the data portal www.medcordex.eu with the atmospheric component of the models defined over a limited domain and driven at the boundary of the domain by the global ERA-Interim reanalyses (Dee et al 2011). As benchmark for model improvement, we also consider evaluation stand-alone atmospheric runs from the ENSEMBLES project (<http://ensemblesrt3.dmi.dk/>). In this case, runs are for the period 1961-2000 at 25 km. As the main goal of this work is to analyze Med-Cordex evaluation runs in terms of their capability to reproduce the time scales longer than the simple year-by-year variability, we always apply a running mean of 5 years (+/- 2 years centered) to each field here presented over the 1979-2011 period with the intent to inform applicability even in the context of projections. For each dataset we consider the anomalies of each field with respect to the corresponding long term mean

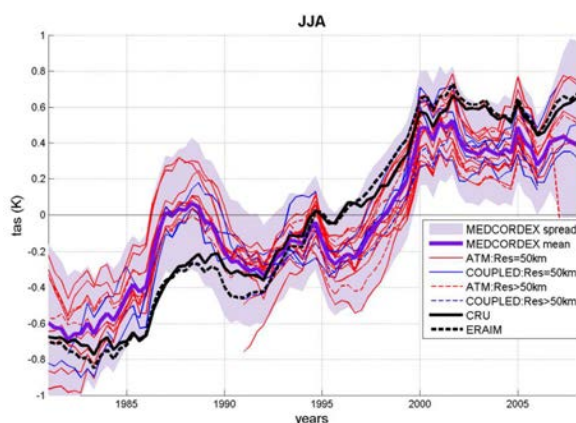


Figure 1. Observed and MEDCORDEX simulated long term climate anomalies in the Mediterranean region (LON: 10W- 40E; LAT: 30N- 48N) over the period 1979-2010. We show the surface air temperature T_a anomalies (T_a , land-only; K); based on CRU ,ERAIM and MEDCORDEX-ERAIM simulations for different seasons. The tick purple line is for the Med-Cordex multi-model ensemble mean, and the grey shaded areas stand for the multi-model spread (+/- 1 standard deviation). The color codes are reported in the legend.

3. Main outcomes for air surface temperature

Probably the most notable feature generally reported when discussing future predictions/projections for a given region is the increase in surface air temperature. Hence, we consider in Fig.1 the ability of the RCMs to reproduce the observed surface air temperature decadal variability and trend when forced by reanalyses. While all Med-Cordex models generally capture the relatively warmer and colder periods (with some relevant exceptions), the amplitude of the simulated anomalies shows errors compared to both CRU and ERA-Interim that are up to 0.5 K; this is true for all seasons considered. In particular, a simulated warm bias with respect to CRU and ERA-Interim is present in the Med-Cordex runs in the late 80s ,especially during MAM (not shown) and JJA, followed by anomalies that are less than observed in the last part of the simulations, since 1995. This leads to Med-Cordex simulated temperature trends that are generally weaker than observed. In general, if one considers the different type of Med-Cordex systems, no clear stratification appears. In fact, it is quite remarkable that in certain periods the amplitude of the anomalies is poorly represented by all the systems (e.g. the period 1985-1990 for MAM and JJA temperatures seems particularly problematic).

Fig.2 provides a comparison of the new Med-Cordex evaluation dataset against the older ENSEMBLES simulations, considered as a benchmark for improvement, over the common 1979-2000 period over the Mediterranean box. In this case, for each dataset only the ensemble mean and the +/- 1 multi model spread (i.e. +/- 1 standard deviation) around the mean are reported rather than individual simulations together with the respective reanalyses drivers (ERA-40 in the case of ENSEMBLES) and CRU observations. A side product of this comparison is to inform on what additional information one could extract from two different datasets of ensemble RCMs runs available for the Euro-Mediterranean region. Overall, the behavior of the Med-Cordex and ENSEMBLES simulations, in the terms of the characteristics described above are very similar. However, during the late 80s Med-Cordex shows warmer features than ENSEMBLES did especially for MAM (not shown) and JJA, while in the same seasons since 1990s Med-Cordex shows colder features. Generally, a smaller spread is displayed by the MedCORDEX runs than the ENSEMBLES dataset even if number of Med-Cordex runs here considered is slightly higher (i.e. 20 runs against 15). Med-CORDEX is overall farther from its ERA-Interim global driver than ENSEMBLES was with respect its ERA40 global driver

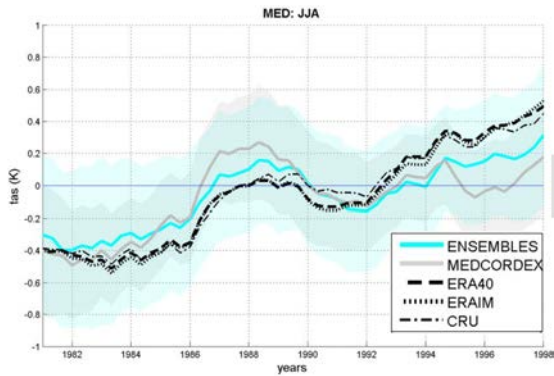


Figure 2 Observed and simulated long term climate anomalies in the Mediterranean region (black box in Fig.1) over the period 1979–2000. We show the surface air temperature T_a anomalies (T_a , land-only; K); based on CRU, ERA40, ERAIM, MEDCORDEX-ERAIM and ENSEMBLES-ERA40 multi-model simulations (we report the multi-model mean ± 1 standard deviation) for JJA period.

4. Conclusions

In this paper we have provided an estimate of the skills of Medcordex regional climate simulations in terms of their capability in reproducing the observed long term changes of some of the most common variables in the impact studies such as surface temperature and precipitation. We are focused onto the Euro-Mediterranean region, recently defined as one of the most vulnerable areas to global climate change (Giorgi 2006). The Medcordex initiative (Ruti et al 2015) tries to respond to the needs of new and reliable climate information for the euro-mediterranean region.

The Med-Cordex simulations are characterized by quite different configuration (atmospheric stand-alone vs ocean atmosphere coupled configurations, wide range of different horizontal resolution between 50 and 12 km, ...). However, no clear stratification can be pointed out: the representation of variability at the selected time scale seems to be not affected by coupling or by the different resolution. The Med-Cordex simulations tend to underestimate the observed trend in air surface temperature, mostly in the summer season, even if the large scale driver at BC (namely, Era-Interim) can be considered as optimal and, inside the domain, reproduces quite closely the observations.

On the other hand, good skills of the ensembles means of Med-Cordex runs in representing the time series of precipitation averaged over the mediterranean box can be figured out (here not shown)

As expected, the greatest discrepancies against the observations occur over JJA when the large scale forcing from Atlantic domain is generally weaker and the local processes can be more relevant in determining the overall tendencies. All the systems experience some problems in representing certain periods: for instance, in the second part of 80s, the the surface air temperature long term climate anomalies for MAM/JJA averaged over the Mediterranean region are generally poorly represented.

Overall, this evaluation suggests limited improvement in Med-Cordex simulations compared to ENSEMBLES with persisting problems likely related to the representation of surface processes that could also affect the viability of future projections (e.g. the estimation of temperature trends).

References

- Dee, D. P., et al. (2011), The ERA-Interim reanalysis: Configuration and performance of the data assimilation system, *Q. J. R. Meteorolog. Soc.*, 137, 553–597.
- Giorgi, F., (2006). Climate change hot-spots. *Geophys. Res. Lett.*, 33:L08707, doi:10.1029/2006GL025734
- Ruti PM and coauthors (2015). Med-CORDEX initiative for Mediterranean Climate studies. Submitted to *Bull. Amer. Meteor. Soc.*

Surface Heat Budget over the North Sea in Climate Change Simulations

Dieterich, C.¹, S. Wang¹, S. Schimanke¹, M. Gröger¹, B. Klein², R. Hordoir¹, P. Samuelsson¹, Y. Liu¹, L. Axell¹, A. Höglund¹, H.E.M. Meier^{1,3}

¹ Swedish Meteorological and Hydrological Institute, Norrköping, Sweden (christian.dieterich@smhi.se)

² Federal Maritime and Hydrographic Agency, Hamburg, Germany

³ Department of Meteorology, Stockholm University, Stockholm, Sweden

1. Introduction

Global and regional scenario simulations show a warming of 2 to 4 C for the North Sea and Baltic Sea region during the 21st century. The increasing temperatures and potential changes in heat, momentum and freshwater fluxes have not been studied with respect to their interaction with regional atmosphere-ocean feedbacks. Global models do not resolve important aspects of regional characteristics and ensembles with regional models have been run with either atmosphere or ocean standalone models. By means of an ensemble of scenario simulations with the coupled regional climate model RCA4-NEMO (Wang et al., 2015) we study the interaction between atmosphere and ocean over the North Sea and how the changing climate affects regional processes and balances.

2. Method

An ensemble of RCP scenarios has been conducted with the SMHI coupled regional climate model RCA4-NEMO. The ensemble consists of dynamically downscaled solutions of five different GCMs and two different RCP scenarios. Certain aspects of the regional solutions are robust features and do not depend on the details of the GCMs or RCPs that are downscaled. This points to regional processes and atmosphere-ocean interaction that are represented in the RCM only, not in the GCMs.

A validation of the ERA40 hindcast of the RCM against gridded datasets (Andersson et al., 2010, Loewe, 1996, Karlsson et al., 2012, Da Silva et al., 1996, Bersch et al., 2013, Sadikni et al., 2013, Berx and Hughes, 2009) shows that the solution of the RCM is in good agreement with observations. Moreover, the control periods of the scenario simulations turn out to exhibit the right annual mean, interannual and seasonal variability with a 95% confidence level.

3. Results

During the 21st century an anomalous pattern of low atmosphere-ocean temperature difference and latent heat loss develops (Figure 1) over the western central North Sea that points to changes in the atmosphere-ocean dynamics of the North Sea. The amplitude of the heat flux signal is of the order of the radiative forcing caused by a CO₂ doubling (4 W/m²). The increased latent heat loss is due to an atmosphere which becomes drier over the western central North Sea. The specific humidity does increase but the 2m temperature increases more rapidly which leads to an increasing dew-point temperature. The decreasing relative humidity allows for extra evaporation and latent heat loss over the North Sea towards the end of the century. The shifting heat loss pattern over the North Sea is in agreement with the analytical model of (Prandle and Lane, 1995) to explain the annual temperature cycle of the North Sea.

4. Acknowledgments

This study was funded by the Swedish Research Council for Environment, Agricultural Sciences and Spatial Planning (FORMAS) within the project "Impact of changing climate on

circulation and biogeochemical cycles of the integrated North Sea and Baltic Sea system" (Grant no. 214-2010-1575). The scenario simulations used in this study have been conducted in the framework of "Impacts of Climate Change on Waterways and Navigation" KLIWAS program. KLIWAS is funded by the Federal Ministry of Transport, Building and Urban Development (BMVBS).

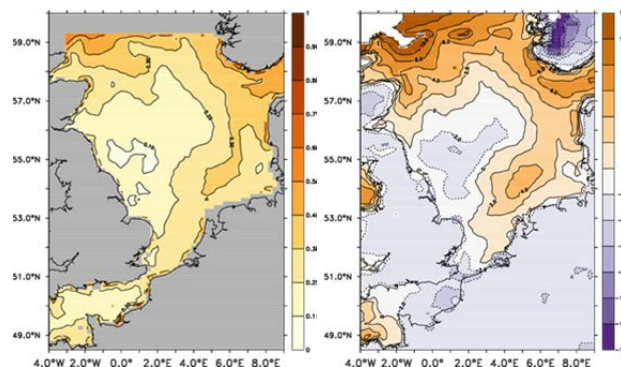


Figure 1. Left: Changes in the ensemble mean atmosphere-ocean temperature difference [C] between the far future (2070-2099) and the recent past (1970-1999). Right: Changes in the ensemble mean non-radiative (sensible plus latent) heat flux [W/m²] between the far future and the recent past.

References

- Wang, S., C. Dieterich, R. Döscher, A. Höglund, R. Hordoir, H.E.M. Meier, P. Samuelsson and S. Schimanke, 2015: Development and evaluation of a new regional coupled atmosphere-ocean model in the North Sea and the Baltic Sea, *Tellus A*, 67, 24284, doi:10.3402/tellusa.v67.24284
- Andersson, A., K. Fennig, C. Klepp, S. Bakan, H. Grassl and J. Schulz, 2010: The Hamburg Ocean Atmosphere Parameters and Fluxes from Satellite Data - HOAPS-3, *Earth Syst. Sci. Data*, 2, 215-234
- Loewe, P. 1996: Surface temperatures of the North Sea in 1996, *Ocean Dynamics*, 48, 175–184
- Karlsson K.-G., A. Riihelä, R. Müller, J.F. Meirink, J. Sedlar, M. Stengel, M. Lockhoff, J. Trentmann, F. Kaspar, R. Hollmann and E. Wolters, 2012: CLARA-A1: The CM SAF cloud and radiation dataset from 28 years of global AVHRR data, *Atmospheric Chemistry and Physics Discussions*, 13, 935–982
- Da Silva, A., C. Young–Molling and S. Levitus, 1996: Revised surface marine fluxes over the global oceans: the UWM/COADS data set, *WCRP Workshop on Air–Sea Flux Fields for Forcing Ocean Models and Validating GCMS*, 762, 13–18
- Bersch, M., V. Gouretski and R. Sadikni, 2013: Hydrographic climatology of the North Sea and surrounding regions, *Centre for Earth System Research and Sustainability (CEN)*, University of Hamburg
- Sadikni R., M. Bersch and A. Jahnke-Bornemann, 2013: Meteorological Climatology of the North Sea and Surrounding Regions, *Centre for Earth System Research and Sustainability (CEN)*, University of Hamburg
- Berx, B. and S.L. Hughes, 2009: Climatology of Surface and Near-bed Temperature and Salinity on the North-West European Continental Shelf for 1971-2000, *Continental Shelf Research*, 29, 2286–2292
- Prandle, D. and A. Lane, 1995: The annual temperature cycle in shelf seas, *Continental Shelf Research*, 1995, 16, 2, 681–704

High-resolution downscaling of ERA40 for region of South East Europe with NMMB model

Vladimir Djurdjevic^{1,3}, Aleksandra Krzic^{2,3}

¹ Institute of Meteorology, Faculty of Physics, University of Belgrade, Serbia (vdj@ff.bg.ac.rs)

² Republic Hydrometeorological Service of Serbia, Belgrade, Serbia

³ South East European Virtual Climate Change Center, Belgrade, Serbia

1. Introduction

Dynamical downscaling is widely accepted approach in climate research (Giorgi 2006). Specifically, reanalysis downscaling has become common practice to verify regional model performance with “perfect” boundary conditions against observed climate over area of interest. On the other side, in recent years horizontal resolution of regional climate models (RCM) approached nonhydrostatic scales (Heikkila et al. 2010, Jacob et al., 2013). The need for these high-resolution runs is mainly driven by the idea of a better representation of the small-scale process, such as convective, which can be crucial for better representation of local climate characteristics. Here we present results of downscaling of ERA40 reanalysis (Uppala et al. 2005) with NMMB model (Janjic and Gall, 2012) for the period 1971-2000 over the region of South East Europe on two horizontal resolutions, 14 and 8 km. Special attention will be given to summer precipitation verification and their dependence on a model resolution.

2. Model

In recent years, the unified Non-hydrostatic Multi-scale Model (NMMB) developed at NCEP (Janjic, 2005; Janjic et al., 2011), has been used for a number of operational and research applications in Republic Hydrometeorological Service of Serbia (Djurdjevic et al., 2013). The NMMB can be run as a global and as a regional model. The main characteristics of the model dynamical core are that horizontal differencing conserves a variety of basic and derived quantities. Model also includes the novel implementation of the nonhydrostatic dynamics (Janjic et al., 2001). For grid-scale convection parameterization Betts-Miller-Janjic scheme (BMJ) is implemented and for turbulence, model use Mellor-Yamada-Janjic (MYJ) closure approach. For radiation user can choose between two radiation schemes, Rapid Radiative Transfer Model (RRTM) and Geophysical Fluid Dynamics Laboratory (GFDL) radiation model. Also two land surface packages are available, NOAH land surface model and Land Ice Seas Surface model (LISS) (Vukovic et al., 2010).

3. Experiment setup and verification data set

Downscaling runs are done for the period 1971-2000 on two horizontal resolutions of 14 (low) and 8 km (high). Domain for low resolution run covers majority of South East Europe (SEE) region while high resolution simulation is done on the smaller domain covering northern and central part of SEE.

Model performance is verified using standard verification scores for daily and monthly mean temperature and daily and monthly precipitation, over territory of Serbia. For score calculation data from 46 stations of

national observational network was used. Also, model verification results are compared with same scores calculated for gridded observation data set EOBS (Haylock et al., 2008) and ERA40 reanalysis.

4. Results

Four scores for daily and monthly mean surface air temperature from 14 and 8 km model runs and from ERA40 and EOBS datasets, are given in Table 1. The largest bias in both cases is for the EOBS data, while according to MAE and RMSE EOBS has the lowest error. Comparing the NMMB results, better results are obtained with high-resolution run. All four datasets have high correlation coefficient (> 0.95).

Table 1. Average scores of daily and monthly mean temperature.

	Data set	BIAS	MAE	RMSE	CC
Daily	ERA40	-0.07	1.5	1.9	0.98
	EOBS	-0.62	1.0	1.2	0.99
	NMMB 14km	-0.04	2.0	2.6	0.96
	NMMB 8km	0.06	1.7	2.2	0.98
Month.	ERA40	-0.07	0.87	1.0	1.0
	EOBS	-0.62	0.79	0.86	1.0
	NMMB 14km	-0.04	1.14	1.36	0.99
	NMMB 8km	0.06	1.0	1.2	0.99

For further analysis on model results we calculated two verification scores, bias and correlation coefficient for daily and monthly precipitation. In Table 2 NMMB scores are presented, together with scores for ERA40 and EOBS data.

Table 1. Average scores of daily and monthly precipitation.

	Data set	BIAS (mm)	BIAS (%)	CC
Daily	ERA40	-0.46	-23.2	0.53
	EOBS	-0.12	-5.1	0.85
	NMMB 14km	-0.18	-9.4	0.40
	NMMB 8km	-0.08	-4.6	0.53
Month.	ERA40	-14.0	-23.2	0.82
	EOBS	-3.5	-5.1	0.98
	NMMB 14km	-5.6	-9.4	0.81
	NMMB 8km	-2.5	-4.6	0.86

Bias score is presented as a mean difference between corresponding data set and observation, averaged over period of 30 years, but also as a ratio of this difference and long term mean of corresponding observation and is presented in percent. As we can see for daily precipitation lowest bias of 0.08 mm/day has high resolution NMMB integration followed by EOBS and 14 km NMMB run. Strongest negative bias is found for ERA40 data set, which is not surprising since reanalysis

data have lowest resolution. Highest correlation coefficient is for EObs data, 0.85. Correlation coefficients for NMMB are 0.53 and 0.4 for 8 km and 14 km runs respectively and 0.53 for ERA40 data. For monthly accumulations correlation coefficients for NMMB runs are significantly higher and high-resolution integration has higher correlation coefficient than reanalysis data set.

In Figure 1 area averaged mean annual cycle of daily precipitation is presented.

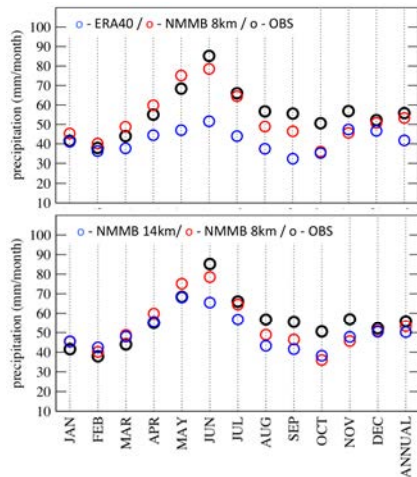


Figure 1. Area averaged annual cycle of precipitation together with annual mean. Symbols for different data sets are indicated on figure.

As we can see ERA40 data has negative bias mainly during period from April to November (upper panel) and it's probably related to pure representation of convective systems, dominantly present during the warmer part of the year. Contrary to this, high-resolution NMMB is capable to better represent small-scale convective processes giving much less biased result especially for period from April to September. Also, comparing two NMMB integrations (lower panel) negative precipitation bias is evident in low-resolution run for summer months when convective processes and related high daily precipitation accumulations strongly contributed to monthly totals in Serbia (Tosic and Unkasevic, 2013).

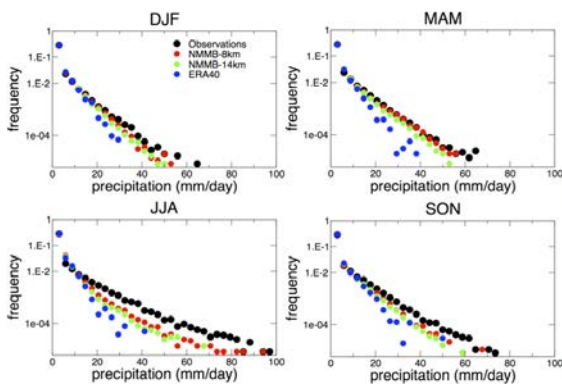


Figure 2. Daily precipitation distributions. Observations (black), NMMB-8km (red), NMMB-14km (green) and ERA40 (blue)

To put more details on precipitation, distributions of daily precipitation are presented in Figure 2. Distributions are calculated for seasons: December-January-February

(DJF), March-April-May (MAM), June-July-August (JJA) and September-October-November (SON). From figures it is evident that ERA40 data set follow observed distributions only for daily accumulation up to 10 mm/day and especially large discrepancies are for accumulations above 20 mm/day. Both results from NMMB downscaling show much better agreement to observations in all seasons. Largest difference between 8 km and 14 km run is for summer months.

5. Conclusions

Presented results shows that higher resolution improved model performance, especially in reduction of negative precipitation bias during summer months. Analysis of daily precipitation distributions revealed that reason for this is probably better representation of summer convection and related episodes with high daily precipitation accumulations.

Acknowledgement

This study was co-funded by the South East Europe Transnational Cooperation Programme – ORIENTGATE project (www.orientgateproject.org). We also acknowledge the support from project III43007 financed by the MEST of the Republic of Serbia.

References

- Djordjevic V. et al. (2013) NCEP's multi-scale NMMB model in the Hydrometeorological Service of Serbia: experiences and recent model developments, EGU General Assembly, Geophysical Research Abstracts, Vol. 15, EGU2013-8217, 2-7 April 2013, Vienna.
- Giorgi, F. (2006) Regional climate modeling: Status and perspectives. *Phys.*, 139,101-118, doi:10.1051/jp4:2006139008
- Haylock, M.R. et al. (2008) A European daily high-resolution gridded dataset of surface temperature and precipitation. *J. Geophys. Res (Atmospheres)*, 113, D20119, doi:10.1029/2008JD10201
- Heikkila U, Sandvik A, Sorterberg A (2010) Dynamical downscaling or ERA-40 in complex terrain using WRF regional Climate model. *Clim Dyn.* doi:10.1007/s00382-010-0928-6.
- Jacob, D. et al. (2013) EURO-CORDEX: new high-resolution climate change projections for European impact research *Regional Environmental Change*, 1-16
- Janjic Z. I., Gerrity J. P. Jr, Nickovic S. (2001) An alternative approach to nonhydrostatic modeling. *Mon. Wea. Rev.* 129: 1164–1178
- Janjic, Z. I. (2005) A unified model approach from meso to global scales, *Geophys. Res. Abstr.*, 7, SRef-ID: 1607-7962/gra/EGU05-A-05582.
- Janjic, Z., Janjic, T., and Vasic, R. (2011) A Class of conservative fourth order advection schemes and impact of enhanced formal accuracy on extended range forecasts, *Mon. Weather Rev.*, 0, null, doi:10.1175/2010MWR3448.1.
- Janjic, Z., and R.L. Gall (2012) Scientific documentation of the NCEP nonhydrostatic multiscale model on the B grid (NMMB). Part 1 Dynamics. NCAR Technical Note NCAR/TN-489+STR, DOI: 10.5065/D6WH2MZX.
- Tosic, I. and Unkasevic, M. (2013) Extreme daily precipitation in Belgrade and their links with the prevailing directions of the air trajectories, *Theor. Appl. Climatol.* 111. 1-2, 97-107.
- Uppala S. M. et al. (2005) The ERA-40 re-analysis. *Q J R Meteorol Soc* 131:2961–3012.
- Vukovic A., Rajkovic B., Janjic Z.: Land Ice Sea Surface Model: Short Description and Verification, 5th International Congress on Environmental Modelling and Software, 5-8 July 2010, Ottawa, Ontario, Canada.

Temperature-precipitation extremes relationship in the Mediterranean: past climate assessment and projection in anthropogenic scenarios

P. Drobinski¹, N. Da Silva¹, G. Panthou², S. Bastin³, C. Muller⁴, B. Ahrens⁵, M. Borga⁶, D. Conte⁷, G. Fossier⁸, F. Giorgi⁹, I. Güttler¹⁰, V. Kotroni¹¹, L. Li¹, E. Morin¹², B. Onol¹³, P. Quintana-Segui¹⁴, R. Romera¹⁵, Torma Csaba Zsolt¹⁶

¹ IPSL/LMD, Palaiseau and Paris, France (philippe.drobinski@lmd.polytechnique.fr), ² IPSL/LSCCE, Gif sur Yvette, France
³ IPSL/LATMOS, Guyancourt, France, ⁴ LADHYX, Palaiseau, France, ⁵ IAU, Goethe-University Frankfurt, Frankfurt, Germany
⁶ University of Padova, Legnaro, Italy, ⁷ CMCC, Lecce, Italy, ⁸ Meteo-France/CNRM, Toulouse, France, ⁹ ICTP, Trieste, Italy
¹⁰ DHMZ, Zagreb, Croatia, ¹¹ NOAA, Athens, Greece, ¹² Hebrew University of Jerusalem, Jerusalem, Israel, ¹³ Istanbul Technical University, Istanbul, Turkey, ¹⁴ Ebro Observatory, Roquetes, Tarragona, Spain, ¹⁵ Environmental Sciences Institute, University of Castilla-La Mancha, Toledo, Spain

1. Introduction

Expected changes to future extreme precipitation remain a key uncertainty associated with anthropogenic climate change. Extreme precipitation has been proposed to scale with the precipitable water content in the atmosphere. Assuming constant relative humidity, this implies an increase of precipitation extremes at a rate of $\sim 7\%/^{\circ}\text{C}$ as indicated by the Clausius-Clapeyron relationship.

This study focuses on the relationship between precipitation extremes and temperature throughout the Mediterranean region, based on quality controlled measurements of surface temperature and precipitation at various weather stations around the Mediterranean, fine scale gridded reanalysis and simulations performed within the context of the HyMeX (Drobinski et al. 2014) and MED-CORDEX programs (Ruti et al. 2015). Our main objective is to investigate the temporal and spatial variability of this relationship and more precisely, to address the following questions:

- What is the spatial variability of the temperature-precipitation extremes relationship around the Mediterranean basin characterized by coastal areas, plains and high mountain ranges, and under the influence of arid and mid-latitude climates?
- What is the uncertainty associated with the simulated temperature-precipitation extremes relationship?
- What are the possible skill changes at high resolution relative to low resolution and the possible effects of ocean-atmosphere feedbacks on the simulation of the temperature-precipitation extremes relationship?
- What is the evolution of the temperature-precipitation extremes relationship in a context of global change?

2. Methodology

We follow the method proposed by Hardwick Jones et al. (2010) and used in Drobinski et al. (2015) and apply it to time series of temperature and precipitation from three different sources: (i) in-situ measurements from surface weather stations across the Mediterranean basin, (ii) E-OBS gridded data products and (iii) regional climate simulations. For the downscaling of ERA-Interim reanalyses, 14 simulations were produced from eight models. Five simulations were carried out with resolution higher than 50 km, and nine with low resolution (50 km). Among these two sets, four simulations were made with the same model and similar setups at high and low resolutions. Among the 14

simulations, 11 were run in atmosphere-only mode, and three runs include an interactive ocean model.

3. Simulation assessment in the present climate

Figure 1 shows the daily precipitation 99th percentile as a function of daily mean temperature at the surface weather stations in Croatia, France, Israel, Italy, Spain and Greece and from the HyMeX/MED-CORDEX simulations at the nearest grid point. The temperature-precipitation extreme curves display a hook shape across the Mediterranean, with negative slope at high temperatures and a slope following Clausius-Clapeyron (CC)-scaling at low temperatures. The temperature at which the slope of the temperature-precipitation extreme relation sharply changes (or temperature break), ranges from about 20°C in the western Mediterranean to less than 10°C in Greece. It is no longer detectable in Israel where the slope is always negative. The models display a very similar relationship, with an accurate representation of the slopes and temperature breaks, despite a systematic underestimation of the precipitation extremes. The GUF-CCLM4-8-18-MED44 simulation is the closest to the observed amount of precipitation extreme (as measured by the 99th percentile) while the CNRM-ALADIN52-MED44 simulation always produces much lower extremes than observed. Besides the averaging effect, sub-CC scaling may also be attributed, to aridity which may limit the rainfall amount as suggested by Hardwick Jones et al. (2010) for Central Australia stations. In the northwestern Mediterranean, Drobinski et al. (2015) also attribute the sub-CC scaling to the arid environment with three consequences. First, the 2-m temperature is no longer a proxy of the temperature of the condensed parcel, as precipitation is produced at much higher altitudes due to enhanced convection. The surface temperature is thus much higher than the temperature of the condensed parcel. Second, the relatively dry air surrounding the precipitating system reduces the precipitation efficiency which thus reduces the slope of the temperature-precipitation extremes relationship. Third, the entrainment of relatively dry unsaturated environment air dilutes the rising saturated air parcels and causes evaporative cooling, which in turn reduces the buoyancy of the convective parcel and the vertical transport of humidity. These processes reduce the slope of the temperature-precipitation extremes relationship and cause the reduction in temperature break as conditions become drier from Spain to Israel along the coast. The

temperature-precipitation extreme curves in Italy and Israel display a negative slope above about 10°C, which is fairly well reproduced by all simulations except CMCC-CCLM4-8-19-MED44. However, contrary to Israel, the slope of the precipitation extreme - temperature curves in Italy are sensitive to time sampling as CC-scaling is found for hourly precipitation extremes.

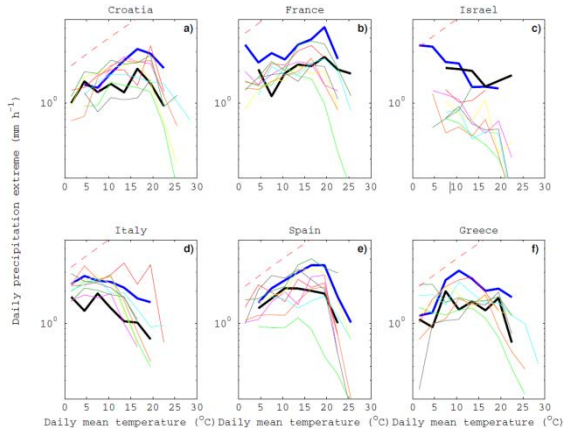


Fig. 1: Daily precipitation extremes (99th percentile) versus daily averaged temperature at the weather stations in Split in Croatia (a), coastal plain in France (b), in Jerusalem in Israel (c), in Telve in Italy (d), in Roquetes in Spain (e) and in Alexandroupoli in Greece (f) from the in-situ data (thick blue line), the E-OBS data at the nearest grid point (thick black line) and from HyMeX/MED-CORDEX simulations at 0.44 resolution (CNRM-ALADIN52-MED44: green; CMCC-CCLM4-8-19-MED44: red; ICTP-RegCM4-3-MED44: orange; ITU-RegCM4-3-MED44: magenta; IPSL-WRF311-MED44: cyan; GUF-CCLM4-8-18-MED44: dark green; UCLM-PROMES-MED44: grey; LMD-LMDZ4NEMOMED8-MED44: yellow) at the nearest grid point. The dashed red line indicate the CC-slope using the August-Roche-Magnus approximation for saturated vapor pressure.

4. Projections in the future climate

Figure 2 shows the daily precipitation extremes as a function of the daily mean temperature at the 6 weather stations and for the GCM-driven HyMeX/MEDCORDEX simulations for the historical period (1979-2005) and the future period 2070-2100. The most striking changes are (i) an increase of the temperature break by about 4-5°C and therefore a broader temperature range over which the slope is close to the CC-scaling; (ii) a still negative but slightly less steep slope at high temperatures. Figure 2 also shows that in the future period at high temperatures (i.e. higher than the temperature break in historical climate), the intensity of the precipitation extremes increases while it remains unchanged at low temperatures, where the slope matches the CC-scaling in the historical period. Such evolution of the temperature-precipitation extreme relationship shows evidence that this relationship cannot be used as a predictor, as instead suggested by Allen and Ingram (2002). The temperature-precipitation extreme curves obtained from the historical simulations corrected assuming the CC-scaling with respect to the temperature change are shown in Fig. 2. They are compared to the projected curve from the RCP8.5 simulations. The results show that the corrected curves match fairly well the projected curves suggesting that despite a negative slope of the temperature-precipitation extremes relationship at high temperatures, the CC law seems to apply in a warming regional climate.

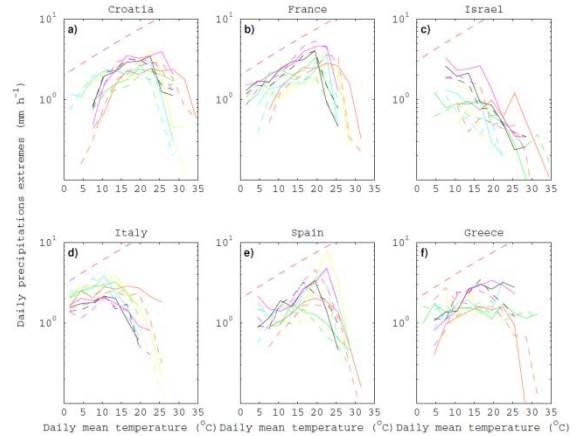


Fig. 2: Daily precipitation extremes (99th percentile) versus daily averaged future temperature at nearest grid point from the weather stations from the HyMeX/MED-CORDEX simulations at 0.44° resolution (CNRM-ALADIN52-MED44: green; ITU-RegCM4BATS-3-MED44: black; ITU-RegCM4CLM-3-MED44: magenta; ICTP-RegCM4-3/MED44 : orange; LMD-LMDZ4NEMO8-MED44-RCP8.5 : yellow) driven by the CMIP5 historical simulations and RCP8.5 scenarios. The solid lines are predictions of future precipitation extreme/temperature relationship computed from the relationship of the historical runs considering climate warming and CC law (constant relative humidity). The dashed curves are the RCP8.5 simulations. The dashed red line indicate the CC-slope using the August-Roche-Magnus approximation for saturated vapor pressure.

5. Conclusion

Despite differences in quantitative precipitation simulation across the various models, the change in precipitation extremes with respect to temperature is robust and consistent. The spatial variability of the temperature-precipitation extremes relationship displays a hook shape across the Mediterranean, with negative slope at high temperatures and a slope following Clausius-Clapeyron (CC)-scaling at low temperatures. The temperature at which the slope of the temperature-precipitation extreme relation sharply changes (or temperature break), ranges from about 20°C in the western Mediterranean to less than 10°C in Greece. In addition, this slope is always negative in the arid regions of the Mediterranean. The simulated temperature-precipitation extremes relationship is insensitive to ocean-atmosphere coupling, while it depends very weakly on the resolution at high temperatures for short precipitation accumulation times. In future climate scenario simulations the temperature break shifts to higher temperatures by a value which is on average the mean regional temperature change due to global warming. The slope of the simulated future temperature-precipitation extremes relationship is close to CC-scaling at temperatures below the temperature break, while at high temperatures, the negative slope is less steep. This indicates more intense precipitation extremes in the future. Correcting the temperature-precipitation extremes relationship in the present climate using the CC law and the temperature shift in the future allows the recovery of the temperature-precipitation extremes relationship in the future climate. This implies negligible regional changes of relative humidity in the future despite the large warming and drying over the

Mediterranean. This suggests that the Mediterranean Sea is the primary source of moisture which counteracts the drying and warming impacts on relative humidity.

References

- Drobinski P, Alonzo B, Bastin S, Da Silva N, Muller C J (2015) Seasonal hysteresis in precipitation extremes-temperature relationship in the French Mediterranean region. *J. Geophys. Res.*:in revision
- Drobinski P, Ducrocq V, Alpert P, Anagnostou E, B\`eranger K, Borga M, Braud I, Chanzy A, Davolio S, Delrieu G, Estournel C, Filali Boubrahmi N, Font J, Grubisic V, Gualdi S, Homar V, Ivancan-Picek B, Kottmeier C, Kotroni V, Lagouvardos K, Lionello P, Llasat M C, Ludwig W, Lutoff C, Mariotti A, Richard E, Romero R, Rotunno R, Rousset O, Ruin I, Somot S, Taupier-Letage I, Tintore J, Uijlenhoet R, Wernli H (2014) HyMeX, a 10-year multidisciplinary program on the Mediterranean water cycle. *Bull. Amer. Meteorol. Soc.* 95:1063--1082
- Hardwick Jones R, Westra S, Sharma A (2010) Observed relationships between extreme sub-daily precipitation, surface temperature, and relative humidity. *Geophys. Res. Lett.* 37:L22805 doi:10.1029/2010GL045081.
- Ruti P, Somot S, Giorgi F, Dubois C, Flaounas E, Obermann A, Dell'Aquila A, Pisacane G, Harzallah A, Lombardi E, Ahrens B, Akhtar N, Alias A, Arsouze T, Raznar R, Bastin S, Bartholy J, B\`eranger K, Beuvier J, Bouffies-Cloche S, Brauch J, Cabos W, Calmanti S, Calvet J C, Carillo A, Conte D, Coppola E, Djurdjevic V, Drobinski P, Elizalde A, Gaertner M, Galan P, Gallardo C, Gualdi S, Goncalves M, Jorba O, Jorda G, Lheveder B, Lebeaupin-Brossier C, Li L, Liguori G, Lionello P, Macias-Moy D, Onol B, Rajkovic B, Ramage K, Sevault F, Sannino G, Struglia M V, Sanna A, Torma C, Vervatis V (2015) MED-CORDEX initiative for Mediterranean climate studies. *Bull. Amer. Meteorol. Soc.*:in revision

Application of the Weather Generator to Bias-correct the Regional Climate Model Output

Martin Dubrovsky^{1,3} and Pierpaolo Duce²

¹ Institute of Atmospheric Physics, Prague, Czech Republic (dub@ufa.cas.cz)

² Institute of Biometeorology, CNR IBIMET, Sassari, Italy

³ CzechGlobe - Center for Global Climate Change Impacts Studies, Brno, Czech Republic

This contribution presents a methodology, which is based on merging information from observations and RCM and is used to produce a gridded parametric daily WG capable to generate realistic synthetic multivariate weather series for weather-ungauged locations. In this procedure, WG is calibrated with RCM-simulated multi-variate weather series in the first step, and then, in the second step, grid-specific WG parameters are de-biased by spatially interpolated correction factors defined by comparing WG parameters derived from gridded RCM weather series vs. spatially scarcer observations. In fact, this procedure may be comprehended from two viewpoints: (1) From a point of view of WG, we may say that the RCM output is used to improve accuracy of interpolated WG. (2) On the other hand, from a point of view of RCM, we may say that WG parameters calibrated from weather data observed in a set of meteorological stations, interpolated into RCM grids and matched with WG parameters derived from RCM output, are used to unbias the RCM. In this case, we should stress that the present methodology allows to unbias not only the means in WG variables, but also the variabilities (standard deviations) and correlations and lag-correlations among the variables.

The quality of the weather series produced by the resultant gridded WG will be assessed in terms of selected climatic characteristics, an emphasis will be put on characteristics related to variability and extremes of surface temperature and precipitation. The validation will be made for two regions: (a) Czech Republic, which represents the climate in the Central Europe, and (b) Sardinia, which represents the Mediterranean climate.

Acknowledgements

The present experiment is made within the frame of projects WG4VALUE (project LD12029 sponsored by the Ministry of Education, Youth and Sports of CR) and VALUE (COST ES 1102 action).

Mediterranean cyclone climatology: Assessment of an ensemble of coupled and uncoupled atmosphere-ocean regional climate models applying six cyclone tracking methods

Flaounas Emmanouil¹, Gaertner Miguel², Kelemen Fanni³, Lionello Piero⁴, Sanchez Emilia⁵, Wernli Heini⁶, Naveed Akhtar⁷, Sandro Calmanti⁸, Dario Conte⁹, Zorica Podrascanin¹⁰, Marco Reale¹¹, Raquel Romera¹², Samuel Somot¹³

¹ National Observatory of Athens, Athens, Greece (flaounas@noa.gr); ² University of Castilla-La Mancha; Toledo, Spain; ³ Institute for Geophysics and Meteorology, University of Cologne, Cologne, Germany; ⁴ CMCC, Lecce, Italy ⁵ CERFACS/CNRS, Toulouse, France; ⁶ ETH, Zurich, Switzerland; ⁷ University of Frankfurt, Germany; ⁸ ENEA, Rome, Italy; ⁹ CMCC, Lecce, Italy; ¹⁰ University of Novi Sad, Serbia; ¹¹ OGS-National Institute of Oceanography and Experimental Geophysics, Trieste, Italy; ¹² Universidad de Castilla – La Mancha, Ciudad Real, Spain; ¹³ CNRM, Toulouse, France

1. Abstract

This study aims to assess how they MED-CORDEX regional climate model simulations reproduce the climatology of Mediterranean cyclones. All simulations were forced at the lateral boundary by the ERA-Interim reanalyses for a common 20-year period (1989-2008). Six different cyclone tracking methods have been applied to all twelve RCM simulations and the ERA-Interim reanalysis.

All models reproduce the main areas of high cyclone occurrence in the region. The skill of the RCM to properly reproduce the cyclone climatology depends strongly on the adopted cyclone tracking method. The modeling of atmosphere-ocean coupling processes has only a weak impact on the climatology and intensity of cyclones.

2. Introduction

Mediterranean cyclones have a strong impact on the regional climate, its variability, change and extremes. Several studies have shown the significant contribution of cyclones to the majority of rainfall and wind extremes in the Mediterranean to the formation of the most prominent high impact weather in the region as well as to the modulation of the hydrological cycle, the circulation and the deep water formation of the Mediterranean Sea (Flaounas et al., 2015a).

It has been demonstrated that, in an area of complex orography and land sea contrast such as the Mediterranean area, RCMs are able to produce realistic climate patterns at spatial scales that the global drivers cannot capture (Calmanti et al., 2015) and are able to improve the quality of input data for impact studies (D'Onofrio et al., 2014). In this paper we aim at assessing the capacity of an ensemble of seven MED-CORDEX regional climate simulations to realistically reproduce cyclone climatology in the Mediterranean.

To identify and track cyclones, we use six different cyclone tracking methods based either on sea level pressure or on relative vorticity at 850 hPa (Hoskins and Hodges, 2002; Neu et al., 2013). Sea level pressure is a low-frequency field that reflects the atmospheric mass, and is representative of atmospheric meso- and large scale processes. On the other hand, relative vorticity is a high frequency field that is representative of the atmospheric circulation at local scales.

Figure 1 provides an example of the uncertainty in tracking of a Medicane (Mediterranean cyclone, presenting visual characteristics of a hurricane) due to the use of different tracking methods. The tracks are calculated by the six tracking methods, applied to ERAI, and are compared to the subjectively drawn track connecting the ERAI sea level pressure local minima in consecutive time-steps. It is evident that all methods captured the cyclone eastward, zonal displacement, however, the life-time (equivalent to the number of track points), the initial and final location, as also the medicane exact path differs from method to method.

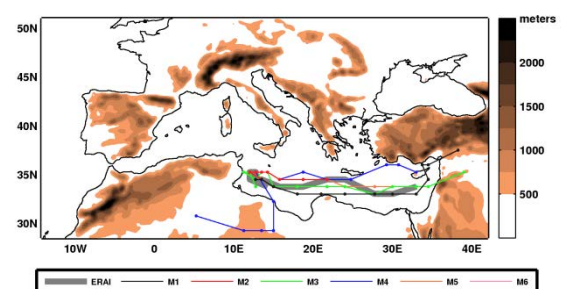


Figure 1. The Mediterranean domain where cyclone-tracking methods have been applied. Terrain elevation is shown in color. Grey thick line depicts the subjectively drawn track of the December 2005 medicane, using the ERAI sea level pressure. The colored lines show the medicane tracks, as diagnosed by the different tracking methods

3. Results

To deepen our analysis on the models' capacity to reproduce the Mediterranean cyclone climatology, Figure 2 shows Taylor diagrams (Taylor, 2001) that compare the CCD between the MED-CORDEX models and ERAI from the perspective of each cyclone tracking method. More precisely, the Taylor diagrams provide a statistical comparison of the spatial representation of the CCD between ERAI and the MED-CORDEX models. The root mean square (RMS) error in Figure 2 provides a measure of the average over- and under estimation of the CCD by each model in the whole domain. Since the CCD is not homogeneous in the region, the standard deviation and the correlation of each model with ERAI reflect the models' capacity to properly represent the level and

location of the regional CCD “hot-spots”, compared to the ERAI reanalysis.

Methods 2, 4 and 6 detect the fewest cyclones (Table 2), and hence for these methods, the CCD model comparison with ERAI in Fig. 4 presents small root mean square error. It can be regarded as a disadvantage of the RMS error that it tends to provide good results for models that produce relatively weak and smooth fields and it “punishes” models that produce variable fields with peaks at the wrong locations (the so-called double-penalty problem discussed in the verification literature, e.g., Wernli et al., 2008). Methods 2 and 6 suggest that all models present statistically equivalent spatial distributions of CCD with the exception of UCLM-PROMES, which is mainly due to the higher CCD of UCLM-PROMES close to the Alps. In fact, for methods 2 and 6, the CCD is higher over the Adriatic, Ionian and western Mediterranean seas (Fig. 2, Online resource 1), where the most intense cyclones are expected to occur (Flaounas et al., 2015b). Indeed, methods 2 and 6 apply a rather strong criterion on cyclone intensity, detecting only cyclones with SLP lower than 1013 hPa and with a SLP gradient greater than 0.5 hPa (100 km)⁻¹, respectively. It is plausible thus to suggest that the MED-CORDEX models capture correctly the occurrence of the most intense cyclones in the central Mediterranean. However, this seems not to be confirmed by method 5, which mainly captures the intense winter cyclones (see discussion above). Method 5 presents the widest spread of the models performance with the COSMO-CLM, the CNRM and the CMCC-CCLM models having a similar CCD standard deviation (about 20%) with ERAI and the highest spatial correlation with the reanalysis.

4. Conclusions

When considering weak and shallow cyclones, the methods based on potential vorticity allow a better understanding of the models capacity to reproduce long lasting vortices. On the other hand, the methods based on SLP provide a measure of the models’ capacity to reproduce deep cyclones and cyclones with strong SLP gradients, respectively. In particular, some of the SLP-based methods, are more adequate in tracking long lasting winter cyclones, while other represent peculiar aspect of cyclones through the detection of SLP deepening pathways.

We have investigated the cyclones’ spatial distribution, seasonal cycle and intensity evolution during the tracks lifetime. Figure 2 shows that no model excels in capturing the climatology of Mediterranean cyclones. Different model performances are mainly linked to the different physical parametrizations and horizontal resolutions, nevertheless all models seem to capture the main “hot-spots” of cyclone occurrence in the Mediterranean. The added value of dynamical downscaling is evident in the Online Resources 1, where the CCD in the models offers more details in the areas that favor cyclone occurrence. The higher detail in the CCD compared to ERAI is surprisingly higher even though the tracks have been calculated after regridding the model outputs in the ERAI grid. When considering the most intense cyclones, all methods tend to capture correctly the tracks (see example in Fig. 1) and their seasonal cycle. In fact we showed that it is more probable for the models to capture the strongest cyclones than the weaker ones.

Concerning the tracks spatiotemporal variability, regardless of the cyclone tracking method used, all model results converge on the weak impact of the coupling of the atmospheric models with an oceanic model. The impact of the coupling on cyclone intensity is also rather weak.

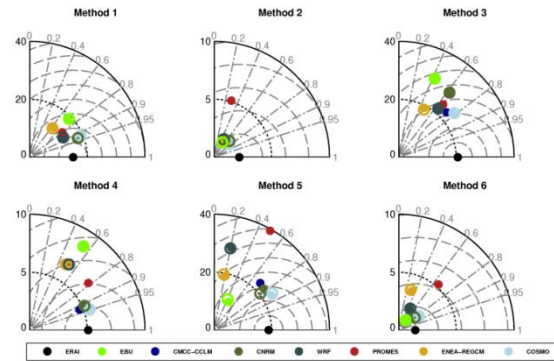


Figure 2. Taylor diagrams for the spatial Cyclone Center Density (CCD) comparison of all MED-CORDEX models (coupled simulations are shown in open circles), regards to ERAI, as shown in Fig. 2. and in Online Resources 1, standard deviation is expressed in per cent units. Note that panels for Methods 2, 4 and 6 are scaled up to 10% of standard deviation. The Root mean square error is plotted with a 5% of interval for Methods 1, 3 and 5 and with a 2 interval for Methods 2, 4 and 6.

References

- Calamanti S, Dell’Aquila A, Maimone F, Pelino V (2015) Evaluation of climate patterns in a regional climate model over Italy using long-term records from SYNOP weather stations and cluster analysis. *Clim Res* 62:173-188
- Flaounas E, Di Luca A, Drobinski P, Mailler S, Arsouze T, Bastin S, Beranger K, Lebeaupin Brossier C (2015a) Cyclone contribution to the Mediterranean Sea water budget, *Climate Dynamics*, 1-15, doi: 10.1007/s00382-015-2622-1
- Flaounas E, Raveh-Rubin S, Wernli H, Drobinski P, Bastin S (2015b) The dynamical structure of intense Mediterranean cyclones, *Climate Dynamics*, 44, 2411-2427, doi: 10.1007/s00382-014-2330-2
- Hoskins BJ, Hodges KI (2002) New Perspectives on the Northern Hemisphere Winter Storm Tracks, *J. Atmos. Sci.*, 59, 1041–1061
- Neu U, and coauthor (2013) IMILAST: A Community Effort to Intercompare Extratropical Cyclone Detection and Tracking Algorithms, *Bull. Amer. Meteor. Soc.*, 94, 529–547. doi: 10.1175/BAMS-D-11-00154.1
- Wernli H, Schwierz C (2006) Surface Cyclones in the ERA-40 Dataset (1958–2001). Part I: Novel Identification Method and Global Climatology. *J. Atmos. Sci.*, 63, 2486–2507.

Analysis of atmospheric and coupled ocean-atmosphere regional climate models capability to simulate tropical-like cyclones over the Mediterranean Sea from MedCORDEX and EUROCORDEX multimodel simulations

M. Á. Gaertner¹, E. Sánchez¹, M. Domínguez¹, R. Romera¹, V. Gil¹, C. Gallardo¹, M. M. Miglietta², Med-CORDEX and EURO-CORDEX teams

¹ University of Castilla-La Mancha, Toledo, Spain (e.sanchez@uclm.es)

² CNR-ISAC, Lecce, Italy

When tropical-like cyclones are observed over the Mediterranean Sea they are usually named as Medicanes. These are intense cyclones with a rather small size compared with other atmospheric structures over wider oceans, and where the sea-atmosphere interaction plays a fundamental role. These characteristics mean a challenging issue for the simulation of such cyclones in climate models. High-resolution (about 0.11°) and ocean-atmosphere coupled regional climate model simulations (RCMs) are being performed in MedCORDEX and EURO-CORDEX european projects during the last years with a domain centered over the Mediterranean, or at least covering almost the whole region. These regional simulations offer interesting and valuable data for the study of this type of cyclones in climate runs, allowing to analyze the impact of high horizontal resolution and ocean-atmosphere coupling on their simulation. The differences obtained when studying these different approaches can be of high interest to improve our understanding and capability to describe these processes. Using multi-model ensembles of simulations nested in reanalysis data, we analyse the ability of regional climate models to represent the characteristics of the observed tropical-like cyclones over the Mediterranean area. The results of these evaluation runs can give an indication of the reliability of the climate change projections for this type of cyclones.

A methodology based on the Picornell et al. (2001) to detect the cyclones and from Hart (2003) to study their vertical structure are used, as it was already shown for RCM runs in Gaertner et al. (2007) work. The work of Miglietta et al. (2013) is the base to compare the modelled results with the available observational information for present climate simulations.

References

- Gaertner MA, Jacob D, Gil V, Domínguez M, Padorno E, Sánchez E, Castro M (2007) Tropical cyclones over the Mediterranean Sea in climate change simulations. *Geophys Res Lett*, 34(14), doi: 10.1029/2007GL029977
- Hart R (2003) A cyclone phase space derived from thermal wind and thermal asymmetry. *Mon Weather Rev*, 131, 585-616
- Miglietta, M. M., Laviola, S., Malvaldi, A., Conte, D., Levizzani, V., Price, C. (2013). Analysis of tropical like - cyclones over the Mediterranean Sea through a combined modeling and satellite approach. *Geophys. Res. Lett.*, 40(10), 2400-2405.
- Picornell MA, Jansà A, Genovés A, Campins J (2001) Automated database of mesocyclones from the HIRLAM-0.5 analyses in the western Mediterranean. *Int J Climatol* 21, 335-354

Response of the Black Sea's benthos ecological functions to an environmental gradient

Grégoire, A.¹, Drion, R.², Gomoiu, M.³, Todorova, V.⁴, Velikova, V.⁵ and Capet, A.⁶

¹Mare Centre, Liege University, 4000 Liège Belgium, mgregoire@ulg.ac.be, ²Mare Centre, Liege University, 4000 Liège Belgium, ³National Institute for Research and Development of marine geology and geoecology (GeoEcoMar), Romania, ⁴Marine biology and ecology, Institute of Oceanology, Varna 9000, Bulgaria, ⁵SuRDEP, Johannesburg, South Africa, ⁶Ecology and Computational Hydrodynamics in Oceanography, OGS, Trieste, Italy

1. Introduction

For decades the Black Sea, and in particular its north-western shelf, has been exposed to multiple stressors like eutrophication, deoxygenation, pollution and overfishing that have affected the health and functioning of its ecosystem. The fact that climate change and acidification may superimpose to these stressors aggravates the situation, and strongly complicates the understanding and prediction of the response of living communities to perturbations. The differentiation of the environmental impact of each single stressor on the ecosystem which is necessary for the spatial planning of human activities in marine areas (in relation to Marine Spatial Planning) in view of achieving or sustaining the Good Environmental Status (GES) requires the development of adequate advanced methodologies.

Here we propose to use an ocean numerical model for mapping physical and environmental conditions and to understand and differentiate the impact of various stressors (eutrophication, climate change) on this mapping. Then, we use specific approaches in order to connect model predictions with descriptors of GES and biodiversity.

2. Methodology

We develop a three dimensional coupled circulation biogeochemical model of the Black Sea in order to assess the status, causes and mechanisms of hypoxia on the north-western shelf (BS-NWS) that was severely impacted by eutrophication in the 80's. Model simulations over the last 3 decades show evidences that hypoxia is still occurring seasonally on a non-negligible area of the bottom waters of the BS-NWS (Capet et al., 2013). This important finding (corroborated by the monitoring of local institutes) is in contradiction with the general idea that bottom hypoxia vanished with the reduction after 1992 of river-borne nutrient discharge. We found that the overestimation of recovering was due to the use of observations concentrated in areas and months not typically affected by hypoxia.

An index H which merges the aspects of the spatial and temporal extension of the hypoxic event is proposed to quantify, for each year, the intensity of hypoxia as an environmental stressor. In order to provide recommendations for the definition of policies aiming to avoid bottom hypoxia and to preserve the GES of the benthic habitat, a simplified statistical model has been derived to link the H index with the level of nutrients loads discharges by the Danube and specific climate drivers of hypoxia.

This approach allows establishing a cost of the local warming in terms of its impact on hypoxia. We find that the potential increase of water stratification in a global change context may promote the occurrence of seasonal hypoxia and this stresses that the definition of future management scheme of river discharges have to integrate the impact of climate change.

We then use statistical tools (Dray et al., 2014) in order to make the link between the wealth of information on the environment provided by the ocean model of the Black Sea with the functions of the BS-NWS benthic ecosystem and indicators of biodiversity. We choose benthos because through the wide diversity of functions it supports (e.g. biomass production, grazing, recycling, bioturbation, filtering, redistribution of food resources, waste decomposition), it is considered as an important ecosystem component for sustaining the delivery of goods and services to humans (e.g. climate regulation, cultural service, to support fisheries through the provision of food or habitat). We opt for a functional description of the macrobenthos using a trait-based approach. It means that the biodiversity of a community will be described by the diversity of the traits of its species (i.e. morphological, physiological, behavioural or phenological feature measurable at the individual level that can ultimately be linked to their performance, Violle et al., 2007).

Statistical methods are used in order to determine the environmental conditions that significantly explain the distribution of the macrobenthos traits. Then, we propose a regionalization of the Black Sea bottom based on the functional composition of its macrofauna (Fig. 1) and we assess how this mapping may evolve under scenarios of environmental changes. The final aim is to support environmental policy makers and managers in the definition of management strategies that would preserve the GES of the benthos as well as of the associated goods and services considering the multiple stressors acting on the systems.

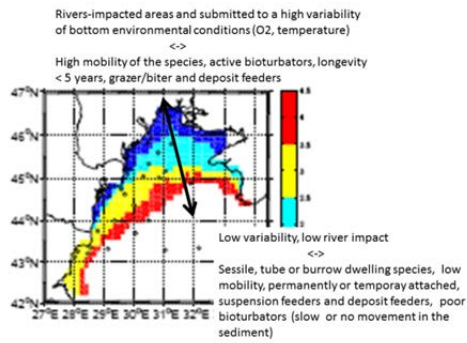


Figure 1: Regionalization of the Black Sea north-western shelf bottom produced by the ocean model based on the similarities of environmental variables that are significantly correlated with the traits of the macrobenthos. Number of the scales refers to the region numbering.

References

- Capet, A., Beckers, JM, Barth A. and Gregoire M, 2013. Drivers, mechanisms and long-term variability of seasonal hypoxia on the Black Sea northwestern shelf – is there any recovery after eutrophication? *Biogeosciences*, 10, 3943-3962.
- Dray S., Choler P., Dolédec S., Peres-Neto P., Thuiller W., Pavoine S., Ter Braak C., 2014. Combining the fourth-corner and the RLQ methods for assessing trait responses to environmental variation. *Ecology*, 95(1),14-21.
- Violle C, Navas M, Vile D., Kazakou E., Fortunel C., Hummer I. and Garnier E., 2007. Let the concept of trait be functional!, *Oikos*, 116(5), 882–892.

Added value of interactive air-sea coupling assessed from hindcast simulations for the North and Baltic seas

Matthias Gröger¹, Christian Dieterich¹, Semjon Schimanke¹, and H.E. Markus Meier^{1,2}

¹ Swedish Meteorological and Hydrological Institute, Norrköping, Sweden (matthias.groger@smhi.se)

² Meteorological Institute, Stockholm University, Stockholm, Sweden

1. The problem

Nonlinear feedback loops between the ocean and the atmosphere will determine the response to climate change as they regulate the energy transfer between these two compartments. In contrast to global climate simulations where interactive coupling is state of the art, regional ocean and atmosphere models are still driven frequently by prescribed forcing fields. In such an idealized setup any change in e.g. the ocean (the atmosphere) like a temperature anomaly is not communicated to the atmosphere (the ocean). Thus, the ocean (atmosphere) lacks an important feedback from the atmosphere (ocean) above (below). We here compare interactively with passively coupled hindcast simulations (Gröger et al., 2015) carried out with the recently developed NEMO-Nordic ocean-atmosphere regional model (Wang et al., 2015; Dieterich et al., in prep.) and aim to identify air-sea coupling effects and address the question whether interactive coupling introduces an added value to regional modeling.

2. Experimental setup

We here analyze basically two different model setups. When applying passive coupling the ocean model NEMO was driven by prescribed atmospheric boundary conditions taken from a downscaled ERA40 hindcast using the regional atmospheric model RCA4. In a second run the ocean model NEMO and the atmospheric model RCA4 interactively exchange mass and energy fluxes online during the simulation in the RCA4-NEMO model (hereafter interactive run).

The lateral boundary conditions were the same for both the setups. The open boundaries for NEMO are taken from an observed climatology (Janssen, 1999). The atmospheric regional model RCA4 is driven by ERA40 reanalysis data.

Coupling effects on the ocean are the main focus here. They are analyzed by comparing the output of the NEMO model from the two setups. Comparison of the two RCA4 outputs give insight to the coupling impact on the atmosphere.

3. Coupling effects in the ocean

In a first step we compare the simulated winter sea surface temperature (SST) with climatological values derived from observations (Fig. 1). During winter storm activity the wind driven mixing is much stronger than in summer. As a consequence, in most regions the mixed layer deepens considerably during the cold season.

Hence, the atmosphere is closer connected to the deeper layers of the ocean. Under these conditions a realistic simulation of ocean-atmosphere heat exchange can be considered important. Fig.1 clearly shows too cold temperatures in both the North Sea, and the Baltic Sea. However, the cold bias is much more pronounced in the model without interactive coupling. We can further conclude that the coupled model performs especially well in highly stratified regions like the Baltic Sea and along the Norwegian coast. In contrast to this, the passively coupled model shows fairly large deviations from the observed climatology. The large difference in performance between the two setups is mainly related to the thermal response of the ocean to atmospheric forcing. During winter the ocean loses heat to the colder atmosphere above which cools the ocean surface. The ocean to atmosphere heat transfer is supported by the deep mixed layer during winter which brings warmer water masses from depth up to the surface. In the coupled model however, the atmosphere considerably warms due to the heat gain from the underlying ocean. In addition the mixed layer is slightly deeper in the coupled model due to stronger wind stress which supports a strong heat transfer to the surface. This results in a warmer SST together with a higher oceanic heat loss at the sea-air interface. However, the oceanic heat loss is damped at the same time by the warming atmosphere. and so the oceanic heat loss is finally controlled by the lateral and vertical advective heat transports in the atmosphere (or in other words) by the atmospheres capability to remove heat).

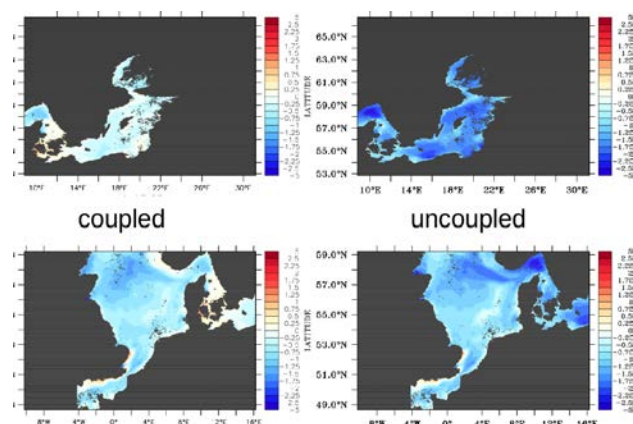


Figure 1. Deviation of simulated sea surface temperature from the observed climatology provided by the Bundesamt fuer Seeschifffahrt und Hydrographie, Hamburg. Shown is the multi-year (1990-2009) winter average (DJF).

In the passive coupled model the ocean heat loss leads not to a warming of the atmosphere and so the heat fluxes are controlled by the local processes alone (i.e. air sea temperature difference, wind mixing etc) whereas atmospheric heat transports are neglected. This leads to an unrealistically fast adaption of the ocean's surface to the cold atmosphere resulting in cooler SST compared to the coupled model. Finally the more realistic treatment of air-sea heat fluxes in the interactive run leads to a closer match to the observed climatology.

Fig. 1 shows that a realistic coupling is especially important in the highly stratified region like the Baltic. In the well mixed North Sea upward mixing of warmer waters from depth is strong in both models which keeps surface waters warmer and hence, the effective capability of the atmosphere to take up heat is less important (but still the coupled model performs better). In accordance with that, the differences between the interactively and the passively coupled model are much smaller during summer when an intensive thermal stratification develops which damps the effective thermal coupling between the ocean and the atmosphere. The strong thermocline weakens the upward mixing of cooler waters to the surface and the thinner mixed layer water can adapt faster to the atmosphere. In this situation an interactive coupling is less essential since heat fluxes are much lower during summer compared to winter.

3. Transient behavior

An important question is, if the two model setups will respond differently to a transient warming as it might be expected in the future. This will depend mainly on the ocean models' capability to absorb and store heat from a warming atmosphere. For the North Sea a recent warming trend has been reported in literature (e.g. Harrison and Carson, 2007; Meyer et al., 2009). Indeed we see this warming trend also in our ERA40 hindcasts and since the ocean model is driven by a fixed mean climatology at the open boundary the only way to warm the North Sea is via the atmosphere. This constitutes an ideal setting to test the ocean models heat uptake.

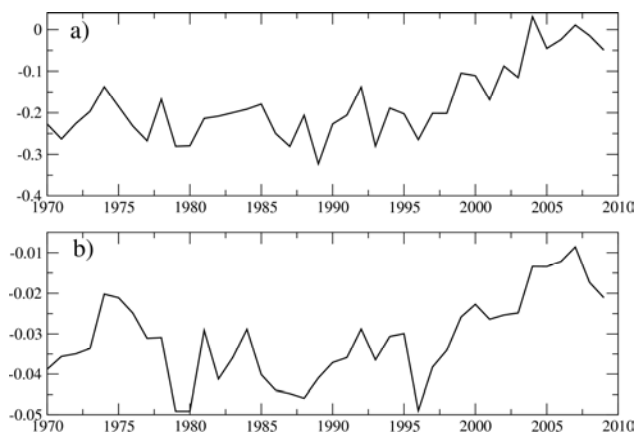


Figure 2: a) Difference in yearly mean North Sea SST (K) passively coupled run minus interactively coupled run. b) Same as a) but for heat content (10^{21} Joule).

Fig. 2a shows that the uncoupled model warms much faster than the coupled model which reduces the cold bias of the uncoupled model compared to the coupled model at the beginning of the 21st century. In order to answer whether this different behavior is only due to a different vertical redistribution of heat we have calculated the 3D heat content of the North Sea in the two setups (Fig. 2b) Indeed, it appears that during the last decade of the simulation the heat content evolves differently indicated by a faster increase in the uncoupled model. Hence the uncoupled model responds faster/stronger to the warming atmosphere.

4. Acknowledgements

This study was funded by the Swedish Research Council for Environment, Agricultural Sciences and Spatial Planning (FORMAS) within the project – Impact of changing climate on circulation and biogeochemical cycles of the integrated North Sea and Baltic Sea system – (Grant no. 214-2010-1575) and from Stockholm University's Strategic Marine Environmental Research Funds Baltic Ecosystem Adaptive Management (BEAM). The simulations have been supported by the National Supercomputer Centre in Sweden (NSC, grants SNIC 2013/11-22 – and SNIC 2014/8-36)

References

- Dieterich, C., Wang, S., Schimanke, S., Gröger, M., Klein, B., Hordoir, R., Samuelsson, P., Liu, Y., Axell, L., Höglund, A., Meier, H.E.M., and Döscher, R., Surface Heat Budget over the North Sea in Climate Change Simulations, in prep.
- Gröger, M., Dieterich, C., Meier, H.E.M., and Schimanke, S., Thermal air-sea coupling in hindcast simulations for the North Sea and Baltic Sea on the NW European shelf, *Tellus*, 67, 26911, DOI:10.3402/tellusa.v67.26911
- Harrison, D. E., Mark Carson, 2007: Is the World Ocean Warming? Upper-Ocean Temperature Trends: 1950–2000. *J. Phys. Oceanogr.*, 37, 174–187.
- Janssen, F., C. Schrum, and J. O. Backhaus, A. 1999, Climatological Data Set of Temperature and Salinity for the Baltic Sea and the North Sea, *Hydrogr. Zeitschrift*, 245 pp.
- Meyer, E.M.I., Pohlmann, T., and Weisse, R. (2009) Hindcast simulation of the North Sea by HAMSOM for the period of 1948 till 2007 – temperature and heat content, GKSS reports 2009/3, ISSN 0344-9629, Helmholtz gemeinschaft, Geestacht. http://www.hzg.de/imperia/md/content/gkss/zentrale_einrichtung_en/bibliothek/berichte/2009/gkss_2009_3.pdf
- Wang, S., Dieterich, C., Döscher, R., Höglund, A., Hordoir, R. and co-authors. 2015. Development of a new regional coupled atmosphere–ocean model in the North Sea and Baltic Sea. *Tellus A.* 67, 24284. <http://dx.doi.org/10.3402/tellusa.v67.24284>

Carbon and total alkalinity budgets for the Baltic Sea

Erik Gustafsson¹, Barbara Deutsch², Bo G. Gustafsson¹, Christoph Humborg^{1,2}, Carl-Magnus Mörtz^{1,3}, Anders Omstedt⁴ and Teresia Wällstedt²

¹ Baltic Nest Institute, Baltic Sea Centre, Stockholm University, Sweden (erik.gustafsson@su.se), ² Department of Environmental Science and Analytical Chemistry, Stockholm University, Sweden, ³ Department of Geological Sciences, Stockholm University, Sweden, ⁴ Marine Sciences: Oceanography, University of Gothenburg, Sweden

1. Introduction

Long-term average budgets for inorganic and organic carbon as well as total alkalinity (TA) have been calculated for the Baltic Sea. These budgets include river loads, atmospheric deposition, air-water gas exchange, internal sources and sinks, as well as the water exchange between the Baltic and North Seas.

The budgets were determined by means of BALTSEM (Baltic Sea long-term large-scale eutrophication model) calculations. The forcing data includes the most complete compilation of Baltic river loads for dissolved inorganic and organic carbon (DIC and DOC) and TA. In addition, we apply the most recent estimates of internal TA generation in the system (Gustafsson et al., 2014b).

2. Sources and sinks for DIC and TOC

River loads dominate the external DIC input to the Baltic Sea; although according to our calculations a net absorption of atmospheric CO₂ makes a substantial contribution as well (Table 1 and Figure 1).

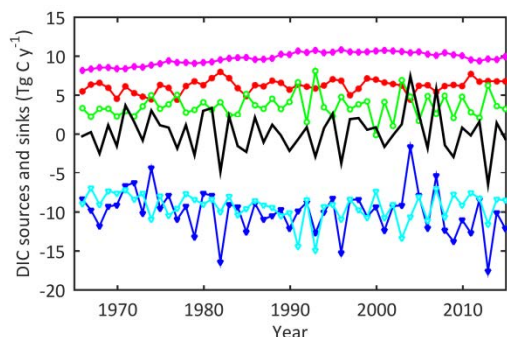


Figure 1. Simulated source and sink terms for DIC (Tg C y⁻¹): river load (red circles), air-water exchange (green circles), net export (blue triangles), net production (cyan triangles), sediment flux (magenta diamonds), and total sources minus sinks (black line). Redrawn from Gustafsson et al. (2015).

The major sources for TOC are river loads and net production (Table 1 and Figure 2). Riverine and atmospheric inorganic and organic carbon supplies are on an annual basis essentially compensated by a net export out of the system, whereas only a minor fraction is permanently buried in the sediments.

Table 1. Average DIC and TOC sources and sinks (Tg C y⁻¹).

	River load	Air-water	Net export	Net prod.	Sed.-water	Total SMS
DIC	6.2	3.2	-9.6	-9.3	9.7	0.20
TOC	4.5	0.43	-3.2	9.3	-11	0.16
Total	11	3.6	-13	0	-1.1	0.36

3. The fate of terrestrial DOC in the Baltic Sea

Our model simulations further indicate that a majority of the organic carbon that is supplied by rivers is mineralized into DIC within the system (Gustafsson et al., 2014a). The result is a decreased capacity to absorb atmospheric CO₂ in some sub-basins of the system, or an enhanced CO₂ evasion from other sub-basins.

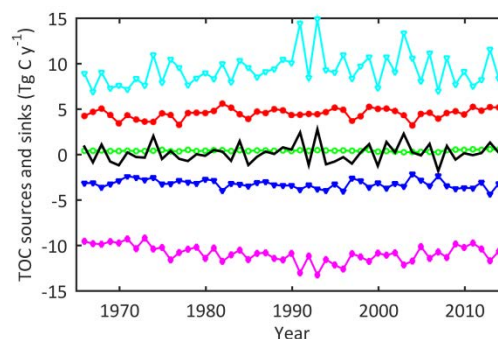


Figure 2. Simulated source and sink terms for TOC (Tg C y⁻¹). Legend: same as in Figure 1. Redrawn from Gustafsson et al. (2015).

4. Sources and sinks for TA

River loads comprise the largest TA source to the Baltic Sea, although the non-riverine sources are substantial (Table 2). The non-riverine sources are a combination of processes such as denitrification, sulfate reduction, silicate weathering, and submarine groundwater discharge (Gustafsson et al., 2014b). Internal TA generation makes a considerable contribution to the buffering capacity of atmospheric CO₂ in the system.

Table 2. Average TA sources and sinks (Gmol y⁻¹).

	Riverine	Non-riverine	Net export	Total SMS
TA	450	370	-810	13

References

- Gustafsson, E., Deutsch, B., Gustafsson, B.G., Humborg, C., Mörtz, C.-M. (2014a) Carbon cycling in the Baltic Sea - the fate of allochthonous organic carbon and its impact on air-sea CO₂ exchange, *J. Mar. Syst.*, 129, 289–302.
- Gustafsson, E., Wällstedt, T., Humborg, C., Mörtz, C.-M., Gustafsson, B.G. (2014b) External total alkalinity loads versus internal generation - the influence of nonriverine alkalinity sources in the Baltic Sea, *Global Biogeochem. Cycles*, 28, 1358-1370.
- Gustafsson, E., Omstedt, A., Gustafsson, B.G. (2015) The air-water CO₂ exchange of a coastal sea – a sensitivity study on factors that influence the absorption and outgassing of CO₂ in the Baltic Sea, *J. Geophys. Res. Oceans*, 120.

A study of the heat budget of the Mediterranean Sea from MedCORDEX forced and coupled simulations.

Ali Harzallah¹, Gabriel Jordà², Clotilde Dubois³, Gianmaria Sannino⁴, Adriana Carillo⁴, Laurent Li⁵, Thomas Arsouze⁶, Leone Cavicchia⁷, Jonathan Beuvier⁸ and Naveed Akhtar⁹

¹ National Institute of Marine Science and Technologies, Salammbô, Tunisia (ali.harzallah@instm.nrnt.tn)

² Institut Mediterrani d'Estudis Avançats, Esporles, Mallorca, Spain

³ Météo France - Centre National de Recherches Météorologiques, Toulouse, France.

⁴ Energy and Environment Modeling Technical Unit, ENEA, Rome, Italy.

⁵ Laboratoire de Météorologie Dynamique, Jussieu, Paris, France.

⁶ Unité de Mécanique, ENSTA-Paris Tech, Palaiseau, France.

⁷ Centro Euro-Mediterraneo sui Cambiamenti Climatici, Lecce, Italy.

⁸ Mercator Océan, Ramonville Saint-Agne, France.

⁹ Institut fuer Atmosphaere und Umwelt, Goethe-Universitaet Frankfurt, Frankfurt/Main, Deutschland.

1. Introduction

The Mediterranean Sea is a semi-enclosed basin; it is connected to the Atlantic Ocean through the narrow Strait of Gibraltar. The Mediterranean Sea gains heat from the Atlantic Ocean through this strait. According to Macdonald et al. (1994), the heat gain is estimated as $+5.2 \pm 1.3 \text{ Wm}^{-2}$. At the sea surface, the Mediterranean Sea losses heat in favor of the atmosphere. Estimates that permit to close the heat budget vary between -3 and -10 Wm^{-2} . However several estimates differ from this accepted range. Estimates based on atmospheric model simulations also show a large spread. Regional downscaling from the ERA40 reanalysis (Dee et al., 2011) show for example a mean value of -9 Wm^{-2} but with a large intermodel spread, 21 Wm^{-2} .

Observation and model simulation of the Mediterranean Sea show a warming and salinification of the Mediterranean waters (Bethoux et al., 1998; Bethoux and Gentili, 1999; Manca et al., 2004). Such changes in the hydrographic conditions are shown to reach the Atlantic Ocean through advection by the outflowing waters at the Strait of Gibraltar (Millot et al., 2006).

In this study we present the mean values and the evolution of the heat budget components in the Mediterranean Sea based on the simulations performed in the frame of the MedCORDEX project (Ruti et al., in revision). Results are compared to available observations and to previous simulations.

2. The models used

The study uses both forced and coupled models. Forced models use downscaled versions of the ERA40/ERAInterim atmospheric reanalyses (Dee et al., 2011) as forcing. Coupled models are driven outside the Mediterranean domain by ERA40/ERAInterim atmospheric fields while kept free to evolve inside. All models take into account the connection between the Mediterranean Sea and the Atlantic Ocean. However models use different approaches for this connection.

The forced simulations are labeled NEMOMED8, NEMOMED12 (two simulations), INSTME06 (two simulations) and MITGCM-REMO. The coupled simulations are labeled CNRM-RCSM4 (two simulations), GUF, MORCE-LMD, CMCC and ENEA. The simulations have different

lengths but the period common to most models (1980-2010) is considered in this study. Details on the models and on the simulations can be found in the MedCORDEX web site: www.medcorex.eu.

3. The heat budget

The time evolution of the Mediterranean thermal state is examined using the average temperature over the entire basin based on the different simulations and on the gridded observations from two data sets, RIXEN (Rixen et al, 2005) and EN3 (Ingleby and Huddleston, 2007). All models show a warming of the Mediterranean Sea waters. The warming is more obvious after the 1980 cooling. The sudden warming in 1990 is also well reproduced by models. The warming rate is around $+4 \cdot 10^{-3} \text{ }^\circ\text{Cyr}^{-1}$ for forced models and $+12.5 \text{ }^\circ\text{Cyr}^{-1}$ for coupled models. Hence coupled models show larger warming but this may partly result from their drift. The most obvious series that illustrates the change of the thermal state of the Mediterranean Sea is the heat accumulation rate, obtained as the derivative of the total heat content. The heat accumulation rate provides an indication of the change of the heat content. It illustrates the difference between the heat gain at the Strait of Gibraltar and the heat loss at the sea surface. Series of the heat accumulation rate are shown in Fig.1. The series are based on the simulations and on the two sets of gridded observations. The figure shows that models simulate close evolutions with variations located inside the limits based on ± 1 standard deviation of the observations. Variations of the heat accumulation rate are found to closely follow those of the surface heat loss which illustrates that the thermal state is driven by the interactions with the atmosphere with almost no effects of the Atlantic Ocean.

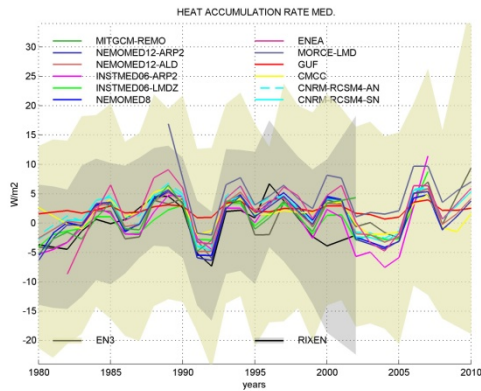


Figure 1. Heat accumulation rate series calculated for the Mediterranean Sea based on the different MedCORDEX simulations and on two observation data sets (with upper and lower limits based on ± 1 standard deviation of the observations). Units are Wm^{-2} .

Mean values of the heat accumulation rate are positive and are larger for the coupled models which recalls the larger trends of the average temperature for these models. At the sea surface the different models show as expected a heat loss with values ranging from -2.6 to $-4.8 Wm^{-2}$. At the Strait of Gibraltar, most models simulate gain values within the range $+3$ to $+6 Wm^{-2}$ with no differences between forced and coupled models. The trends of the heat accumulation rates, calculated for the period 1980-2010, are not significant but most values are positive which indicates that water warming accelerates. In agreement with previous studies this is attributed to a decrease of the heat loss at the sea.

The temperatures of the inflowing and outflowing waters at the Strait of Gibraltar are estimated from the ratios between heat and water fluxes. This approach shows larger than observed simulated inflow temperatures. At the opposite, it shows that the simulated outflow temperatures are close to the observed ones. Significant trends are found for the outflowing waters, which illustrates changes of the hydrographic conditions inside the Mediterranean Sea.

4. Conclusions

The heat budget components of the Mediterranean Sea are studied using an ensemble of simulations performed in the frame of the MedCORDEX project. The simulations reevaluate the Mediterranean evolution during the last decades. The used models successfully reproduce the water warming at a rate ranging from $+4 \cdot 10^{-3} \text{ } ^\circ\text{Cyr}^{-1}$ for forced models to $+12.5 \text{ } ^\circ\text{Cyr}^{-1}$ for coupled models. Models also show an acceleration of the warming but trends are not always significant. The heat accumulation rate is seen to be driven mainly by interactions at the sea surface with almost no effects of the heat exchange at the Strait of Gibraltar. The simulated temperatures of the outflowing waters are found to increase with significant trends, which shows that changes in the characteristics of the Mediterranean Sea waters have an influence on the heat through the Strait of Gibraltar.

References

- Bethoux, J.-P., Gentili, B., and Tailliez, D. (1998) Warming and freshwater budget change in the Mediterranean since the 1940s, their possible relation to the greenhouse effect. *Geophys. Res. Lett.*, 25, 1023–1026.
- Bethoux, J.P. and Gentili, B. (1999) functioning of the Mediterranean Sea: past and present changes. *Journal of Marine Systems*, 20, 33–47.
- Ingleby, B., and Huddleston M. (2007) Quality control of ocean temperature and salinity profiles - historical and real-time data. *Journal of Marine Systems*, 65, 158-175 [10.1016/j.jmarsys.2005.11.019](http://dx.doi.org/10.1016/j.jmarsys.2005.11.019).
- Manca, B., Burca, M., Giorgetti, A., Coatanoan, C., Garcia, M.-J., and Iona, A (2004) Physical and biochemical averaged vertical profiles in the Mediterranean regions: an important tool to trace the climatology of water masses and to validate incoming data from operational oceanography. *Journal of Marine Systems*, 48(1–4), 83–116.
- Millot, C., Candela, J., Fuda, J.-L. and Tber, Y. (2006) Large warming and salinification of the Mediterranean outflow due to changes in its composition. *Deep-Sea Research I* 53, 656–666.
- Rixen, M., Beckers, J.M., Levitus, S., Antonov, J., Boyer, T., Maillard, C., Fichaut, M., Baloupos, E., Iona, S., Dooley, H., Garcia, M.-J., Manca, B., Giorgetti, A., Manzella, G., Mikhailov, N., Pinardi, N., Zavatarelli, M. (2005) The Western Mediterranean Deep Water: a proxy for climate change. *Geophysical Research Letters* 32, L12608. <http://dx.doi.org/10.1029/2005GL022702> (2949-2952).
- Ruti PM, Somot S, Giorgi F, Dubois C, Flaounas E, Obermann A, Dell’Aquila A, Pisacane G, Harzallah A, Lombardi E, Ahrens B, Akhtar N, Alias A, Arsouze T, Aznar R, Bastin S, Bartholy J, Béranger K, Beuvier J, Bouffies-Cloch e S, Brauch J, Cabos W, Calmanti S, Calvet J-C, Carillo A, Conte D, Coppola E, Djurdjevic V, Drobinski P, Elizalde-Arellano A, Gaertner M, Gal n P, Gallardo C, Gualdi S, Goncalves M, Jorba O, Jord  G, L’Heveder B, Lebeaupin-Brossier C, Li L, Liguori G, Lionello P, Maci s D, Nabat P, Onol B, Raikovic B, Ramage K, Sevault F, Sannino G, MV Struglia, Sanna A, Torma C, Vervatis V (2015) MED-CORDEX initiative for Mediterranean Climate studies, BAMS, in revision.

Generation of heavy rainfall during the Oder flood event in July 1997: On the role of soil moisture

Ha Thi Minh Ho-Hagemann¹, Stefan Hagemann² and Burkhardt Rockel¹

¹Institute for Coastal Research, Helmholtz-Zentrum Geesthacht, Geesthacht, Germany (Ha.Hagemann@hzg.de)

²Max-Planck Institute for Meteorology, Hamburg, Germany

1. Introduction

Soil moisture-atmosphere feedback effects play an important role in the regional climate in several regions worldwide (Seneviratne et al., 2010). Land surface processes can effect extreme events (Pitman et al., 2012), and several studies have noted that soil moisture at the beginning of an event can have a significant impact on the extent and severity of droughts and heat waves (Lorenz et al., 2010; Quesada et al., 2012).

However, the potential impact of soil moisture on extreme rainfall events has been less often a scientific focus until now. Recent studies of climate change projections (e.g., Gutowski et al., 2004; Pan et al., 2004) suggest that summer precipitation strongly depends on surface processes, notably in the simulation of regional extremes (Randall et al., 2007). Therefore, in the present study, we conduct an in-depth investigation of the extreme rainfall event occurring from 18-20 July 1997, which led to the peak of the “Oder flood” in July 1997. Here, we present a regional climate modelling study, which indicates that the state of soil moisture preceding the event largely influenced the formation of the associated extreme rainfall over Central Europe.

2. Model and experiments

The atmospheric model COSMO-CLM (Rockel et al., 2008; hereafter, CCLM) was applied in two configurations in this study. First, the CCLM version `cosmo4.8_clm17` was applied in an uncoupled mode using sea surface temperature (SST) from the ERA-Interim reanalysis (hereafter, ERA-Int; Dee et al., 2011) over ocean surfaces. Second, CCLM is a component of the coupled system model COSTRICE (Ho-Hagemann et al., 2013), which also comprises the ocean model TRIMNP and the sea ice model CICE. In both configurations, CCLM is set up with a horizontal grid mesh size of 50 km and 32 vertical atmosphere layers for the CORDEX Europe domain and is driven by the 6-h ERA-Int reanalysis data as the initial and lateral boundary conditions. TRIMNP is constructed with a 12.8 km grid and 50 vertical ocean levels for the North and Baltic Seas. Initial and boundary conditions of TRIMNP are updated using ECMWF ORAS-4 reanalysis data (Balmaseda et al., 2013) for deep water levels, AVHRR2 SST of NOAA and a climatology surface salinity data (Levitus and Boyer, 1994). CICE calculates 5 categories of ice on a 12.8km grid for Baltic Sea and Kattegat, a part of the North Sea. Initial conditions of CICE are determined using the AVHRR2 SST.

Two long-term experiments (EXPs) were conducted: an uncoupled EXP using the standalone CCLM (hereafter, UNCPL) and a coupled EXP using the COSTRICE system (hereafter, CPL). For CPL, the CCLM, TRIMNP and CICE models exchange data every hour. The runs started in January 1979 and ended in December 2009. In addition, three one-month sensitivity EXPs were designed to simulate

the Oder flood extreme event, and these EXPs were restarted on 1 July 1997 (Table 1).

Table 1. Sensitivity experiments (EXPs) using different sea surface temperature (SST) data for the coupling area, and the restart conditions on 1 July 1997.

EXPs	SST	Restart conditions
UNCPL	ERA-Int	UNCPL
CPL	TRIMNP	CPL
UNCPL_SSTCPL	CPL	UNCPL
UNCPL_resCPL	ERA-Int	CPL
UNCPL_SST_resCPL	CPL	CPL

The ERA-Int data on a grid of ca. 0.7° and the E-OBS data on a 0.22° grid (Haylock et al., 2008) are interpolated to the CCLM grid for comparisons.

3. Analysis of sensitivity experiments

The Oder flood event was widespread over Central Europe, and both of its two major phases had relatively long durations (Kundzewicz et al., 1999). Randall et al. (2007) noted that large-scale and long-duration extreme events generally result from the persistence of weather patterns associated with air-sea and air-land interactions. Therefore, it is expected that the CPL and UNCPL will yield rather different simulations, as air-sea interactions are only taken into account by the CPL.

For the first phase of the event (4-8 July), however, the CPL and UNCPL behave similarly, as both of them underestimate the heavy rainfall over Poland compared with the E-OBS data. This underestimation seems to be related to the fact that both experiments miss the low over the Mediterranean Sea and its movement to the north that brought heavy rainfall along the trajectory.

In Phase 2 (18-20 July), ERA-Int data show a joining of three major rainfall sources in Central Europe, one from the depression over the Mediterranean Sea moving northward, one from a low over the North Atlantic Ocean crossing the North Sea, and a smaller branch from the North Atlantic Ocean crossing England. In addition, rainfall was also locally generated over Central Europe due to convection. This phenomenon is not found in the UNCPL; instead, a heavy rainfall area formed in an area further north-east one to two days later (Fig. 1b). The joining is better captured by the CPL. However, again, the branch from the Mediterranean Sea is not captured by the CPL. Consequently, the CPL's heavy rainfall area (Fig. 1c) has a smaller area and a lower intensity than that of the E-OBS data (Fig. 1a).

To investigate whether the better temporal resolution (i.e. 1-h) of SST in the CPL caused the better simulation of the heavy rainfall event during the second phase, the CPL's SST was used as a lower boundary condition for the uncoupled CCLM that was restarted on 1 July 1997 (UNCPL_SSTCPL). However, the heavy rainfall from 18-20 July is not captured with this setup either (Fig. 1d).

When both SST and the restart file of the CPL are applied (UNCPL_SST_resCPL, Fig. 1e) or only the restart file of the CPL is replaced (UNCPL_resCPL, Fig. 1f), the second phase of the event is captured with a similar rainfall area to that of the CPL, though with the smaller intensity. Hence, the restart state on 1 July plays an important role in reproducing the rainfall extreme event occurring from 18-20 July 1997. As most of the atmosphere/land-influencing synoptical-scale processes in July comprise only a small amount of memory, it can be concluded that soil moisture is a key player in transmitting this memory, especially giving its known importance in land-climate interactions.

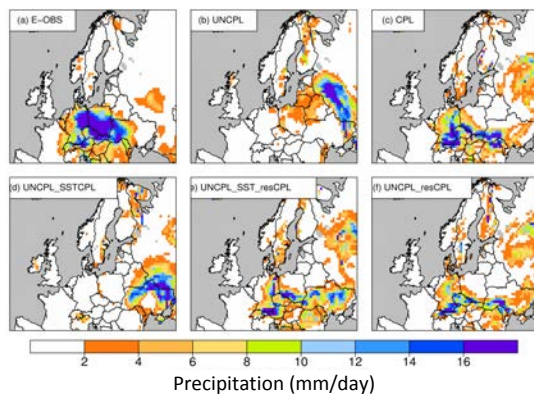


Figure 1. Mean precipitation (mm/day) of E-OBS data and the various experiments averaged for 18-20 July 1997.

On 1 July, over Central Europe, soil moisture in the 6 upper soil layers of the UNCPL and UNCPL_SSTCPL is noticeably lower than in the CPL and the other two experiments using the restart file from the CPL. The wetter soil moisture conditions of the CPL are due to the higher amount of precipitation in June. The CPL's better performance in June is likely associated with the beneficial impact of the coupling over the Baltic Sea and North Sea; the CPL could thus better reproduce the observed sequence of weather events in the weeks preceding the flood event and provide, in turn, a better restart condition than the UNCPL for July 1997.

4. Role of soil moisture

Further analyses of CPL and UNCPL fields in the time period prior to the second phase reveal a positive feedback loop: Higher soil moisture content in CPL than in UNCPL leads to more evaporation and latent heat fluxes from the land into the atmosphere. This causes more humidity in the atmosphere so that more cloud water and consequently more clouds are created, which eventually leads to more precipitation in CPL than in UNCPL on 18 July. Nevertheless, high soil moisture content is a necessary, though insufficient, condition for triggering the heavy rainfall event in this case study. By comparing results for 6 July (phase 1) and 18 July (phase 2) of the UNCPL and CPL simulations, we can see that although soil moisture content of the CPL on 6 July is as high as it is on 18 July, the heavy rainfall area over Central Europe on 6 July is not captured, which may be associated with a rather low moisture convergence on that day. An area of moisture divergence over the North Sea in the CPL on 18 July implicitly suggests that a source of moisture from the sea was transferred to Central Europe. Consequently, high soil moisture content, together with the large-scale circulation moisture transport, can be seen to

contribute to the phase 2 extreme event. This means that soil moisture may impact the generation of heavy rainfall events for conditions like in phase 2 where local feedbacks are at least as important as the large-scale circulation features. In situations in which this is not the case (such as for phase 1), soil moisture differences will not have a discernible impact on the characteristics of an extreme event.

5. Conclusion

In this study, we highlighted the impact of soil moisture on an extreme rainfall event associated with the Oder flood in July 1997. However, soil moisture is not a unique factor that generates heavy rainfall; instead, the lateral convergence of moisture from the North Sea and the Mediterranean Sea also plays an important role, as it brings moisture from the seas to the land. We also noted the added value that the atmospheric model coupled with an ocean model has on the simulation of the event.

However, our findings are for a specific extreme event while the impact of soil moisture seems to be dependent on many factors such as extreme events, the RCM, domain and integration period, model configuration (e.g. with or without spectral nudging, spatial resolution, number of vertical layers). Further analyses are planned for other heavy rainfall events with respect to the impact of soil moisture and whether coupling leads to an improved capturing of these events.

References

- Balmaseda, M. A., Mogensen, K. and Weaver, A. T. (2013) Evaluation of the ECMWF ocean reanalysis system ORAS4, *Q.J.R. Meteorol. Soc.*, 139: 1132–1161. doi: 10.1002/qj.2063.
- Dee, D.P., Uppala, S., Simmons, A.J., Berrisford, P., Poli, P., Kobayashi, et al. (2011) The era-interim reanalysis: Configuration and performance of the data assimilation system, *Q. J. R. Meteor. Soc.*, 137, 553–597.
- Gutowski, W.J., Otieno, F., Arritt, R.W., Takle, E.S., and Pan, Z. (2004) Diagnosis and attribution of a seasonal precipitation deficit in a US regional climate simulation, *J. Hydrometeorol.*, 5, 230–242.
- Haylock, M.R., Hofstra, N., Klein Tank, A.M.G., Klok, E.J., Jones, P.D., and New, M. (2008) A European daily high-resolution gridded data set of surface temperature and precipitation for 1950–2006, *J. Geophys. Res.*, 113, 1–12.
- Ho-Hagemann, H.T.M., Rockel, B., Kapitza, H., Geyer, B., and Meyer, E. (2013) COSTRICE – an atmosphere – ocean – sea ice model coupled system using OASIS3, HZG Technical Report, No. 2013-5, 26pp.
- Kundzewicz, Z.W., Szamalek, K., and Kowalczak, P. (1999) The Great Flood of 1997 in Poland, *Hydrol. Sci. J.*, 44, 855–870.
- Levitus, S., Boyer, T.P. (1994) *World Ocean Atlas 1994, Volume 4: Temperature*, number 4.
- Lorenz, R., Jaeger, E.B., and Seneviratne, S.I. (2010) Persistence of heat waves and its link to soil moisture memory, *Geophys. Res. Lett.*, 37, L09703.
- Pan, Z., Christensen, J.H., Arritt, R.W., Gutowski, W.J., Takle, E.S., Jr., and Otieno, F. (2004) Evaluation of uncertainties in regional climate change simulations, *J. Geophys. Res.*, 106, 17735–17752.
- Pitman, A.J., De Noblet-Ducoudré, N., Avila, F.B., Alexander, L.V., Boisier, et al. (2012) Effects of land cover change on temperature and rainfall extremes in multi-model ensemble simulations, *Earth Sys. Dyn.*, 3, 213–231.
- Quesada, B., Vautard, R., Yiou, P., Hirschi, M., and Seneviratne, S.I. (2012) Asymmetric European summer heat predictability from wet and dry southern winters and springs, *Nat. Clim. Change*, 2, 736–741.
- Randall, D.A., Wood, R.A., Bony, S., Colman, R., Fichefet, et al. (2007) *Climate Models and Their Evaluation*, In: *Climate Change 2007: The Physical Science Basis, Contribution of Working Group I to the Fourth Assessment Report of the IPCC*.
- Rockel, B., Will, A., and Hense, A. (Editorial) (2008) Special issue Regional climate modelling with COSMO-CLM (CCLM), *Meteorologische Zeitschrift*, 17, 347–348.
- Seneviratne, S.I., Corti, T., Davin, E., Hirschi, M., Jaeger, E.B., et al. (2010) Investigating soil moisture-climate interactions in a changing climate: A review, *Earth Sci. Rev.*, 99, 125–161.

Coupling of regional atmospheric-ocean models (WRF-ROMS) for climate applications in the Mediterranean basin

Pedro Jiménez-Guerrero, Juan P. Montávez

Physics of the Earth, Department of Physics. Regional Campus of International Excellence "Campus Mare Nostrum", Murcia, Spain (pedro.jimenezguerrero@um.es)

1. Introduction

Nowadays, most regional climate models (RCMs) have been essentially composed by an atmospheric component coupled to a land surface scheme and driven over ocean areas by prescribed sea surface temperature (SST). Although such a RCM can be sufficient for many applications, there are cases (like in the Mediterranean basin) in which the fine scale feedbacks associated with air-sea interactions can substantially influence the spatial and temporal structure of regional climates.

Therefore, in this work we present the first testing phase of the application of an atmospheric-ocean regional climate model (AORCM) for the Mediterranean basin under the framework of the CORWES project. CORWES is a Spanish consortium of research groups using the Weather Research and Forecasting (WRF) model to contribute to the Coordinated Regional Climate Downscaling Experiment (CORDEX).

2. Methodology

The modelling system covers the period 2001-2010 and consists of the Advanced Research WRF atmospheric model coupled to the ROMS regional oceanic model. The WRF model (Skamarock et al., 2005) is a community mesoscale model designed for a wide range of applications. It consists of a fully compressible non-hydrostatic dynamical core with a run-time hydrostatic option and a full suite of physics enabling its use in a broad spectrum of applications across scales ranging from tens of meters to thousands of kilometers. The NOAA Land Surface Model is included in WRF to represent land surface processes. The parameterizations used for WRF in this study include the Rapid Radiative Transfer Model (RRTM) longwave radiation scheme, the Dudhia shortwave radiation scheme, the WRF Single-Moment 3-class scheme microphysics scheme, and the Yonsei University planetary boundary layer scheme, a non-local k-profile scheme with an explicit treatment of entrainment processes at the top of the boundary layer.

ROMS (Shchepetkin and McWilliams, 2005) solves the hydrostatic, free-surface primitive equations in 3D curvilinear coordinates that follow the bottom orography and sea level exactly (i.e., a generalized r-coordinate), and the coastline approximately. ROMS contains accurate algorithms for extremum-preserving advection, the pressure-gradient force, the seawater equation of state compressibility, and split-explicit time-stepping for the barotropic/baroclinic mode coupling. The ROMS-AGRIF version is used in the coupled model. Coupling between WRF and ROMS is achieved in the following way: on a prescribed interval of 2 h, WRF sends wind stress, surface heat and water fluxes to ROMS time-averaged over the previous two hours. One hour later, and also with a prescribed interval of 2 h, ROMS sends time-averaged SST to WRF.

The resolution of the domain used in WRF is 12 km. The number of vertical levels is 30 for WRF. The ROMS domain, with 32 vertical levels, is slightly smaller than WRF innermost nest and has a higher resolution of 4 km (Figure 1). The analyses are focused on the area encompassed by the ROMS domain, where WRF and ROMS are coupled. Results from ROMS are first interpolated to the WRF 12 km grid. The lateral atmospheric boundary conditions for WRF are extracted from ERA-Interim reanalysis. The lateral oceanic boundary conditions for ROMS come from the downscaling of the Simple Ocean Data Assimilation analysis (SODA) by an uncoupled nested ROMS simulation covering the Mediterranean. The atmospheric forcing for this simulation is also extracted from ERA-Interim. To isolate effects of coupling on the atmosphere solutions, an atmosphere-only WRF simulation forced by ERA-Interim has been run. The domains are identical to the ones used for WRF in the coupled model, and its SSTs is derived from ERA-Interim 0.7 degree dataset.

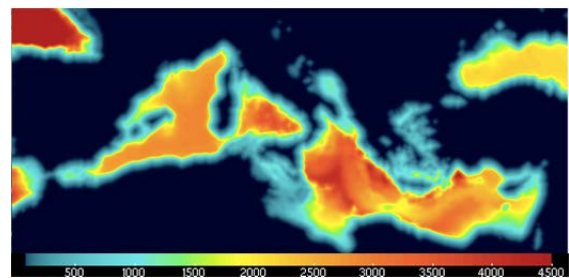


Figure 1. Domain for the ROMS simulation and corresponding bathymetry. Units are m.

3. Results

The results indicate that there is an overall good agreement between WRF-ROMS simulations and the E-OBS gridded dataset. During winter (DJF), the land temperature fields over most subregions in both WRF-ROMS and WRF achieve a closer agreement with E-OBS than ERA-Interim reanalyses, as a consequence of the dynamical downscaling. During summer (JJA) the regional simulations exhibit a cold bias with respect to E-OBS, somehow corrected by coupled simulation. WRF-ROMS and WRF present, however, similar average temperatures during all the annual cycle.

During summer (Figure 2), WRF-ROMS provides higher temperatures in the southern Mediterranean (Alboran, Benghazi, Mersa Matrouh) and lower temperatures in the Adriatic and the north-eastern Levantine basin than the atmosphere-only WRF simulations.

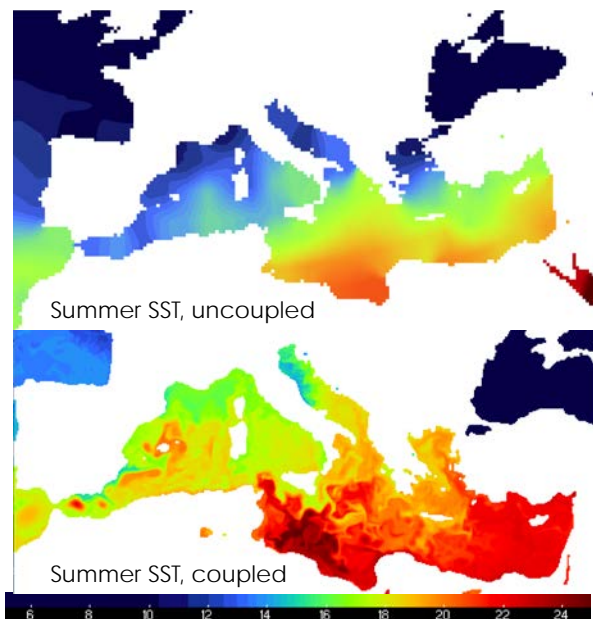


Figure 2. Comparison of sea surface temperature (SST, degrees Celsius):. Top: ERA-Interim prescribed SST; Bottom: WRF-ROMS resolved SST

According to Artale et al. (2010), this pattern corresponds to the prevailing anti-cyclonic oceanic structures along the southern coasts and to the cyclonic structures along the northern Mediterranean coasts, the two being separated by the Mid-Mediterranean jet. Also, the 2-m air temperatures for summertime for coupled vs. uncoupled simulations are marked by the differences in SST. WRF-ROMS and WRF-alone have similar temperature averages. Main differences are found over coastal areas (but are lower than 0.2 °C for all the Mediterranean basin). Therefore, the atmosphere-ocean coupling over this region does not significantly change the simulations of present climate 2-m temperature (Figure 3).

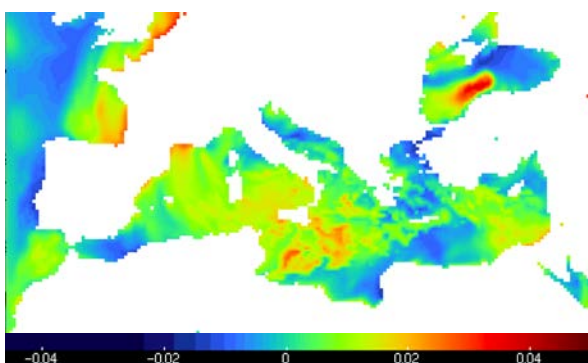


Figure 3. Difference in summertime (JJA) 2-m temperature (degrees Celsius) Coupled vs. uncoupled simulations

Moreover, the precipitation in the WRF-ROMS and WRF simulations do not present substantial differences for total precipitation, suggesting a weak effect of air-sea feedbacks on seasonal mean of land precipitation in our modelling system. This result is somewhat expected from the well established notion that the Mediterranean area is mainly subject to large scale orographic precipitation associated to synoptic systems travelling eastward from the North Atlantic.

In the WRF-ROMS coupled simulation, mostly in the warm seasons, we find less convective rainfall over the Adriatic and the northeastern Levantine basin (more convective rainfall over southern coasts and the eastern Mediterranean) than in the atmosphere-only simulation. The differences in convective precipitation are associated to the differences found for SST in the coupled vs. uncoupled simulations (Figure 4).

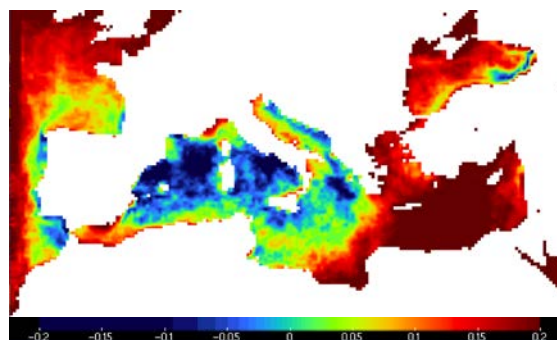


Figure 4. Difference in JJA convective precipitation (mm/day) Coupled vs. uncoupled simulations

4. Conclusions

The climatology of the coupled model over land is in good agreement with the results of the stand-alone version of the atmospheric model, whose performance is in line with that of other state-of-the-art regional climate models.

In the Euro-Mediterranean area, the two-way interaction with the ocean does not impair the quality of the predicted atmospheric fields, despite the presence of a temperature bias over the sea (as also stated by Somot et al., 2008, Artale et al., 2010).

The most important contribution of the WRF-ROMS coupled modelling is providing high-resolution oceanic components and fluxes over the area of analysis.

Acknowledgements

This work was funded by the Spanish Ministry of Economy and the "Fondo Europeo de Desarrollo Regional" (FEDER) (projects CGL2010- 22158-C02-02 and CGL2014-59677-R). The CORWES project team and is specially acknowledged for the fruitful discussions.

References

- Artale, V., et al. (2010) An atmosphere-ocean regional climate model for the Mediterranean area: assessment of a present climate simulation, *Climate Dynamics*, 25(5), 721-740.
- Skamarock, W.C., et al. (2005) A Description of the Advanced Research WRF Version 2. NCAR Technical note NCAR/TN-468+STR.
- Shchepetkin, A. F., McWilliams, J.C. (2005) The regional ocean modeling system (ROMS): A split-explicit, free-surface, topography-following-coordinate oceanic model. *Ocean Modeling*, 9(4), 347-404
- Somot S. , Sevault F., Déqué M., Crépon M. (2008) 21st century climate change scenario for the Mediterranean using a coupled Atmosphere-Ocean Regional Climate Model. *Global and Planetary Change*, 63(2-3), 112-126.

Arctic regional atmosphere-ocean-sea ice coupling, sensitivity to the domain geographical location.

Nikolay V. Koldunov¹, Dmitry V. Sein², Joaquim G. Pinto³ and William Cabos⁴

¹ Climate Service Center Germany (GERICS) Helmholtz-Zentrum Geesthacht, Hamburg, Germany (nikolay.koldunov@hzg.de)

² Alfred Wegener Institute, Germany.

³ Institute for Geophysics and Meteorology, University of Cologne, Germany.

⁴ Department of Physics, University of Alcalá, Spain

1. Introduction

The choice of the model domain for the regional ocean-atmosphere coupling is often based more on geographical reasons (e. g. inclusion of the certain countries, or continents) rather than on geophysical reasons (e. g. centers of atmospheric circulation, storm pathways, air-sea interaction). Here we investigate sensitivity of the regional coupled model climate simulations over the Arctic region to different configurations of the model domain. We are going to show how inclusion or exclusion of certain regions influences model results.

2. Model setup

The REgional atmosphere MOdel (REMO; Jacob and Podzun, 1997; Jacob, 2001) is coupled to the global ocean-sea ice model MPIOM (Marsland et al., 2003) with increased resolution in the Arctic. The models are coupled via the OASIS (Valcke et al., 2003), which provides the exchange between the ocean and atmosphere models. The coupled system is called ROM and is described in (Sein et al., 2015). We use NCEP/NCAR reanalysis data as an external forcing.

Five different coupled setups (Fig. 1) were used for five ensemble simulations. The coupled model setups share the same ocean-model configuration. Each ensemble contained five ensemble members. The coupled domain of each setup includes the Arctic and additionally a specific region, that is, Asia, Atlantic, Pacific, in order to investigate the impact of this region on Arctic climate variability.

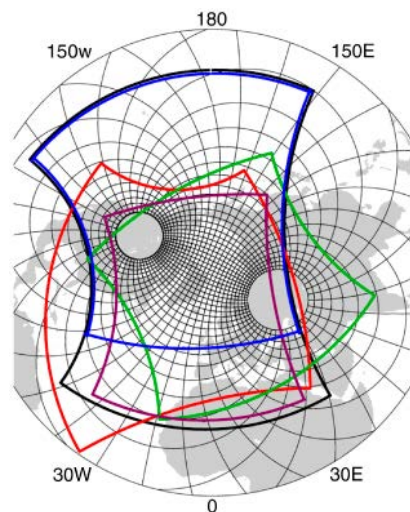


Figure 1. Coupled setups. Colors of spherical rectangles indicate different domains: Arctic (violet), Asia (green), Atlantic (red), Pacific (blue), Atlantic-Pacific (black). Domains are defined on REMO grid. Thin black lines – MPIOM grid (every 12th grid line).

3. Results

We compare our simulations to ERA-40 reanalysis. Comparison shows that in terms of 2m temperatures the differences between domains lay mostly in the absolute values, while spatial distribution of temperature is similar. The Pacific setup shows largest amplitudes of the temperature biases. The mean sea level pressure (MSLP) differences show a more diverse distribution among setups compared to 2m temperatures. The Arctic and Atlantic setups show the smallest biases compared to the reanalysis, while the Pacific and AP setups present an anomalous anticyclonic flow over most of the Arctic.

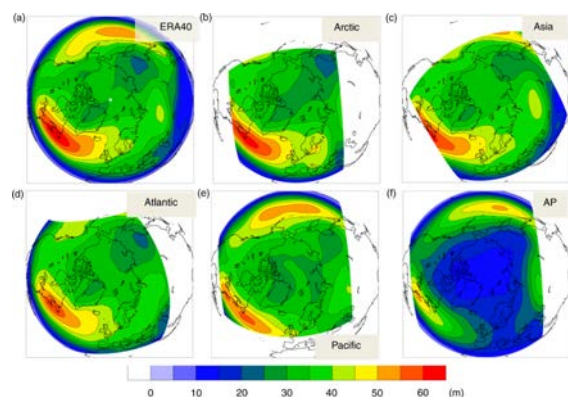


Figure 2. Storm track calculated as a standard deviation of bandpass (2.5 – 6 d) filtered DJF 500 hPa geopotential height (m), see main text for more details.

Analysis of heat transport and storm tracks (Fig. 2) show that differences in atmospheric circulation is the main cause of the differences between setups. It turns out that large-scale modes like the AO are only reproduced properly when North Pacific is not included in the domain (Arctic, Asia and Atlantic setups). When North Pacific is included (Pacific and Atlantic-Pacific setups), model AO becomes an “internal” mode, and correlation with observed AO drops significantly.

4. Conclusions

Our investigation shows that for a regional coupled ocean-atmosphere-sea ice model, the results of climate simulations can be quite different from those of the driving global model or reanalysis and strongly depend on the model domain. More detailed analysis of the mechanisms responsible for differences between the coupled model simulations over different domains and contribution of internal modes to Arctic climate variability is presented in Sein et al., 2014. We conclude that the choice of model domain should be based on the physical knowledge of the atmospheric and ocean processes. An

adequate choice of model domain is particularly important in the Arctic region due to the complex feedbacks between the components of the regional climate system taking place in that region.

References

- Marsland, S. J., Haak, H., Jungclaus, J. H., Latif, M. and Roeske, F. (2003) The Max-Planck-Institute global ocean/sea ice model with orthogonal curvilinear coordinates. *Ocean Model.* 5, 91–126.
- Jacob, D. and Podzun, R. (1997) Sensitivity studies with the regional climate model REMO. *Meteorol. Atmos. Phys.* 63, 119–129
- Sein D.V., Mikolajewicz U., Gröger M., Fast I., Cabos W., Pinto J.G., Hagemann S., Semmler T., Izquierdo A., Jacob D. (2015) Regionally coupled atmosphere - ocean - sea ice - marine biogeochemistry model ROM: 1. Description and validation. *J Adv Model Earth Syst* 7:268–304 doi:10.1002/2014MS000
- Sein D.V., Koldunov N.V., Pinto J.G., Cabos W. (2014) Sensitivity of simulated regional Arctic climate to the choice of coupled model domain. *Tellus A* 66:23966. doi:10.3402/tellusa.v66.23966

Improved Regional Climate Model Simulation of Precipitation by a Dynamical Coupling to a Hydrology Model

Morten Andreas Dahl Larsen¹, Martin Drews¹, Jens Hesselbjerg Christensen², Michal Brian Butts³ and Jens Christian Refsgaard⁴

¹ Dept. of Management Engineering, Technical University of Denmark, Kgs. Lyngby, Denmark (madla@dtu.dk)

² Dept. of Research and Development, Meteorological Institute of Denmark, Copenhagen, Denmark

³ Dept. of Water and Environmental management, DHI, Hørsholm, Denmark

⁴ Dept. of Hydrology, Geological Survey of Denmark and Greenland, Copenhagen, Denmark

1. Abstract

The complexity of precipitation processes makes it difficult for climate models to reliably simulate precipitation, particularly at sub-grid scales, where the important processes are associated with detailed land-atmosphere feedbacks like the vertical circulations driven by latent heat that affect convective precipitation systems. As a result climate model simulations let alone future projections of precipitation often exhibit substantial biases. Here we show that the dynamical coupling of a regional climate model to a detailed fully distributed hydrological model - including groundwater-, overland- and river flow as well as land surface-atmosphere fluxes of water (evapotranspiration) and energy - significantly reduces precipitation bias compared to the regional climate model alone. For a six year simulation period (2004 – 2010) covering a 2500 km² catchment substantial improvements in the reproduction of local precipitation dynamics are seen for time scales of app. Seasonal duration and longer. We show that these results can be attributed to a more complete treatment of land surface feedbacks. The local scale effect on the atmosphere suggests that coupled high-resolution climate-hydrology models including a detailed 3D redistribution of sub- and land surface water have a significant potential for improving climate projections even diminishing the need for bias correction in climate-hydrology studies.

2. Introduction

The importance of correctly reproducing interaction between the land surface and the atmosphere is well documented (Seneviratne et al. 2006). Horizontal model grid scale (Rauscher et al. 2010) and the ability to account for non-linearity and variability (Deser et al. 2012) play a significant role in the ability to simulate precipitation systems. Land surface representation is however also crucial (Dirmeyer et al. 2009) and even more so on local to regional scales (Fosser et al. 2014). Recent improvements in modelling approaches include higher spatio-temporal scales (Kendon et al. 2014), improved physical representation (Quillet et al. 2010), higher quality of forcing data (Silva et al. 2007) and increased computational resources. However, state-of-the-art regional climate models (RCM's) still suffer from deficiencies in feedback from the sub- and land surface to the atmosphere (Rummukainen 2010) and these are often related to simplifications (e.g. lack of groundwater representation) in some cases degrading model performance under specific conditions (Boberg and Christensen 2012).

3. Method

The hydrological model is used over the 2500 km² Skjern River catchment and is based on the MIKE SHE model in 500 m resolution (Højberg et al. 2013). The model uses an integrated description of groundwater flow (3D), unsaturated flow (1D Richards equation), overland flow (2D kinematic routing) and river routing (1D). Further, the model includes the SWET land surface model (Overgaard 2005) accommodating energy based fluxes. The HIRHAM regional climate model (Christensen et al. 2007) version 5 is used for atmospheric simulations in an 11 km rectangular grid resolution using a 90 sec. time step over a 2800 km x 4000 km domain.

The coupling of MIKE SHE and HIRHAM operates across platforms using a Windows PC and a parallelized CRAY XT5 supercomputer respectively and both models have been modified for compatibility with the OpenMI open source coupling tool (Gregersen et al. 2007). The setup is described in Butts et al. (2014) and Larsen et al. (2014) describes multiple simulations assessing the optimal cross-model data transfer interval (30 min. as used in the present study), variability etc. HIRHAM delivers the six driving climatic variables of precipitation, surface temperature, surface pressure, relative humidity, global radiation and wind speed, whereas MIKE SHE in return delivers sensible heat (recalculated from surface temperature) and latent heat thereby essentially replacing the HIRHAM land surface scheme over the hydrological catchment.

The coupled simulations were performed from 1 May 2004 to 31 July 2010 discarding the first 3 months as spin-up. An off-line warm-up has been used for the hydrological model for realistic groundwater levels. RCM output and observations were spatially and temporally matched (RCM grid/daily values) before the analyses. The analyses include I) coupled/uncoupled performance (RMSE) on varying period length (1 to 365 days), II) coupled/uncoupled performance (RMSE) on the 75-99.5% high-precipitation percentiles, III) plots of precipitation totals for the entire period as well as the 2009-2010 period where evapotranspiration was also available (surface area weighted values from three flux towers within the catchment representing the three dominating surfaces) and IV) a distributed plot of the RMSE difference between the coupled and uncoupled simulations.

4. Results

Between the coupled and uncoupled simulations an equal performance was found for period lengths up to app. 3 months (i.e. seasonal length) whereas for longer periods the coupled simulations showed distinctly lower RMSE levels. Similarly, the coupled simulations were superior when analyzing the 75-97.5% heavy precipitation percentiles.

For the 2004-2010 and 2009-2010 periods, the coupling is seen to significantly increase the precipitation totals more closely resembling the observed levels. A large part of this increase is seen to derive from an increase in convective precipitation. For the 2009-2010 period where observed evapotranspiration was available the coupled simulation is also superior in reproducing the total period evapotranspiration as well as showing a better RMSE for the daily values as compared to the uncoupled simulation (0.85 vs. 0.99 mm/day respectively).

The distributed plot showed the effect of the coupling (RMSE larger than model variability) to be highly local over the hydrological catchment extending app. 1-3 cells outside the catchment with the largest effect to the north-east somewhat in the downstream direction of the domination weather systems in Denmark.

5. Discussion

The superior coupled precipitation simulation results for periods over seasonal time scales as compared to the uncoupled results implies that the addition of sub-soil processes and overall improvements in the hydro-physical schemes become important when approaching time scales typical for climate models. For Denmark having a flat topography and high net precipitation groundwater generally exerts a high influence on soil moisture (Stisen et al. 2013). The increase in convective precipitation for the coupled simulation and the corresponding superior performance for heavier precipitation further implies a better treatment of processes as e.g. soil moisture has been shown to affect convective precipitation (Hauck et al. 2011). The improved evapotranspiration results for the coupled simulation, and thereby the overall water balance, also supports the interpretation of a positive effect of greater detail in associated process, spatio-temporal resolution and numerical layering.

6. Conclusions and perspectives

It is shown that the addition of higher detail in the full range of sub- and land surface processes by a fully dynamical coupling between and RCM and a hydrological model improves the RCM precipitation output significantly also with regards to heavy and convective precipitation. This could imply a potential for increased confidence in RCM simulation of projected changes in the hydrological cycle and the obvious possibility of increasing the coupled area with the increase in calibration efforts this would then require. The results clearly show the potential of having a higher spatio-temporal detail in the land- and subsurface hydrology of RCM's by coupling to an external hydrology model for studies of the hydrological cycle in a climate system.

References

- Boberg, F. & Christensen, J. H. (2012) Overestimation of Mediterranean summer temperature projections due to model deficiencies. *Nat Clim Chang* 2, 433–436
- Butts, M. et al. (2014) Embedding complex hydrology in the regional climate system – Dynamic coupling across different modelling domains. *Adv Water Resour* 74, 166–184
- Christensen, O. B., Drews, M., Christensen, J. H., Dethloff, K., Ketelsen, K., Hebestadt, I., and Rinke, A. (2006) The HIRHAM regional climate model version 5, Danish Meteorological Institute Technical Report 06-17, Danish Meteorological Institute, Copenhagen
- Deser, C., Phillips, A., Bourdette, V. & Teng, H. (2012) Uncertainty in climate change projections: the role of internal variability. *Clim Dyn* 38, 527–546
- Dirmeyer, P. A., Schlosser, C. A. & Brubaker, K. L. Precipitation, Recycling, and Land Memory: An Integrated Analysis. *J Hydrometeor* 10, 278–288 (2009)
- Fosser, G., Khodayar, S. & Berg, P. (2014) Benefit of convection permitting climate model simulations in the representation of convective precipitation. *Clim Dyn* 44, 45–60
- Gregersen, J. B., Gijbbers, P. J. A. & Westen, S. J. P. (2007) OpenMI: Open modelling interface. *J Hydroinform* 9, 175
- Hauck, C., Barthlott, C., Krauss, L. & Kalthoff, N. (2011) Soil moisture variability and its influence on convective precipitation over complex terrain. *Q.J.R. Meteorol Soc* 137, 42–56
- Højberg, A. L., Troldborg, L., Stisen, S., Christensen, B. B. S. & Henriksen, H. J. (2013) Stakeholder driven update and improvement of a national water resources model. *Environ Model Softw* 40, 202–213
- Kendon, E. J. et al. (2014) Heavier summer downpours with climate change revealed by weather forecast resolution model. *Nat Clim Chang* 4, 570–576
- Larsen, M. A. D. et al. (2014) Results from a full coupling of the HIRHAM regional climate model and the MIKE SHE hydrological model for a Danish catchment. *Hydrol Earth Syst Sci* 18, 4733–4749
- Overgaard, J. (2005) Energy-based land-surface modelling: new opportunities in integrated hydrological modeling, Ph.D. Thesis, Institute of Environment and Resources, DTU, Technical University of Denmark, Lyngby
- Quillet, A., Peng, C. & Garneau, M. (2010) Toward dynamic global vegetation models for simulating vegetation–climate interactions and feedbacks: recent developments, limitations, and future challenges. *Environ Rev* 18, 333–353
- Rauscher, S. A., Coppola, E., Piani, C. & Giorgi, F. (2010) Resolution effects on regional climate model simulations of seasonal precipitation over Europe. *Clim Dyn* 35, 685–711
- Rummukainen, M. (2010) State-of-the-art with Regional Climate Models. *Wiley Interdisciplinary Reviews: Clim Change* 1, 82–96
- Seneviratne, S. I. et al. (2010) Investigating soil moisture–climate interactions in a changing climate: A review. *Earth-Sci Rev* 99, 125–161
- Silva, V. B. S., Kousky, V. E., Shi, W. & Higgins, R. W. (2007) An Improved Gridded Historical Daily Precipitation Analysis for Brazil. *J Hydrometeor* 8, 847–861
- Stisen, S., Sonnenborg, T. O., Refsgaard, J. C. (2013) Investigating the importance of groundwater for near surface flux and state simulation through a multi-constraint analysis of a complex surface-subsurface-atmosphere model. *Climate And Land Surface Changes In Hydrology*, eds Boegh et al. (IAHS Press), Proceedings of IAHS-IAPSO-IASPEI Assembly, Gothenburg, Sweden. 359:146-151

Very High Resolution Observations of Regional Climate from Offshore Platforms near the German Coast

Tina Leiding, Birger Tinz and Lydia Gates

Deutscher Wetterdienst, Marine Climate Monitoring Centre, Hamburg, Germany (tina.leiding@dwd.de)

1. Introduction

In order to investigate conditions for offshore wind power generation in the German coastal areas, three research platforms were constructed in the North Sea (FINO1 and 3) and the Baltic Sea (FINO2). The observations from these masts are shown to be a valuable source of multi-level and sub-hourly maritime atmospheric data in an otherwise data-sparse region which may be used for the evaluation of fine-scale modelling and assimilation. The measurement masts at the offshore platforms are either square or triangular shaped and have different boom constellations. They are equipped with a range of meteorological sensors at heights of 30 to 100 m above sea level (Fig. 1).

The research project “FINO-Wind” focusses on defining standards for the quality control, analysis and interpretation of the data which is necessary to make the results of the different platforms comparable and more useful for users.



Fig. 1: Mast designs with different foundations. [Source: FuE-Zentrum FH Kiel GmbH].

2. Quality Control

Standards for wind turbines given in the IEC (International Electrotechnical Commission) can only be partly applied as some requirements are not applicable to offshore masts. Therefore, a standardization method for data quality checking is developed by introducing a consecutive checking scheme. The sequence of steps (Fig. 2) consists of formal checks, followed by climatological, temporal, repetition and consistency checks. After successful completion of each part of this sequence, the data are assigned standardized quality flags. As a default, 10-minute data are processed.

The quality criteria are either derived from existing meteorological standards or carefully chosen from several years of experience with the analysis of measurements and data from the three FINO platforms.

The core procedure of the routine was originally developed and tested in the observations network operated by the National German Meteorological Service Deutscher Wetterdienst (DWD). It was adapted to the specific requirements of the meteorological data in a marine environment and the application for measurements at different heights.

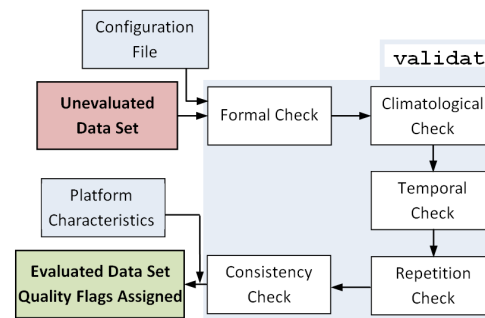


Fig. 2: DWD data quality control routine.

3. Further Investigations

The question how mast effects on the flow affect the wind measurements, observations at all three masts are intensively investigated in comparison to LiDAR, Computational Fluid Dynamics (CFD) calculations, the Uniform Ambient Mast flow (UAM) method and wind tunnel measurements. A thorough evaluation of these analyses yielded an optimized correction method for wind measurements which will be included in the final data set.

Over the last few years offshore wind farms were built in the vicinity of FINO1, 2 and 3 and further wind farms are expected to be added in the coming years. In a later phase of the “FINO-Wind” project, wake effects at the three masts from existing and planned wind farms will be investigated and analyzed with regard to wind speed reduction and turbulence intensity increase.

4. Conclusion

The project provides a range of new quality standards of high-resolution meteorological data as well as consistent data storage and ease of access to the data base. Best practices and procedures will be described.

5. Acknowledgment

The authors acknowledge funding for this research project on atmospheric conditions for renewable energy generation through the ‘Wind Energy Initiative’ of the German Federal Ministry for Economic Affairs and Energy and Projektträger Jülich for the period 2013 to 2016. Deutscher Wetterdienst implements this project as a federal government-business enterprise in collaboration with the Federal Maritime and Hydrographic Agency (BSH), UL International GmbH - DEWI, Fraunhofer IWES, DNV GL, and Wind-consult GmbH. FINO-Wind project webpage: www.dwd.de/fino-wind.

Projected acidification of the Mediterranean Sea

Briac Le Vu¹, James C. Orr¹, Julien Palmier¹, Jean-Claude Dutay¹, Florence Sevault², and Samuel Somot²

¹ LSCE/IPSL, Laboratoire des Sciences du Climat et de l'Environnement, CEA-CNRS-UVSQ, Gif-sur-Yvette, France (james.orr@lsce.ipsl.fr)

² CNRM/Météo-France, Toulouse, France

1. Introduction

Along with climate change, the Mediterranean Sea is also experiencing acidification. That is, its surface pH is declining as atmospheric CO₂ continues to increase. Ocean acidification is a well understood chemical process that occurs because CO₂ is not only a greenhouse gas; it is also an acid gas. Seawater has a high capacity to absorb CO₂ due to its high alkalinity (acid neutralizing capacity).

The Mediterranean Sea has 10% higher alkalinity than average ocean waters and is thus more chemically capable of absorbing CO₂. Further enhancing this capacity to absorb anthropogenic carbon is the relatively rapid ventilation of its deep waters. Nonetheless, recent model simulations over the historical industrial era have demonstrated that the rate of acidification of Mediterranean surface waters does not differ from typical ocean surface waters (Palmieri et al., 2015). Here we provide the first projections of ocean acidification over the 21st century.

2. Methods

To make these projections, we have exploited output from a regional climate model from Somot et al. (2006), which couples the ARPEGE atmospheric model to the NEMO-MED8 regional eddying ocean model. That model is forced under historical forcing as well as the IPCC A2 scenario over the 21st century (Somot et al., 2006). Results from those simulations are used to pilot a offline configuration of the same ocean model Calibri. The figure should be at least 300 dpi and details should be well recognizable in this small space printing.

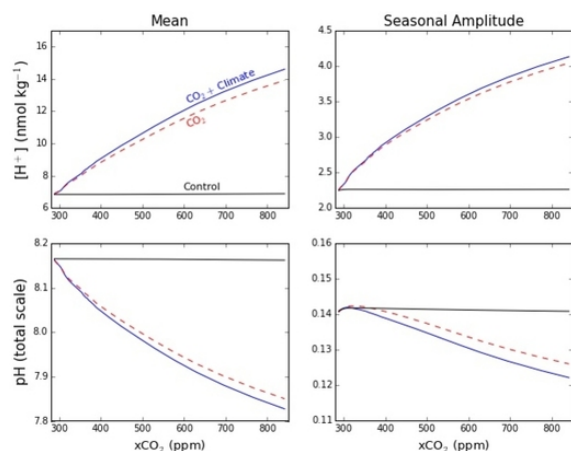


Figure 1. Change in [H⁺] (top) and pH (bottom) from 1860 to 2100 for the Mediterranean Sea's mean concentration (left) and mean seasonal amplitude (right). Atmospheric CO₂ varies from 288 to 845 ppm during 1860 to 2100.

3. Results

During the simulation (1860 to 2100) the level of free acidity (hydrogen ion concentration [H⁺]) doubles as does the amplitude of the seasonal cycle of [H⁺] (Figure 1). Simultaneously, pH (equal to -log₁₀[H⁺]) declines by -0.35 while the amplitude of its seasonal cycle is reduced by 0.02 units. Changes in pH are slightly larger in the western basin relative to the eastern basin, which is warmer and has greater alkalinity (Figure 2). These changes are due almost entirely to increasing atmospheric CO₂; climate change has little effect.

4. Conclusion

The Mediterranean Sea will probably experience a doubling of its natural level of free acidity during the 21st century. Seasonal extreme events will become more extreme due to simultaneous doubling of the seasonal amplitude.

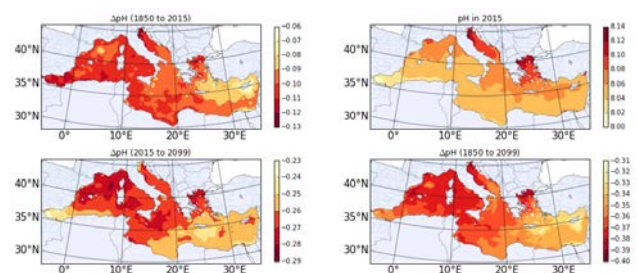


Figure 2. Maps of (a) 1850-to-2015 change in surface pH, (b) surface pH in 2015, and changes in pH (c) from 2015 to 2099 and (d) from 1850 to 2099.

References

- Adloff F, Somot S, Sevault S et al. (2015) Mediterranean Sea response to climate change in an ensemble of twenty first century scenarios, *Clim. Dyn.*, DOI 10.1007/s00382-015-2507-3.
- Aumont, O. and Bopp, L. (2006) Globalizing results from ocean in-situ iron fertilization studies, *Global Biogeochem. Cy.*, 20, GB2017, doi:10.1029/2005GB002591.
- Palmieri, J., Orr, J. C., Dutay, J.-C., Béranger, K., Schneider, A., Beuvier, J., and Somot, S. (2015) Simulated anthropogenic CO₂ storage and acidification of the Mediterranean Sea, *Biogeosciences*, 12, 781-802, doi:10.5194/bg-12-781-2015, 2015.
- Somot S, Sevault F, Déqué M (2006) Transient climate change scenario simulation of the Mediterranean Sea for the twenty-first century using a high-resolution ocean circulation model. *Clim. Dyn.* 27(7–8):851–879

Heat and salt redistribution in the Mediterranean Sea. Insights from the MedCORDEX model ensemble

J.Llasses¹, G.Jordà¹, D.Gomis¹, F.Adloff², D.Macías-Moy³, A.Harzallah⁴, T.Arzouse⁵, B.Ahrens⁶, L.Li⁷, A.Elizalde⁸, G.Sannino⁹

¹ Mediterranean Institute for Advanced Studies (IMEDEA), Mallorca, Spain (josep.llasses@uib.es)

² Centre National de Recherches Météorologiques, Toulouse, France

³ Insitute for Environment and Sustainability, Ispra, Italy

⁴ Institut National des Sciences et Technologies de la Mer, Salambo, Tunisia

⁵ ENSTA-ParisTech, Palaiseau, France

⁶ Institute for Atmospherica and Environmental Sciences, Frankfurt, Germany

⁷ Laboratoire de Météorologie Dynamique, Paris, France

⁸ Max-Planck-Institute für Meteorologie, Hamburgt, Germany

⁹ ENEA Centro Ricerche Casaccia, Roma, Italy

The evolution of the heat and salt content of the Mediterranean Sea can differ significantly among different ocean regional climate models (ORCMs). The main source of discrepancies is the differences in the forcing, either through the air-sea interface or the lateral boundaries (Strait of Gibraltar, Dardanelles Strait or rivers). However, an additional source of discrepancies is how each model redistributes the heat and salt that is introduced in the system through the boundaries. This determines the regional differences in heat and salt content as well as the long term evolution of the Mediterranean, especially if the heat and salt are transferred to depths where the residence time is very long (i.e. below the sills of the Strait of Gibraltar or the Sicily Channel).

In this contribution, our goal is twofold. First, we will characterize the main patterns of heat and salt fluxes inside the Mediterranean using a box-model with 8 compartments (4 layers and 2 regions). The NEMOMED8 simulation (Beuvier et al., 2010) will be analysed in detail in order to understand the magnitude and time variability of the fluxes among the different compartments of the box model. Second, we will use the same box-model to describe the behaviour of an ensemble of 15 simulations contained in the MedCORDEX database. The similarities and the discrepancies in the heat and salt redistribution patterns of the different models will be described. We will also try to explain them in terms of differences in the forcings and/or model configuration. This will help us to determine which elements of the model configuration are more sensitive for a proper representation of the Mediterranean heat and salt content evolution.

Climate change and anthropogenic impacts on Mediterranean Sea ecosystems for the end of the 21st century.

Diego Macias¹, Adolf Stips¹ and Elisa Garcia-Gorriz

European Commission. Joint Research Center. Via E. Fermi, I-21027, Ispra, Italy (diego.macias-moy@jrc.ec.europa.eu)

1. Abstract

The Mediterranean Sea is considered as a hotspot for climate change because of its location in the temperate region and because it is a semi-enclosed basin surrounded by highly populated and developed countries.

Some expected changes include an increase in air temperature and changes in the periodicity and spatial distribution of rainfall. Alongside, demographic and politics changes will alter freshwater quantity and quality. All these changes will have an impact on the ecological status of marine ecosystems in the basin.

We use a 3D hydrodynamic-biogeochemical coupled model of the entire Mediterranean Sea to explore potential changes in primary productivity under two emission scenarios (rcp4.5 and rcp8.5) and considering two socio-economic scenarios (Global Orchestration and Adaptive Mosaic, from Millennium Ecosystem Assessment).

Climatic changes will alter the hydrodynamic properties of the simulated basin by modifying the surface forcing to the ocean and the rivers' water flow, while the socioeconomic scenarios will modify the nutrients loads in the riverine waters.

Our model simulation indicate that the most important changes in marine productivity levels and distribution could be attributed, in order of importance, to (i) changes in atmosphere-ocean interactions, (ii) changes in the baroclinic water masses balance of the basin because of freshwater inputs modifications and (iii) changes in nutrient loads in riverine waters.

2. Material and Methods

The 3-D General Estuarine Transport Model (GETM) was used to simulate the hydrodynamics in the Mediterranean Sea. A detailed description of the GETM equations could be found in Stips *et al.* (2004) and at <http://www.getm.eu>. The configuration of the Mediterranean Sea (Fig. 1) has a horizontal resolution of 5' x 5' and includes 25 vertical layers.

The ocean model is forced at surface every 6 hours by the following atmospheric variables, wind velocity at 10 meters (U10 and V10), air temperature at 2 m (t2), specific humidity (sh), cloud cover (tcc) and sea level pressure (SLP) provided by the different realizations of the atmospheric model described in the next section. Bulk formulae are used to calculate the corresponding relevant heat, mass and momentum fluxes between atmosphere and ocean (Macias *et al.*, 2013).

Atmospheric forcings are provided by the Cosmos-CLM (<http://www.clm-community.eu/>) RCM implemented within the EuroCORDEX initiative (<http://www.euro-cordex.net/>). This RCM is forced at the boundaries with conditions provided by two global circulation models (GCMs) included in the CMIP5 exercise, MPI and EcEarth (<http://cmip-pcmdi.llnl.gov/cmip5/>). For each GCM two emission scenarios as defined by IPCC are considered; rcp4.5 and rcp8.5 (Meinhausen *et al.*, 2011).

The present configuration of the ocean model includes 37 rivers discharging along the Mediterranean coast (blue stars in Fig. 1). The corresponding present-day river discharges were derived from the Global River Data Center (GRDC, Germany) database. Actual nutrient content (nitrate and phosphate) of freshwater runoff were obtained from Ludwig *et al.* (2009)

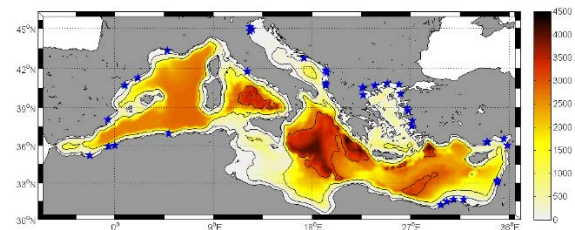


Figure 1. Model domain with main bathymetric lines and included rivers (blue stars).

To determine the relative change in freshwater flow for the end of the 21st century the change in precipitation-evaporation in the different catchments (as defined in the WISE river basin districts) have been computed for each of the RCM realizations (see example in Fig. 2).

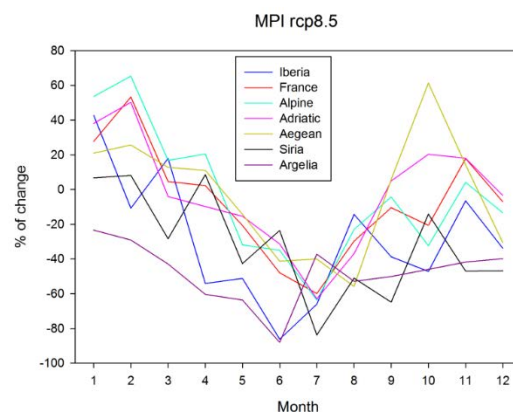


Figure 2. Monthly relative anomalies of precipitation-evaporation for each catchment area. CCLM-MPI rcp8.5 realization.

Changes in nutrient loads for Mediterranean rivers are more difficult to assess as they are heavily dependent on socio-economic changes. We have used the river scenarios proposed by Ludwig *et al.* (2010) to assess potential changes on nitrogen and phosphate loads for different Mediterranean and Black Sea rivers under four different socio-economic scenarios used in the Millennium Ecosystem Assessment exercise (Carpenter *et al.*, 2006). From the four options included in this exercise we have chosen the worst and best case scenarios (Global Orchestration and Adaptive Mosaic respectively).

3. Results

We first run the ocean model under the different climate scenarios without changing the rivers' conditions (flow and nutrient) in order to isolate the effect of changing atmospheric forcing. This exercise showed a consistent trend towards oligotrophy in the western basin and increased production in the eastern basin (Macias *et al.*, submitted) and provides the baseline to evaluate the effect of river modifications.

In the second set of simulations the final decade of the 21st century was simulated again for each climate model realization but changing the river flows (leaving untouched the nutrient loads in the freshwater). Surface chlorophyll and primary production rates in these simulations were evaluated against the corresponding runs without river changes. It was found that changes in sea surface temperature (SST) were strongly correlated with productivity changes but with regional-specific correlation patterns. In the open sea a negative correlation was found, i.e., an increase in SST corresponded with a decrease in primary production. On the other hand, in coastal areas the correlation was positive, with increasing SST accompanied by increasing primary production (Fig. 3).

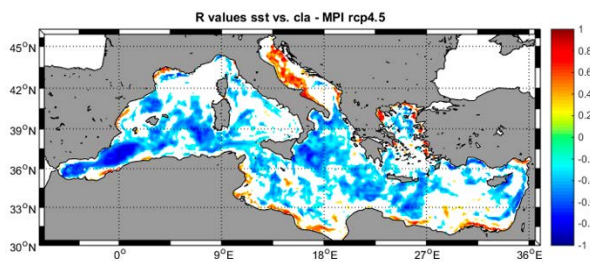


Figure 3. Correlation coefficient between SST and surface production anomalies (simulation river flow modified – simulation river flow cte) for MPI under emission scenario rcp4.5.

The third set of simulations consisted in adding the nutrient load changes considered from the socio-economic scenarios. Surface productivity changes were evaluated against the previous set of simulations (only changing freshwater flow). It was found that the effect of these modifications were much more limited in space, with substantial changes in marine productivity in the regions nearby rivers' mouths (Fig. 4).

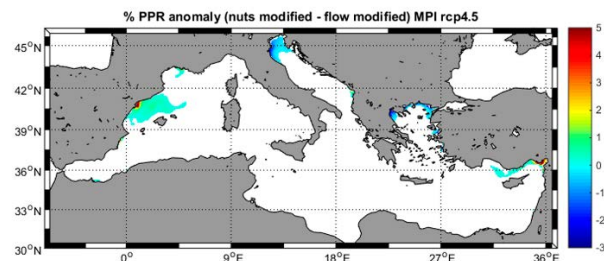


Figure 4. % of change in surface primary production rate between the worst case scenario for riverine nutrient and the simulation with modified flows (MPI – rcp4.5 forced run).

4. Conclusions

The three sets of simulations performed here allows to identify and isolate the impact of different drivers within future scenarios for the marine productivity of the Mediterranean Sea. We have found that the largest

influence comes from the direct effect of the modifications of atmospheric conditions that changes the surface stratification properties in the basin, altering the mixing efficiency and changing the distribution of primary production with respect to present-day conditions.

Altering the magnitude of the freshwater flows has a relatively smaller impact on primary production levels but has basin-wide consequences. In open sea regions a negative correlation between SST and production is found, meaning that where stratification is enhanced (higher SST), production decreases. The contrary is found for coastal areas where increasing water temperature leads to higher production.

Finally, our simulations indicate that changing the nutrient loads for the end of the next century will have only marginal effects on primary production, with the strongest effect concentrated around the river mouths. However, some regions as the Adriatic Sea, Aegean Sea or the NE basin could be significantly affected.

References

- Carpenter, S. R., P. L. Pingali, E. M. Bennett, and M. B. Zurek (Eds.) (2006), *Ecosystems and Human Well-Being*, vol. 2, Scenarios, 515 pp., Island Press, Washington, D. C.
- Ludwig W, Dumont E, Meybeck M, Heussner S (2009) River discharges of water and nutrients to the Mediterranean and Black Sea: Major drivers for ecosystem changes during past and future decades? *Progress in Oceanography*, **80**, 199-217.
- Ludwig, W., A. F. Bouwman, E. Dumont, and F. Lespinas (2010), Water and nutrient fluxes from major Mediterranean and Black Sea rivers: Past and future trends and their implications for the basin-scale budgets, *Global Biogeochem. Cycles*, **24**, GB0A13, doi:10.1029/2009GB003594.
- Macias D, García-Gorriz E, Stips A (2013) Understanding the Causes of Recent Warming of Mediterranean Waters. How Much Could Be Attributed to Climate Change? *Plos One*, **8**, e81591.
- Macias D, García-Gorriz E, Stips A (submitted) Productivity changes in the Mediterranean Sea for the 21st century in response to climate scenarios. *Frontiers in Marine Science*.
- Meinshausen M, Smith SJ, Calvin K, Daniel JS, Kainuma MLT, Lamarque JF, Matsumoto K, Montzka SA, Raper SCB, Riahi K, Thomson A, Velders GJM, Van Vuuren DPP (2011) The RCP greenhouse gas concentrations and their extensions from 1765 to 2300. *Climatic Change*, **109**, 213-241.
- Stips A, Bolding K, Pohlman T, Burchard H (2004) Simulating the temporal and spatial dynamics of the North Sea using the new model GETM (general estuarine transport model). *Ocean Dynamics*, **54**, 266-283.

A downscaling investigation of multi-model uncertainty of hindcasted and projected regional temperatures

Brian R. MacKenzie¹ and Markus Meier²

¹Section for Ocean Ecology and Climate, 4National Institute for Aquatic Resources, Technical University of Denmark (DTU-Aqua), Denmark; brm@aqu.dtu.dk,

²Swedish Meteorological and Hydrological Institute, Norrköping, Sweden, and Department of Meteorology, Arrhenius Laboratory, Stockholm University, Sweden

1. Introduction

Different model parameterisations used for projecting future states of ecosystems and foodwebs can contribute uncertainty to projected outcomes (Stock et al. 2011; Meier et al., 2012; Hollowed et al. 2013; Payne et al. submitted). This uncertainty is particularly evident when multiple models are available for estimating the same response (e. g., sea temperature, biomass of a fish population) in a given system. Knowledge of the magnitudes and sources of uncertainty in climate projections of oceanographic and ecosystem variables is needed so that estimates of risk and vulnerability of climate-dependent processes and variables can be estimated more reliably and for developing effective climate mitigation and adaptation strategies.

2. Methods

Here we evaluate the level of uncertainty in projections of an abiotic variable (sea temperature) as estimated by three different regional models of a large marine ecosystem (Baltic Sea), which are coupled via downscaling to a global model of climate-ocean dynamics. The outputs of the models (RCO-SCOBI, ERGOM, BALTSEM) were generated within a BONUS project (ECOSUPPORT) focussed on coupling downscaled global climate model outputs to regional oceanographic-biogeochemical-fish population models (Meier et al. 2012; MacKenzie et al. 2012; Niiranen et al. 2013). The main forcing dataset used were results from a regional atmosphere model (Samuelsson et al. 2011), driven with ERA40 re-analysis data (Uppala et al. 2005) at the lateral boundaries.

3. Results

Using historical observations (1970-2005), we show that each of the three regional oceanographic models performs reasonably well, but has its own specific biases and uncertainties. Moreover, biases differ depending on season of the year, indicating that generalisations of uncertainty for a given season may not apply to other seasons. All three models produce simulated temperatures whose variance underestimates that seen in nature.

4. Discussion and Conclusions

These analyses quantify some of the uncertainty that is present in model hind- and forecasts at a regional level. This uncertainty can subsequently impact perceptions of how temperature – dependent ecosystem variables (e. g., timing of plankton blooms, duration of growth seasons for biota, occurrence of physiologically stressful temperatures for local and immigrating biota) could be affected depending on model choice (Jones et al. 2012; MacKenzie

et al. 2012; Niiranen et al. 2013). Potential approaches for incorporating inter-model uncertainty in climate projections of oceanographic and ecosystem responses could include bias corrections and development of unweighted or weighted ensemble averages of hind- or forecasts, as well as continued development and implementation of process knowledge related to the phenomenon of interest.

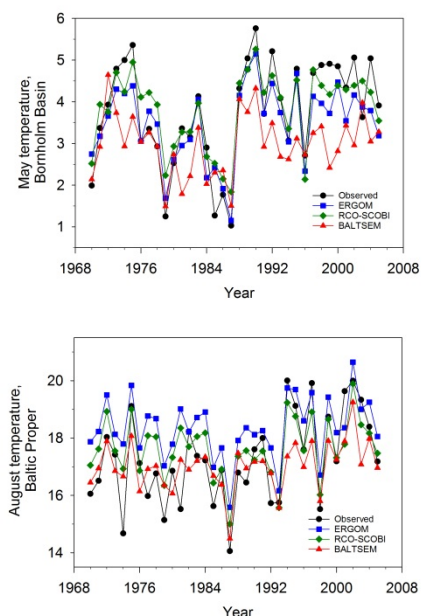


Figure 1. Inter-annual variability in sea temperatures as estimated by three regional oceanographic models for the Baltic Sea based on ERA40 hindcast outputs, and as estimated from in situ observations contained in the ICES hydrographic database. Top panel: temperatures at 45-65 m depth in the Bornholm Basin during May; bottom panel: temperatures at 0-10 m in the Baltic Proper during August.

Some preliminary results of weighted and unweighted ensemble averages will be presented at the meeting.

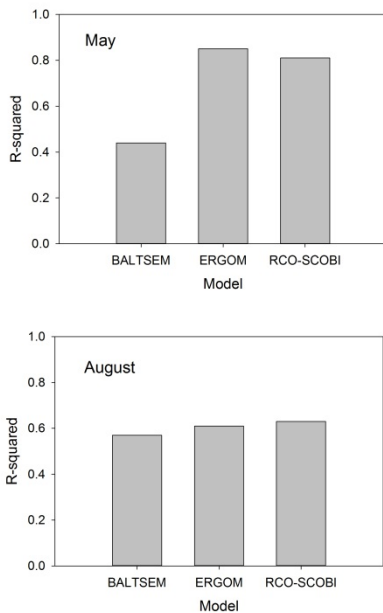


Figure 2. Explained variance (R^2) as measure of goodness-of-fit between in situ observations of sea temperature and modelled temperatures derived from three regional oceanographic models for May (Bornholm Basin, 45–65 m) and August (Baltic Proper, 0 – 10 m). The comparison is based on annual May and August data for 1970–2005.

References

- Hollowed, A. B., Barange, M., Beamish, R., Brander, K., Cochrane, K., Drinkwater, K., Foreman, M., Hare, J., Holt, J., Ito, S., Kim, S., King, J., Loeng, H., MacKenzie, B. R., Mueter, F., Okey, T., Peck, M. A., Radchenko, V., Rice, J., Schirripa, M., Yatsu, A., Yamanaka, Y. 2013. Projected impacts of climate change on marine fish and fisheries. *ICES. J. Mar. Sci.* 70:1023–1037
- Jones, M. C., Dye, S. R., Pinnegar, J. K., Warren, R., and Cheung, W. W. L. 2012. Modelling commercial fish distributions: Prediction and assessment using different approaches. *Ecological Modelling*, 225: 133–145.
- MacKenzie, B. R., Meier, H. E. M., Lindegren, M., Neuenfeldt, S., Eero, M., Blenckner, T., Tomczak, M., Niiranen, S. 2012. Impact of climate change on fish population dynamics in the Baltic Sea – a dynamical downscaling investigation. *Ambio* 41: 626–646; doi: 10.1007/s13280-012-0325-y
- Gårdmark, A., Lindegren, M., Neuenfeldt, S., Blenckner, T., Heikinheimo, O., Müller-Karulis, B., Niiranen, S., Tomczak, M. T., Aro, E., Wickström, A., Möllmann, C. 2013. Biological ensemble modelling to evaluate potential futures of living marine resources. *Ecological Applications*, 23: 742–54.
- Meier, H. E. M., Andersson, H. C., Arheimer, B., Blenckner, T., Chubarenko, B., Donnelly, C., Eilola, K., Gustafsson, B. G., Hansson, A., Havenhand, J., Hoglund, A., Kuznetsov, I., MacKenzie, B. R., Müller-Karulis, B., Neumann, T., Niiranen, S., Piwowarczyk, J., Raudsepp, U., Reckermann, M., Ruoho-Airola, T., Savchuk, O. P., Schenk, F., Schimanke, S., Vali, G., Weslawski, J.-M., Zorita, E. 2012. Comparing reconstructed past variations and future projections of the Baltic Sea ecosystem—first results from multi-model ensemble simulations. *Environ. Res. Lett.* 7 (2012) 034005 (8pp); doi:10.1088/1748-9326/7/3/034005
- Niiranen, S.; Yletyinen, J.; Tomczak, M.; Blenckner, T.; Hjerne, O.; MacKenzie, B. R.; Müller-Karulis, B.; Neumann, T.; Meier, M. 2013. Combined effects of global climate change and regional ecosystem drivers on an exploited marine food web. *Global Change Biology* 19: 3327–3342.
- Payne, M. R., Barange, M., Batchelder, H. P., Cheung, W. W. L., Cormon, X., Eddy, T. D., Fernandes, J. A., Hollowed, A. B., Jones, M. C., Link, J. S., MacKenzie, B. R., Neubauer, P., Ortiz, I., Queirós, A. M., Paula, J. R. 2015. Uncertainties in projecting climate change impacts in 1 marine ecosystems. Submitted to *ICES J. Mar. Sci.*
- Samuelsson, P., C.G. Jones, U. Willen, A. Ullerstig, S. Gollvik, U. Hansson, C. Jansson, E. Kjellstrom, et al. 2011. The Rossby centre regional climate model RCA3: Model description and performance. *Tellus Series A-Dynamic Meteorology and Oceanography* 63: 4–23. doi:10.1111/j.1600-0870.2010.00478.x.
- Stock, C. A., Alexander, M. A., Bond, N. A., Brander, K. M., Cheung, W. W. L., Curchitser, E. N., Delworth, T. L., Dunne, J. P., Griffies, S. M., Haltuch, M. A., Hare, J. A., Hollowed, A. B., Lehodey, P., Levin, S. A., Link, J. S., Rose, K. A., Rykaczewsk, R. R., Sarmiento, J. L., Stouffer, R. J., Schwing, F. B., Vecchi, G. A., Werner, F. E. 2011. On the use of IPCC-class models to assess the impact of climate on Living Marine Resources. *Prog. Oceanog.* 88: 1–27.
- Uppala, S., P. Kallberg, A. Simmons, U. Andrae, V. Bechtold, M. Fiorino, J. Gibson, J. Haseler, et al. 2005. The ERA-40 re-analysis. *Q. J. R. Meteorological Society* 131: 2961–3012. doi: [10.1256/qj.04.176](https://doi.org/10.1256/qj.04.176).

The Regional Earth System Model (RegESM) using RegCM4 coupled with the MITgcm ocean model: First assessments over the MED-CORDEX domain.

Laura Mariotti¹, Ufuk Utku Turunçoğlu^{2,1}, Riccardo Farneti¹, Gianmaria Sannino³, Giovanna Pisacane³, MariaVittoria Struglia³, Adriana Carillo³, Alessandro Dell'Aquila³, Sandro Calmanti³, Lina Sitz¹, Ramon Franco Fuentes¹, Fabio Di Sante¹

¹ The Abdus Salam International Centre for Theoretical Physics- ICTP, Trieste, Italy (mariotti@ictp.it)

² Informatics Institute, Istanbul Technical University, Istanbul, Turkey

³ SSPT-MET-CLIM Laboratory - ENEA Centro di ricerche, Roma, Italy

In the framework of global climate studies, there is an increasingly growing concern about the vulnerability of the Mediterranean region, where high population density and intense exploitation activities pose severe questions on the sustainability of terrestrial water management, both for the present and the future. On the other hand, ocean modelling studies suggest that the Mediterranean thermohaline circulation could be weakened in conditions of global greenhouse warming (Thorpe et al, 2000, Somot et al. 2006), an event which would undoubtedly affect regional climate, possibly triggering global feedback processes. Somot et al. (2008) suggested that ocean-atmosphere coupled models might be necessary for a reliable assessment of local climate over the Mediterranean, as they observed an amplification of the climate change signal with respect to analogous experiments performed with standalone atmospheric models. Such a result was attributed to better consistency between the high resolution SST field and to the improved simulation of energy fluxes at the atmosphere-ocean interface and of the vertical structure of the atmosphere. Experiments with the atmosphere-ocean coupled system developed within the HyMEX framework during the last years confirmed that a good comprehension of Mediterranean processes requires the explicit inclusion of the feedbacks between the atmospheric and the oceanic components, thus achieving a complete, fully coupled description of the Mediterranean hydrological cycle, at the same time gaining new insights in our current ability to reproduce the atmospheric hydrological processes (e.g. the repartition of precipitation between water and snow) and to close the hydrological balance. However, such tests also highlighted the need for substantial spatial resolution enhancement and for more frequent coupling of the two components, in order to avoid lags in their separate evolution between successive coupling times. These issues are addressed by the upgraded PROTHEUS system which was jointly developed by ENEA and ICTP.

Here we present a first evaluation of the performances of the new PROTHEUS system (called PROTHEUS 2.0) composed by the regional climate model RegCM4 (Giorgi et al. 2012) coupled with both the ocean model MITgcm (Marshall J. et al. 1997a,b) and the HD river model (Max-Planck's HD model; Hagemann and Dümenil, 1998) using RegESM (Regional Earth System Model) as a driver.

The three-component (atmosphere, ocean and river routing) fully coupled model exchanges sea surface temperature (SST) from the ocean to the atmospheric model, surface wind stress, energy and freshwater fluxes from the atmosphere to the ocean model, surface and sub-

surface runoff from the atmospheric component to the river routing model (Max-Planck's HD model; Hagemann and Dümenil, 1998). In order to have water conservation within the system, the river routing component sends the calculated river discharges to the ocean model.

The evaluation is presented for the MED-CORDEX region (Fig. 1) using three simulations: the first one uses the regional climate model RegCM4 driven by the perfect boundary conditions provided by ERA-Interim and prescribed SST; the second one is performed only with the ocean component driven by a downscaled ERA-Interim data; and the third one is performed with the fully coupled modeling system (RegCM4 ,MITgcm and HD).

The fully coupled Regional Earth System Model (RegESM) is also been tested over the Central-American and the South Asia CORDEX regions.

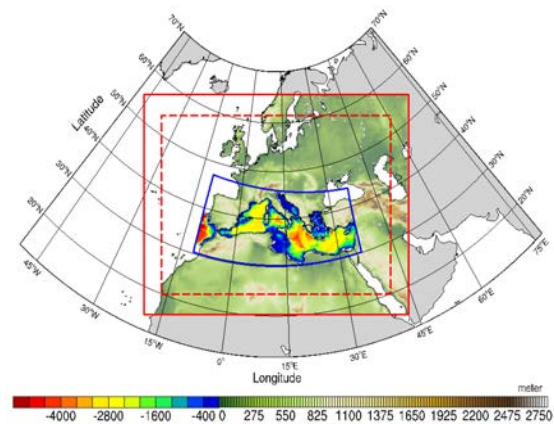


Figure 1. The domain map for the RegESM simulation with topography of atmosphere model (RegCM) and bathymetry of ocean component (MITgcm). The solid red box indicates full atmospheric model domain, relaxation zone is indicated between solid and dashed red box. The blue solid box shows ocean model domain.

References

- Giorgi F., Coppola E., Solmon F., Mariotti L. and others (2012) RegCM4: model description and preliminary tests over multiple CORDEX domains. *Clim. Res.*, 52, pp.7-29
- Marshall J. et al. (1997a) A finite-volume, incompressible navier stokes model for studies of the ocean on parallel computers, *J. Geophys. Res.*, 102(C3), pp. 5753-5766
- Marshall J. et al. (1997b) Hydrostatic, quasi-hydrostatic, and non-hydrostatic ocean modeling, *J. Geophys. Res.*, 102(C3), pp.5733-5752
- Hagemann S. and Dümenil Gates L. (2001) Validation of the hydrological cycle of ECMWF and NCEP reanalyses using the MPI hydrological discharge model. *J Geophys Res.*, 106, pp1503-1510
- Somot, S., Sevault F. and M. Deque: Transient climate change scenario simulation of the Mediterranean Sea for the twenty-first century using a high-resolution ocean circulation model, *Climat Dynamics*, 27, 851–879, DOI 10.1007/s00382-006-0167-z, 2006
- Somot, S., Sevault F., M. Deque and M. Crepon: 21st century climate change scenario for the Mediterranean using a coupled atmosphere–ocean regional climate model, *Global and Planetary Change*, 63(2-3), 112-126, 2008
- Thorpe, R. B. and G. R. Bigg: Modelling the sensitivity of the Mediterranean outflow to anthropogenically forced climate change, *Climate Dynamics*, 16, 355-368, 2000

Evaluating the utility of dynamical regionalization of climate for predicting climate impacts on forests”

Nicolas Martin-StPaul¹, Marc Stéfanon², Joannès Guillemot³, Julien Ruffault⁴, Christophe François³, Samuel Somot⁵, Eric Dufrêne³, Paul Leadley³

¹ Ecologie des Forêts Méditerranéennes, INRA, UR629, F-84914 Avignon, France

² Laboratoire des Sciences du Climat et de l'Environnement (LSCE) - Institut Pierre Simon Laplace, CEA/CNRS/UVSQ, Gif sur Yvette, France (marc.stefanon@lsce.ipsl.fr)

³ Laboratoire d'Écologie Systématique et Évolution (ESE), (UMR 8079 CNRS/Univ. Paris-Sud/AgroParisTech), Orsay, France

⁴ CEFÉ, CNRS, Campus du CNRS, 1919, route de Mende 34293 Montpellier, France

⁵ Météo-France CNRM, 42 av. Gaspard Coriolis, 31057, Toulouse Cedex, France

Ecological studies have demonstrated that fine resolution climate products are required for a proper assessment of climate change impacts on ecosystem services and biodiversity. Most of the current climate products used in impact studies ultimately come from climate modelling and particularly from the dynamic regionalization of climate performed with regional climate models (RCM). It therefore appears important to assess whether the dynamic regionalization of climate help to improve the prediction of ecosystem services and biodiversity. We drew on the regional climate simulations from the MedCordex initiative to evaluate whether finer resolution climate products may improve the simulations of forest growth and tree distributional range (oak and beech).

To test this, we compared measured and simulated forest growth using the model CASTANEA forced by different climate products derived from: (1) Climate simulations at 3 different resolutions (140km, 44km, 12 Km) from the RCM Aladin forced by Era-Interim at the boundaries (Ala-ERAi); (2) climate simulations at 140km from the GCM CNRCM (CNRCM); (3) climate simulation from the RCM Aladin at 12km forced by CNRCM at the boundaries (Ala-CNRCM) and finally (4) the re-analysis ERA-Interim (~60km resolution) and SAFRAN (8km) as references. We found that when CASTANEA was forced with Aladin-ERAi, increasing the spatial resolution from 140 km to 12 km greatly improved the simulations of forest growth and ranges. Goodness of fit (R^2 and best TSS) between simulated and observed biometric variables (growth and presence/absence) using Aladin-ERAi climate at 12km yielded very close result that what was obtained with the reanalysis SAFRAN. Conversely, when we used CNRCM climate (140km) as

forcing entries, goodness of fit between simulated and observed biometric variables were better than when using the regionalization at 12km from Ala-CNRCM. Our results indicate that climate regionalization can improve the prediction of forest ecological impacts only when reanalysis (closer to real data) are used to force the RCM at the boundaries. Consequently much effort should be invested to improve the climate data used to force RCM at their boundaries, to help improving assessments of climate change impacts on forests.

References

- Chebib A, Badeau V, Boe J, et al. Climate change impacts on tree ranges: model intercomparison facilitates understanding and quantification of uncertainty. *Ecol Lett.* 2012;15(6):533-44. 1.
- Dufrene E, Davi H, Francois C, le Maire G, Le Dantec V, Granier A. Modelling carbon and water cycles in a beech forest Part I: Model description and uncertainty analysis on modelled NEE. *Ecol Modell.* 2005;185(2-4):407-436.
- Radu R, Déqué M, Somot S. Spectral nudging in a spectral regional climate model. *Tellus A.* 2008;60(5):898-910.
- Randin CF, Engler R, Normand S, et al. Climate change and plant distribution: local models predict high-elevation persistence. *Glob Chang Biol.* 2009;15(6):1557-1569.
- Stéfanon, M., Martin, N., Leadley, P., Bastin, S., Dell'Aquila, A., Drobinski, P., Gallardo, C., (2015), Testing climate models using an impact model: what are the advantages?, *Climatic Change*, p.1-13, doi:10.1007/s10584-015-1412-4
- Trivedi MR, Berry PM, Morecroft MD, Dawson TP. Spatial scale affects bioclimate model projections of climate change impacts on mountain plants. *Glob Chang Biol.* 2008;14(5):1089-1103.

Regional climate system modelling for European sea regions – aims of the workshop

H.E. Markus Meier^{1,2}, Marcus Reckermann³, Anna Rutgersson⁴, Gianmaria Sannino⁵ and Samuel Somot⁶

¹ Leibniz-Institute for Baltic Sea Research Warnemünde, Department of Physical Oceanography and Instrumentation, Rostock, Germany (markus.meier@io-warnemuende.de)

² Swedish Meteorological and Hydrological Institute, Norrköping, Sweden

³ Department of Earth Sciences Uppsala University, Uppsala, Sweden

⁴ International Baltic Earth Secretariat, Helmholtz Zentrum Geesthacht, Geesthacht, Germany

⁵ Italian National Agency for New Technologies, Energy and Sustainable Economic Development, Rome, Italy

⁶ Centre National de Recherches Météorologiques (Météo-France/CNRS, CNRM-GAME), Toulouse, France

1. Introduction to Baltic Earth and HyMeX

Baltic Earth (Fig. 1) is an international, interdisciplinary and curiosity driven science program and the successor to BALTEX (1992-2013) (Meier et al., 2014). The vision of Baltic Earth is to achieve an improved Earth System understanding of the Baltic Sea region based upon a holistic view that encompasses processes in the atmosphere, land, and sea as well as in the anthroposphere. Within the program scientists formulate research challenges that will regularly be updated. Examples of grand challenges that are currently in focus are the salinity dynamics in the Baltic Sea, land-sea biogeochemical feedbacks, natural hazards and extreme events, sea level dynamics and regional variability of water and energy exchange. In addition, thematic assessments of particular research topics, compiled by expert groups, are performed with the intention to identify gaps in the current knowledge. An example for such a thematic assessment with a benefit for society is the Assessment of Climate Change for the Baltic Sea Basin (BACC author team, 2008; BACC II author team, 2015) which summarizes the available knowledge on past, present and future climates in the Baltic Sea region.

HyMeX (HYdrological cycle in the Mediterranean Experiment, Fig. 2) is an international, multi-disciplinary and coordinated science program (Drobinski et al. 2014). The HyMeX scientific challenges and strategies to address them have been defined by the international community for the decade 2010-2020 in the HyMeX International Science Plan and the International Implementation Plan. HyMeX aims at a better understanding and quantification of the hydrological cycle and related processes in the Mediterranean, with emphasis on high-impact weather events, inter-annual to decadal variability of the Mediterranean coupled system, and associated trends in the context of global change (Ducrocq et al. 2014). The main strategies are: (1) monitoring and modelling the Mediterranean atmosphere-land-ocean coupled system (Ruti et al. 2015), its variability from the event to the seasonal and interannual scales, and its characteristics over one decade (2010-2020) in the context of global change and (2) assessing the social and economic vulnerability to extreme events and adaptation capacity. The multidisciplinary research and the database developed within HyMeX should contribute to improve observational and modelling systems, especially for coupled systems, better predict extreme events, simulate the long-term water-cycle more accurately, and provide guidelines for

adaptation measures, especially in the context of global change.



Figure 1. Logo Baltic Earth - An Earth System Science Program for the Baltic Sea Region.



Figure 2. Logo HyMeX – Hydrological Cycle in Mediterranean Experiment.

2. A review of regional climate system modeling

General Circulation Models (GCMs) are needed because changing climate is a global phenomenon. However, GCMs are usually too coarse to resolve regional scales of interest in climate change impact studies and very often fail to deliver reliable information on regional scales like the Baltic Sea or Mediterranean Sea. To overcome this scale problem basically two methods are used, statistical and dynamical downscaling. Applying the dynamical downscaling method means that a simulation with a regional climate model (RCM) with higher spatial resolution is performed driven with GCM output at the lateral boundaries. The other method is statistical downscaling where a statistical relationship between observed local and large scale variables is established and applied to GCM output.

Since the 1990s more and more regional scenario simulations for European seas became available. To investigate how physical and biogeochemical variables of regional seas may change in a future climate, a consistent dynamical downscaling approach is needed. This requires a sufficiently highly resolved coupled physical-biogeochemical model, driven with appropriate atmospheric forcing (i.e. air-sea fluxes of momentum, energy and matter including the atmospheric deposition of nitrogen and carbon fluxes), hydrological forcing (volume, carbon and nutrient flows from the catchment area) and lateral boundary data. In addition, model consistent initial conditions are needed. If only time slices of present and future climates are calculated instead of the transient evolution under changing climate, initial conditions for both time slices are needed.

In recent years, coupled atmosphere – sea ice – ocean regional climate models were further elaborated by using a hierarchy of sub-models for the various components of the regional climate system combining atmosphere regional climate models, inter alia, with physical ocean, surface waves, land vegetation, hydrology and land biochemistry, natural and anthropogenic aerosols, marine biogeochemistry, the marine carbon cycle, marine biology and food web modelling. Hence, there is a tendency to develop so-called Regional Climate System Models (RCSMs) or Regional Earth System Models (RESMs) with the aim to investigate the impact of various climate components on the regional climate variability and change using high-resolution representation of the different drivers. This new generation of regional climate models is also able to provide for the first time an integrated view of the impacts of climate change on the entire marine environment.

In this presentation we will briefly review the state-of-the-art in regional climate system modeling for European sea regions, like the Baltic Sea, North Sea, Mediterranean Sea, Black Sea, Arctic Ocean and North East Atlantic.

3. Aims of the workshop

During this workshop, challenges in regional climate system modelling and possibilities for collaboration will be discussed. One aim is to define broad scientific questions that can gather the various geographical communities of the European Seas (or even at larger scales). Some selected questions are (the list is open to further questions to be discussed at the workshop):

- What are the expected integrated impacts of climate change over the European Seas?
- What is the role of the various regional climate drivers in the past climate variability and trends in Europe (e.g. regional aerosols, regional land-use, regional SST)?
- What are the regional climate drivers missing in low-resolution GCMs to estimate a consistent regional climate change evolution (regional aerosols, regional land-use, regional SST)?
- What is the added value of using RCSM or RESM when studying key regional climate phenomena?
- What kind of new climate/ocean services could be developed from the use of RCSM or RESM?

The overarching goal of the workshop is the establishment of a common research community across regions for collaboration in joint projects.

References

- BACC Author Team (2008) Assessment of Climate Change for the Baltic Sea basin. Springer Verlag, Berlin, Heidelberg
- BACC II Author Team (2015) Second Assessment of Climate Change for the Baltic Sea basin. Springer Verlag, Berlin, Heidelberg
- Drobinski P., V. Ducrocq, P. Alpert, E. Anagnostou, K. Béranger, M. Borga, I. Braud, A. Chanzy, S. Davolio, G. Delrieu, C. Estournel, N. Filali Boubrahmi, J. Font, V. Grubisic, S. Gualdi, V. Homar, B. Ivančan-Picek, C. Kottmeier, V. Kotroni, K. Lagouvardos, P. Lionello, M. C. Llasat, W. Ludwig, C. Lutoff, A. Mariotti, E. Richard, R. Romero, R. Rotunno, O. Roussot, I. Ruin, S. Somot, I. Taupier-Letage, J. Tintore, R. Uijlenhoet, and H. Wernli (2014) HYMEX, a 10-Year Multidisciplinary Program on the Mediterranean Water Cycle. BAMS 95(7), DOI:10.1175/BAMS-D-12-00242.1
- Ducrocq, V., Braud, I., Davolio, S., Ferretti, R., Flamant, C., Jansa, A., Kalthoff, N., Richard, E., Taupier-Letage, I., Ayrat, P.-A., Belamari, S., Berne, A., Borga, M., Boudevillain, B., Bock, O., Boichard, J.-L., Bouin, M.-N., Bousquet, O., Bouvier, C., Chiggiato, J., Cimini, D., Corsmeier, U., Coppola, L., Cocquerez, P., Defer, E., Delanoë, J., Di Girolamo, P., Doerenbecher, A., Drobinski, P., Dufournet, Y., Fourrié, N., Gourley, J.J., Labatut, L., Lambert, D., Le Coz, J., Marzano, F.S., Molinié, G., Montani, A., Nord, G., Nuret, M., Ramage, K., Rison, W., Roussot, O., Said, F., Schwarzenboeck, A., Testor, P., Van Baelen, J., Vincendon, B., Aran, M., Tamayo, J. (2014) HyMeX-SOP1: The field campaign dedicated to heavy precipitation and flash flooding in the northwestern Mediterranean. BAMS, 95(7), pp. 1083-1100.
- Ruti, P., Somot S., Giorgi F., Dubois C., Flaounas E., Obermann A., Dell'Aquila A., Pisacane G., Harzallah A., Lombardi E., Nabat P., Onol B., Rajkovic B., Ramage K., Sevaut F., Sannino G., Struglia M.V., Sanna A., C. Torma, V. Vervatis MED-CORDEX initiative for Mediterranean Climate studies (2015) BAMS 09/2015; DOI: 10.1175/BAMS-D-14-00176
- Meier, H. E. M., A. Rutgersson, and M. Reckermann (2014) Baltic Earth - A new Earth System Science Program for the Baltic Sea Region. EOS, Trans. AGU, 95(13), 109-110

Which complexity of regional climate system models is essential for downscaling of anthropogenic climate change for the North Sea?

Uwe Mikolajewicz, Moritz Mathis and Alberto Elizalde

Max-Planck-Institut f. Meteorologie, Hamburg, Germany (uwe.mikolajewicz@mpimet.mpg.de)

1. Introduction

The spatial resolution of the current generation of global climate models, which have been used e.g. in the framework of CMIP5 to project anthropogenic climate change, is so coarse, that these models are generally not suitable to adequately simulate the current ocean climate on the Northwest European Shelf, the Baltic, the Mediterranean and the Black Seas. On the other side these regions are intensely economically utilized and many people live around their coasts. Thus, projections of the effect of anthropogenic climate change on these seas are highly demanded.

In atmospheric sciences dynamical downscaling of results from global climate models using regional atmospheric models is a widely used standard procedure. For the shelf seas the appropriate methodology is much less mature. The simplest approach is to force a regional ocean model with atmospheric forcing either directly from a global atmosphere model or from an atmospheric downscaling simulation. The oceanic change at the domain margins of the regional ocean model are specified according to the changes in the coarse resolution global ocean model. Often the forcing applied to the regional ocean model has been 'bias-corrected' meaning that the only the anomalies from the global model are passed to the regional ocean model. At the high end of complexity, regionally coupled climate models (or climate system models) have recently been developed and successfully applied. These models are computationally far more expensive and increase the complexity of model tuning and application. For the North Sea recently a set of simulations with three different coupled model systems has been performed and analyzed (Bülow et al. 2014). However, it is not fully clear yet, what the benefit of this gain in complexity is, and whether some questions can still be answered reliably with simpler model systems. Here we will present results from a set of experiments, where different ocean-downscaling approaches for the North Sea have been applied.

2. Model system

The simulations used here have been performed either with the complete regionally coupled climate model system developed at the MPI-M (Mikolajewicz et al. 2005, Sein et al. 2015) or with reduced subsystems. The model system consists of the formally global ocean model MPIOM with grid poles located in SW Germany and near Chicago, yielding maximal resolution along the German and Dutch North Sea coasts. This model is fully coupled to the regional atmosphere model REMO (Majewski 1991, Jacob et al. 2001) in a set-up covering the EURO-CORDEX domain. The hydrological cycle is closed with a terrestrial run-off model (Hagemann and Dümenil-Gates 2001).

3. Experiments

This model system has been used to downscale a CMIP5 simulation of the MPI-ESM-LR model to the northwest European Shelf. The complexity of the ocean-downscaling approach ranges from direct application of the atmospheric forcing interpolated from the global climate model to application of a fully coupled regional earth system model. A set of transient experiments have been performed starting with the historical simulation in 1920 until the end of the RCP8.5 scenario simulation ending in year 2100.

4. Preliminary results

The planned set of simulation has not been completed yet, some simulations are still ongoing. The results are compared with the original results of the global climate model.

First results indicate that in the North Sea the large scale SST change at the end of the century is essentially determined by the global model. However, there are a few noticeable exceptions. Near the coasts the regional coupling clearly modifies the pattern of anthropogenic climate change, showing marked differences in simulated SST change to the results from e.g., the uncoupled ocean-only downscaling simulation. The higher spatial resolution and the inclusion of tides in the regional ocean model have a marked impact on the simulated temperature change in the English Channel and near the shelf edge in the Norwegian Sea in comparison to the global climate model.

The simulated general freshening of the North Sea is largely determined by the inflowing water masses from the Atlantic which originates from the global climate model. The ocean regionalization and the modified river run-off allow for the additional development of a band of low salinities along the continental coast of the North Sea. The enhanced outflow of freshwater from the Baltic is reflected in a band of negative salinity anomalies along the Norwegian coast.

The cyclonic circulation of the North Sea is intensified in winter independent of the downscaling approach. In summer the reduced inflow of Atlantic water masses through the English Channel seems to be a robust feature among the downscaling simulations.

5. References

- Bülow, K., et al. (2014), Comparison of three regional coupled ocean atmosphere models for the North Sea under today's and future climate conditions, KLIWAS-27/2014, 265 pp., Koblenz, BfG, Koblenz, Germany, doi:10.5675/Kliwas_27/2014.
- Hagemann, S., and L. Dümenil Gates (2001), Validation of the hydrological cycle of ECMWF and NCEP reanalyses using the MPI hydrological discharge model, *J. Geophys. Res.*, 106, 1503–1510.
- Jacob, D., et al. (2001), A comprehensive model intercomparison study investigating the water budget during the BALTEX-PIDCAP period, *Meteorol. Atmos. Phys.*, 77(1-4), 19–43.
- Majewski, D. (1991), The Europa modell of the Deutscher Wetterdienst, in Seminar Proceedings ECMWF, vol. 2, pp. 147–191, ECMWF, Reading, U. K.
- Mikolajewicz, U., D. Sein, D. Jacob, T. Kahl, R. Podzun, and T. Semmler (2005), Simulating Arctic sea ice variability with a coupled regional atmosphere-ocean-sea ice model, *Meteorol. Z.*, 14(6), 793–800.
- Sein, D.V., U. Mikolajewicz, M. Gröger, I. Fast, W. Cabos, J.G. Pinto, S. Hagemann, T. Semmler, A. Izquierdo and D. Jacob (2015). Regionally coupled atmosphere-ocean-sea ice-marine biogeochemistry model ROM. Part 1: Description and validation. *Journal of Advances in Modeling Earth Systems*, 7, 268-304. doi:10.1002/2014MS000357

Direct and semi-direct aerosol radiative effect on the Mediterranean climate variability using a coupled regional climate system model

Pierre Nabat, Samuel Somot, Marc Mallet, Florence Sevault, Marc Chiacchio and Martin Wild

Laboratoire Aerologie, UPS/CNRS, Toulouse, France, (marc.mallet@aero.obs-mip.fr)

1. Motivation

The Mediterranean region is one of the regions which have the highest aerosol loads owing to air masses carrying numerous and various aerosol types (Lelieveld et al. 2002). These anthropogenic and natural aerosols lead to strong effects on the regional radiative budget and climate of the Mediterranean (Rosenfeld et al. 2001). This diversity results in a large variety in physico-chemical and optical aerosol properties over the basin. Numerous studies have used in-situ measurements and radiative transfer models to quantify the direct effect of different aerosol types over the basin: notably dust aerosols (Meloni et al. 2004), biomass burning (Formenti et al. 2002) and anthropogenic aerosols (Markowicz et al. 2002). Up to now, aerosol radiative and climatic effects have essentially been studied using numerical simulations covering short-time periods. In this study the objective is to assess the direct and semi-direct effects of aerosols on the regional climate of the Mediterranean, as well as their role in the radiation-atmosphere-ocean interactions, using the fully coupled regional climate system model developed at CNRM, namely CNRM-RCSM4.

2. Methodology

CNRM-RCSM4 includes the regional climate atmospheric model ALADIN-Climate (50 km resolution, version 5.2, Déqué and Somot 2008), the land-surface model ISBA, the river routing scheme TRIP and the regional ocean model NEMOMED8. ALADIN includes the Foucart and Morcrette radiation scheme, based on the ECMWF model incorporating effects of greenhouse gases, direct effects of aerosols as well as the first indirect effect of sulfate aerosols.

The domain chosen for this study includes the official domain of the Med-CORDEX program. The model ALADIN-Climate incorporates a radiative scheme to take into account the direct and semi-direct effects of five aerosol types (sea salt, desert dust, sulfates, black and organic carbon aerosols) through AOD climatologies (Nabat et al. 2013), who proposed a new AOD monthly inter-annual climatology over the period 2003–2009, based on a combination of satellite-derived and model-simulated products.

Different configurations have been used for simulations in the present work, depending on the presence of aerosols, and on the use of the whole RCSM or the atmospheric model only. The simulation defined as the reference for this study, called C-AER, has used the fully coupled RCSM described previously with the mentioned aerosol fields. The lateral boundary conditions are provided by the ERA-INTERIM reanalysis (Dee et al. 2011). The simulation covers the period 2003–2009, after a spin-up period of 2 years (beginning in 2001). Ensembles of 6 simulations for each configuration (with and without aerosols, with the fully system or the atmospheric model only) have been carried out using the same methodology.

3. Results

Our simulations show a major impact of aerosols on the regional climate. Figure 1 presents the average aerosol net direct radiative forcing (DRF) at the surface and at the TOA for SW (b) and LW (c) radiation calculated in the C-AER simulations. The scattering and absorption of the incident radiation by the various aerosols cause a negative direct radiative forcing in SW radiation at the surface. Over Europe, the surface SW DRF is estimated at -19.4 Wm^{-2} and reaches its maximum in summer (-25 Wm^{-2} in July). It is dominated throughout the year by the sulfate forcing with a maximum in absolute terms in June, and accentuated in July by organic and dust aerosols. With regards to LW radiation, only dust aerosols have a significant impact because of their microphysical properties, and notably the presence of coarse dust mode.

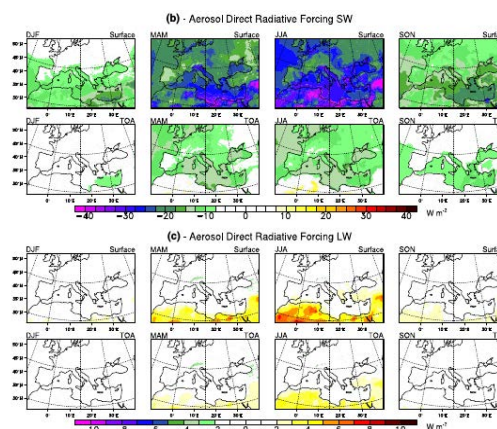


Figure 1. Direct radiative forcing (SW and LW) of aerosols at the surface and top of the Atmosphere (TOA).

Figure 2 presents the seasonal average difference between C-AER and C-NO (without aerosols) in terms of SST, latent heat loss, surface specific humidity and precipitation. With regards to SST, the decrease is estimated at $0.5 \text{ }^\circ\text{C}$ on average over the Mediterranean Sea, and can reach $1 \text{ }^\circ\text{C}$ in summer in the Adriatic Sea and near the African coast. The modification of SST by aerosols involves changes in the heat budget over the Mediterranean Sea including air-sea fluxes (Figure 2). The sensible heat loss has substantially decreased over Europe (-4.7 Wm^{-2}) and northern Africa (-8.5 Wm^{-2}), especially in summer, probably due to a decrease in surface temperature. Moreover, aerosols cause a significant decrease in the latent heat loss over the Mediterranean Sea, reaching -13.6 Wm^{-2} in summer and -13.5 Wm^{-2} in autumn.

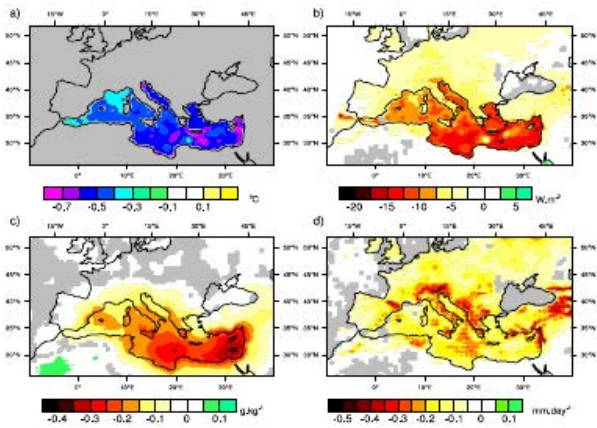


Figure 2. Differences in SST, latent heat fluxes, specific humidity and precipitation between two simulations including or not aerosol radiative forcing.

As a result of the decrease of the latent heat loss, surface specific humidity also decreases with the presence of aerosols. This diminution ranges from -0.1 g/kg in winter to -0.5 g/kg in summer near the western coasts and in the Ionian basin. In line with this decrease in humidity, the comparison of simulations reveals a decrease of cloud cover, (ranging from -1 to -3 % over the Mediterranean Sea and Europe, in spring and summer). Consequently, aerosols also tend to reduce precipitation: -0.2 mm/day on annual average over the Mediterranean Sea.

4. Conclusion and perspectives

This study allows characterizing the aerosol radiative and climatic effects over the Mediterranean. Because of the absorption and scattering of the incident solar radiation, the SW surface direct effect is negative, equal on average to -20.9 Wm $^{-2}$ over the Mediterranean Sea, -14.7 Wm $^{-2}$ over Europe and -19.7 Wm $^{-2}$ over northern Africa. The LW surface direct effect is weaker as only dust aerosols contribute. This direct cooling effect is partly counterbalanced by a positive semi-direct SW forcing over the Mediterranean Sea (4.7 Wm $^{-2}$ on average) and Europe (3.0 Wm $^{-2}$) due to changes in cloud cover and atmospheric circulation. The net (semi-direct plus direct) aerosol surface effect is consequently negative over Europe, the Mediterranean Sea and northern Africa and is responsible for a decrease in land (-0.4 °C over Europe and -0.5 °C over northern Africa) and sea surface temperature (-0.5 °C for the Mediterranean Sea).

The coupled system used in this work highlights for the first time the consequences of the decrease of SST due to aerosols on the Mediterranean climate. Such changes in SST are shown to decrease the latent heat loss (-11.0 Wm $^{-2}$ on average over the Mediterranean Sea) resulting in a decrease in specific humidity in the lower troposphere, and a reduction in cloud cover and precipitation.

References

- Dee DP. et al. (2011) The era-interim reanalysis: configuration and performance of the data assimilation system. *Q J R Meteorol Soc* 137:553–597. doi:10.1002/qj.828.
- Dequé, M, Somot S. (2008) Extreme precipitation and high resolution with aladin. *Idöjaras QJ Hung Meteorol Serv* 112(3–4):179–190.
- Formenti P. et al. (2002) Staaarte-med 1998 summer airborne measurements over the aegean sea 2. Aerosol scattering and absorption, and radiative calculations. *J Geophys Res* 107:D21. doi:10.1029/2001JD001536.
- Lelieveld J. et al. (2002) Global air pollution crossroads over the mediterranean. *Science* 298:794–799. doi:10.1126/science.1075457.
- Markowicz KM. et al. (2002) Absorbing mediterranean aerosols lead to a large reduction in the solar radiation at the surface. *Geophys Res Lett* 29:1968. doi:10.1029/2002GL015767.
- Meloni D. et al. (2004) Direct radiative forcing of saharan dust in the mediterranean from measurements at lampedusa island and misr space-borne observations. *J Geophys Res* 109(D08):206. doi:10.1029/2003JD003960.
- Nabat P et al. (2013) A 4-d climatology (1979–2009) of the monthly tropospheric aerosol optical depth distribution over the mediterranean region from a comparative evaluation and blending of remote sensing and model products. *Atmos Meas Tech* 6:1287–1314. doi:10.5194/amt-6-1287-2013.
- Nabat P. et al. (2015) Direct and semi-direct aerosol radiative effect on the Mediterranean climate variability using a coupled Regional Climate System Model. *Clim. Dyn.* 44, 1127–1155, DOI:10.1007/s00382-014-2205-6.
- Rosenfeld D. et al. (2001) Desert dust suppressing precipitation: a possible desertification feedback loop. *Proc Natl Acad Sci USA* 98:5975–5980. doi:10.1073/pnas.101122798.

Mistral and Tramontane time series in (un)coupled regional climate simulations

Anika Obermann and Bodo Ahrens

IAU, Goethe University Frankfurt, Germany (Obermann@iau.uni-frankfurt.de)

1. Motivation

The Mistral and Tramontane are mesoscale winds in the Mediterranean region that travel through valleys in southern France. The cold and dry Mistral blows from the north to northwest, and travels down the Rhône valley, between the Alps and Massif Central. The Tramontane travels the Aude valley between the Massif Central and Pyrenees. Over the sea, these winds cause deep-water generation, and thus impact the hydrological cycle of the Mediterranean Sea. In this study, we evaluate coupled and uncoupled regional climate simulations in terms of Mistral and Tramontane permitting sea level pressure patterns.

2. Data

The simulations used in this work were downloaded from the Med-CORDEX database. Reanalysis runs with ERA-Interim as driving data, projections and hind casts with several models of the Med-CORDEX framework are available. The Mistral and Tramontane time series are derived from gust observations in the Mistral and Tramontane areas. Gust time series were provided by Valérie Jacq, Météo-France.

3. Time Series

To evaluate the sea level pressure patterns, a classification algorithm – comprising EOF analysis and a Bayesian network – is used (Obermann et al. 2015). Figure 1 shows the number of Mistral and Tramontane days per year for simulations with COSMO-CLM (Doms et al. 2011) and ALADIN-climate (Herrmann et al. 2011) compared to ERA-Interim.

4. Results & Outlook

ERA-Interim driven regional climate simulations are able to correctly simulate Mistral and Tramontane permitting sea level pressure patterns about 80 % of the time in 2000–2008 (Obermann et al. 2015). The simulated time series of Mistral and Tramontane days per year show a correlation with observations of about 0.6–0.7. The influence of coupling on the occurrence of Mistral and Tramontane permitting patterns will be studied. Furthermore, we want to study the development of Mistral and Tramontane situations per year/season in climate projections.

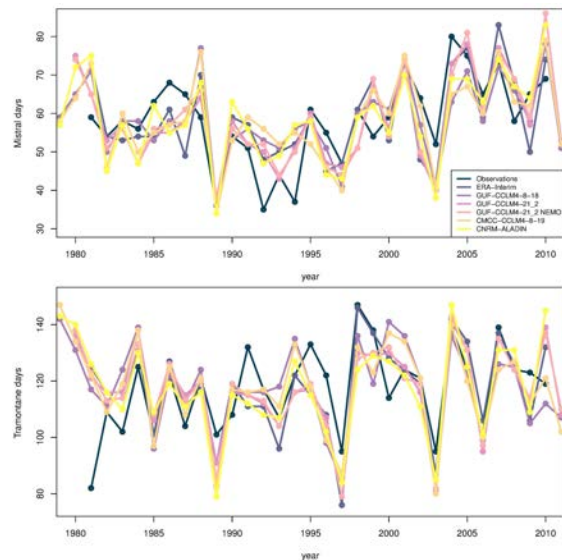


Figure 1. Number of Mistral and Tramontane days per year for several regional climate simulations.

References

- JG. Doms, J. Foerstner, E. Heise, H.-J. Herzog, D. Mironov, M. Raschendorfer, T. Reinhardt, B. Ritter, R. Schrodin, J.-P. Schulz, G. Vogel (2011): A Description of the Nonhydrostatic Regional COSMO Model, Part II: Physical Parameterization
- M. Herrmann, S. Somot, S. Calmanti, C. Dubois, F. Sevault (2011): Representation of daily wind speed spatial and temporal variability and intense wind events over the Mediterranean Sea using dynamical downscaling: impact of the regional climate model configuration, *Nat. Hazards Earth Syst. Sci.*, 11, 1983-2001
- A. Obermann, S. Bastin, S. Belamari, D. Conte, MA. Gaertner, L. Li, B. Ahrens (2015): Mistral and Tramontane wind speed and wind direction patterns in regional climate simulations (in preparation for *Climate Dynamics*)

Modeling the heat and the water balances including sea levels in the Mediterranean Sea

Anders Omstedt¹ and Mohamed Shaltout^{1,2}.

¹ Department of Marine science, University of Gothenburg, Goteborg, Sweden (anders.omstedt@gvc.gu.se)

² Department of Oceanography, University of Alexandria, Faculty of Science, Alexandria, Egypt

1. Summary

This research presents a one, two and multi basin modeling approach (PROBE-MED) when calculating the water and heat balances of the Mediterranean Sea using available meteorological and hydrological data. Through construction of nets of sub-basins the exchange of water, heat and salinity between the sub-basins were analyzed forming the base also for sea level studies. Sea levels were analyzed using gridded Mediterranean altimetry sea level (i.e dynamic topography). The future sea level changes along the Mediterranean Egyptian coast were projected using the outputs from three realizations of the Geophysical Fluid Dynamics Laboratory (GFDL) model.

2. Water and heat balances Modeling description

PROBE-MED version 1.0 was designed for analyzing the water and heat balances for the Eastern Mediterranean sub-basin (EMB), PROBE-MED version 2.0 was designed for analysing the water and heat balances in the western Mediterranean sub-basin (WMB) and EMB, PROBE-MED version 3.0 was designed for study the local features of WMB as 6 sub-basins. In future, PROBE-MED version 4.0 will be designed for study the local features of the Mediterranean Sea as 16 sub-basins. The modeling approach uses the PROBE general equation solver (Omstedt, 2011; Shaltout and Omstedt, 2015) and couples the different sub-basins using models of the inverse estuarine circulation. The basic model dynamics apply a transient Ekman flow model in each sub-basin with in- and outflows calculating the inverse estuarine circulation. A two-equation turbulent model of the turbulent kinetic energy (k) and its dissipation rate (e) was used to estimate the turbulence in the surface boundary layer. In the deep layers, the deep-water mixing was parameterized based on the stratification. The turbulent model's initial conditions for the turbulent kinetic energy and its dissipation rate assumed constant and small values. The initial temperature and salinity conditions for the two sub-basins were taken from January 1800 to avoid spin-up calculation errors. The different simulation was forced laterally using Atlantic Ocean surface properties (annual average values of 19.8 °C and 36.85 g kg⁻¹). The model was run from 1800 to 2010 with a vertically resolved 190-cell grid extending from sea surface to sea bottom and with a 600-s temporal resolution.

3. Sea level modeling description

The spatial and temporal distributions of Mediterranean sea-level variation are studied using the dynamic topography (DT) dataset over a 21-year period, focusing on seasonal and inter-annual distributions of average values and linear trends. Linear trends are calculated using ordinary least squares estimation and

tested for significance using t-tests at a 95% significance level.

The results of the three GFDL realizations for the 1993–2013 period were first examined using the DT data. Next, the realization that best simulated the current sea-level changes was used in scenario studies. The GFDL ZOS (ZOS= modeled sea level using climate models) calculations were corrected for the sea level pressure (SLP) effect. Monthly and annual averages of ZOS and DT were then calculated for a 21-year control period, 1993–2013. Biases in the linear trends were calculated (as

$$100 \times \frac{\text{GFDL ZOS linear trend} - \text{Altimetry DT linear trend}}{\text{Altimetry DT linear trend}} (\%)$$

and used to test the quality of each GFDL simulation. Only GFDL simulations that simulated current sea levels reasonably well were used to illustrate the uncertainty of the projected sea level based on the CMIP5 scenarios. Finally, the projected sea-level changes were compared with SRTM digital elevation data to study the flooding probability in the study area and to determine whether or not the Nile Delta coast will be threatened by the projected SLR during the twenty-first century.

4. Validation of the PROBE-MED modeled results

Validations of the PROBE-MED version 2.0 model were performed for surface temperature, surface salinity, evaporation, net heat loss, solar radiation, and total heat loss through the two sub-basins. In both the WMB and EMB, five of the six studied parameters are well modeled. However, monthly average sea surface salinities are not modeled satisfactorily over the two studied sub-basins (Fig. 1).

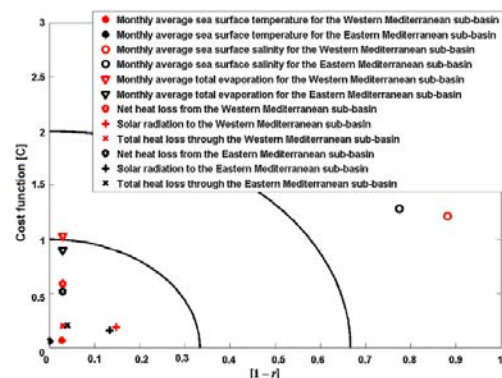


Figure 1. The dimensionless quality metrics r (the correlation coefficient) and C (the volume-weighted mean of the cost function) of the Mediterranean Sea, 1963–2002. Red (black) represents the Western (Eastern) Mediterranean sub-basin. The inner field represents good agreement, the middle field reasonable agreement, and the outer field poor agreement.

5. Water balance

The annual mean net flow through the WMB is larger than through the EMB (Fig. 2); moreover, the net flows through the WMB and EMB display positive trends of $5.2 \cdot 10^3 \text{ m}^3 \text{ s}^{-1} \text{ yr}^{-1}$ and $3.3 \cdot 10^3 \text{ m}^3 \text{ s}^{-1} \text{ yr}^{-1}$, respectively. The net precipitation is negative for the Mediterranean Sea, especially over the EMB, indicating that evaporation is larger than precipitation and without any trends. Annual river discharge into the EMB is larger than river discharge into the WMB because we have treated the Black Sea outflow as river input into the EMB. The river discharge displays no trend for the WMB.

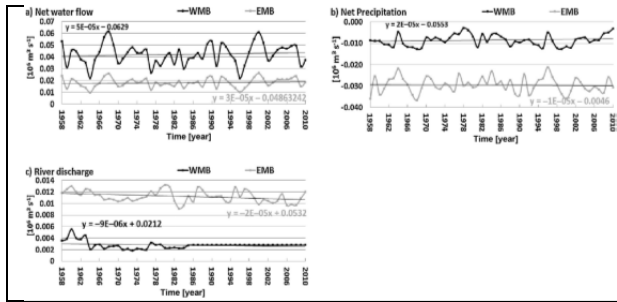


Figure 2. Annual mean modelled water balance components for the Western and Eastern Mediterranean sub-basin water components: (a) net water flow, (b) net precipitation rates, and (c) river discharge.

6. Heat Balances

There is no trend in F_n over the WMB and EMB, but a negative trend in F_s^0 indicates an increasing heat gain in the sub-basins (Fig. 3), especially over EMB, probably due to changes in total cloud cover over the study period. The total heat loss displays no net trend for the WMB but a decreasing trend ($0.6 \text{ W m}^{-2} \text{ yr}^{-1}$) for the EMB.

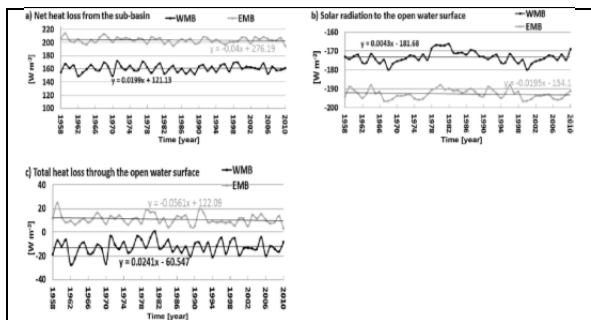


Figure 3. Annual mean modelled heat balance components for the Western and Eastern Mediterranean water components: (a) net heat loss from the sea (F_n), (b) solar radiation to the open water surface (F_s^0), and (c) total heat loss through the open water surface (F_{loss}).

7. Spatial and temporal distribution of the Mediterranean sea level

The annual average Mediterranean DT ranges from 27 cm to -15 cm (Figure 4a). The maximum values occurred in the Alboran sub-basin, partly indicating two Alboran anticyclonic gyres, while the minimum values occurred near the Gulf of Lion and in the Rhodes gyre, indicating two regions of cyclonic circulation (This two areas represents source of dense water formation).

The trend distribution of the Mediterranean DT (Figure 4b) illustrates how the annual Mediterranean DT trends range from $11.6 \text{ cm decade}^{-1}$ (centre of the Pelops gyre) to $-5.8 \text{ cm decade}^{-1}$ (centre of the Levantine deep-water formation region), averaging $2.6 \text{ cm decade}^{-1}$. The Mediterranean DT is positive and increasing everywhere except in the northern Ionian sub-basin. In addition, the Egyptian Mediterranean coast provides an example of high trends, with an annual rate of $3.5 \text{ cm decade}^{-1}$, most markedly along the coast near Marsa Matrouh ($6.5 \text{ cm decade}^{-1}$). This area coincides with the area of Marsa Matrouh anticyclonic eddy (Poulain et al., 2012 and Shaltout et al., 2015).

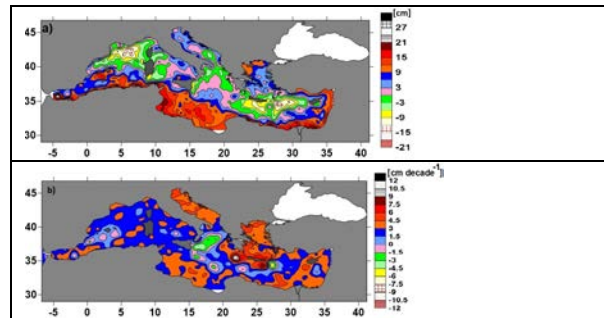


Figure 4. Spatial distribution of a) dynamic topography (cm) and b) Trend (cm decade^{-1}) calculated from an 18-year period (1993–2010).

8. Spatial and temporal distribution of the Mediterranean sea level

The GFDL simulations illustrates that Egypt's Mediterranean coast will experience substantial sea-level rise (SLR) this century as seen in Fig. 5. The estimated uncertainty over the study area was 4 to 22 cm by 2100, with the emission assumptions dominating the sources of studied uncertainties. Comparing the projected SLRs with digital elevation data illustrates that Egypt's Mediterranean coast will only be safe from flooding by 2100 if effective adaptation methods are applied.

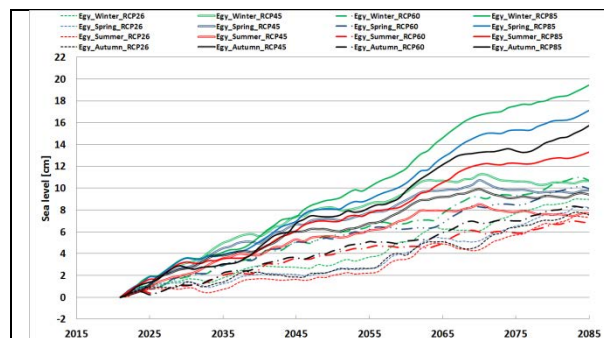


Figure 5. Thirty-year running annual mean sea levels for different seasons and emission scenarios relative to the 2006–2035 period for the GFDL ensemble simulation.

References

- Omstedt, A., 2011. Guide to Process Based Modelling of Lakes and Coastal Seas. Springer-Praxis Books in Geophysical Sciences. Springer-Verlag, Berlin/Heidelberg, <http://dx.doi.org/10.1007/978-3-642-17728-6>.
- Shaltout.M. and Omstedt., A (2015). Modelling the water and heat balances of the Mediterranean Sea using a two-basin model and available meteorological, hydrological, and ocean data. *Oceanologia Journal*, 57 (2), 116—131.
- Poulain P., Menna M. and Mauri E. (2012). Surface Geostrophic Circulation of the Mediterranean Sea Derived from Drifter and Satellite Altimeter Data. *J. Phys Oceanogr*, 42, 973–990.
- Shaltout. M., Tonbol, K., and Omstedt., A (2015). Sea-level change and projected future flooding along the Egyptian Mediterranean coast. *Oceanologia Journal* (Accepted and INPRESS)

The role of the atmospheric coupling in the ability of ORCHIDEE to simulate droughts

Jan Polcher¹, Marc Stéfanon²

¹ Laboratoire de Météorologie Dynamique (LMD) - Institut Pierre Simon Laplace, (CNRS/Ecole Polytechnique/ENS/UPMC), Palaiseau, France

² Laboratoire des Sciences du Climat et de l'Environnement (LSCE) - Institut Pierre Simon Laplace, CEA/CNRS/UVSQ, Gif sur Yvette, France (marc.stefanon@lsce.ipsl.fr)

Droughts are a typically coupled process where the large scale atmospheric conditions set-up the conditions but it is the response of the land surface, through its vegetation and hydrological processes, which generate the impact societies will face from a prolonged lack of rainfall. In this study we will evaluate the importance of the surface/atmosphere fluxes in the establishment of an ecological or hydrological drought.

To perform this study we have the ORCHIDEE land surface model which is on the one hand run offline forced by the ERA-Int re-analysis and on the other the WRF/ORCHIDEE coupled model driven by the atmospheric component of this same re-analysis. In both cases the observed long dry-spell over the 1979-2012 period are present. The impact of these drought on the land surface in both configuration will be presented. In the off-line mode, ORCHIDEE cannot modify the atmospheric conditions through the turbulent fluxes it computes. On the

other hand in the coupled mode the fluxes of the land surface model will alter the atmospheric conditions and avoid run-away effects into a dry condition. This leads to very different evolutions of the simulated ecological and hydrological droughts.

References

- Stéfanon, M., P. Drobinski, F. D'Andrea, and N. deNoblet-Ducoudré (2012), Effects of interactive vegetation phenology on the 2003 summer heat waves, *J. Geophys. Res.*, 117, D24103, doi:10.1029/2012JD018187.
- Drobinski, P., Anav, A., Lebeaupin Brossier, C., Samson, G., Stéfanon; M., et al. (2012) Model of the Regional Coupled Earth system (MORCE): Application to process and climate studies in vulnerable regions, *Environmental Modelling & Software* 35, 1-18.

Feedback of Coastal Upwelling on the Near-Surface Wind Speed at the Baltic Sea

Thomas Raub¹, Andreas Lehmann² and Daniela Jacob¹

¹ Climate Service Center Germany (GERICS), Helmholtz-Zentrum Geesthacht, Hamburg, Germany (thomas.raub@hzg.de)

² GEOMAR-Helmholtz Centre for Ocean Research Kiel, Germany

1. Background

Due to its narrow and elongated basin, coastal upwelling plays an important role in the Baltic Sea. During the thermally stratified period from spring to autumn, a seasonal thermocline separates warm water at the surface from colder water below. A sufficiently strong upwelling event can cause the thermocline to reach the surface leading to a drop of the sea surface temperatures (SSTs). The different SSTs directly affect the turbulent heat fluxes between the ocean and the atmosphere and thus the near-surface air temperature. As consequence, the stability of the atmospheric boundary layer is increased which reduces the vertical momentum transport from the free atmosphere toward the surface. This can cause considerably lower near-surface wind speeds.

2. Model and Experiment

In this study, we use a coupled regional climate model, consisting of the atmospheric model REMO and the Baltic Sea Ice Ocean model BSIOM, to investigate the described mechanism at the Baltic Sea. We analyze a twenty-year long simulation from 1989 to 2008 with the ERA-Interim reanalysis as lateral boundary forcing.

3. Upwelling detection

To detect upwelling we use an automatic algorithm adapted from Lehmann et. all (2012) which uses SST anomalies. Figure 1 shows the mean upwelling frequencies in summer for the simulation period 1989 to 2008.

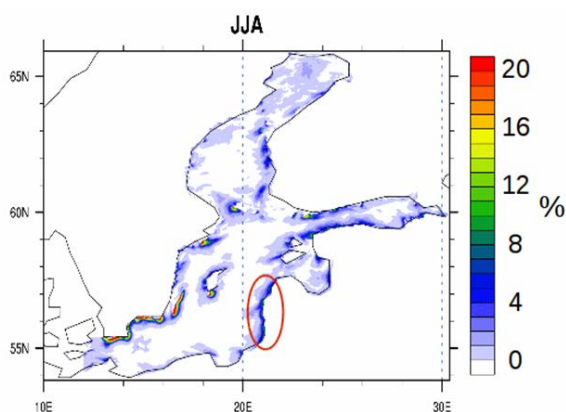


Figure 1. Mean upwelling frequencies in summer for the period 1989-2008.

This study focuses at a specific site at the eastern coast of the Baltic Proper (indicated in red). In total, 47 upwelling events with an average duration of about 8 days are detected during the 20-years period. The mean effect and the mean temporal evolution of all detected upwelling events is investigated.

4. Effect on wind speed

To separate the coupling effects from large-scale influences, the results are compared to an uncoupled atmosphere-only simulation using the SSTs from ERA-Interim. Figure 2 shows the difference of the 10m wind speed from the coupled and uncoupled simulation. On average, the SST drops by about 3°C leading to a considerable reduction of the 10m wind speed of about 0.6 m/s.

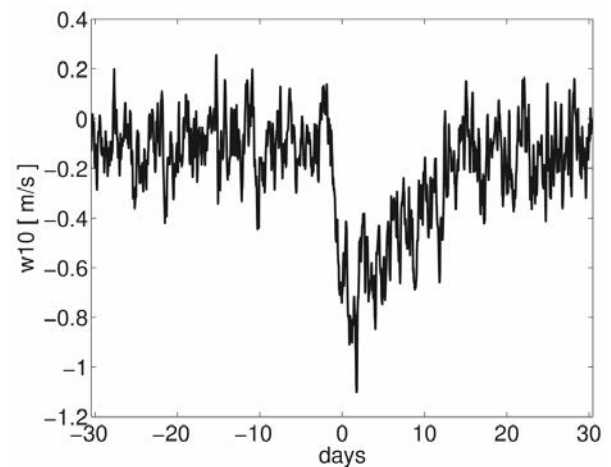


Figure 2. Mean difference of the 10m wind speed from the coupled and uncoupled simulation.

References

- Lehmann, A., K. Myrberg, and K. Höflisch (2012) A statistical approach to coastal upwelling in the Baltic Sea based on the analysis of satellite data for 1990-2009. *Oceanologia*, 54, 4, pp. 369-393.
- Sweet, W., Fett, R., Kerling, J., LaViolette, P. (1981) Air-Sea Interaction Effects in the Lower Troposphere Across the North Wall of the Gulf Stream, *Monthly Weather Review*, 109, pp. 1042-1052.

Spatiotemporal characterization of very long dry spells in the Mediterranean region

Florian Raymond¹, Albin Ullmann¹, Pierre Camberlin¹ and Philippe Drobinski²

¹ CRC, Biogéosciences, CNRS/University of Burgundy, Dijon, France (florian.raymond@u-bourgogne.fr)

² IPSL/LMD, Palaiseau and Paris, France

1. Introduction

The Mediterranean basin has quite a unique character that results both from physiographic and climatic conditions and historical and societal developments. Because of the latitudes it covers, the Mediterranean basin is a transition area under the influence of both mid-latitudes and tropical variability. Because in such transition area, the Mediterranean basin is very sensitive to global climate change. Regarding on-going climate change, the Mediterranean area is considered as one major “hotspots” with strong warming and drying (IPCC, 2013). The vulnerability of the Mediterranean population may thus increase with higher probability of occurrence of events conducive to heat waves and droughts which are among the most devastating natural hazards.

There is thus strong motivation to understand and model the Mediterranean climate system and specifically the processes at various time and spatial scales leading to heat waves and droughts, not only as separate processes within each Earth compartment, but as coupled mechanisms with feedback loops. This is indeed crucial to characterize how these processes will respond to climate change, in order to make decision on development of adaptation strategies to face risks related to changing climate.

The study focuses on the identification of very long dry spells (VLDS) in the Mediterranean region, relying on observations. It also assesses the ability of regional climate simulations performed within the context of the HyMeX (Drobinski et al. 2014) and MED-CORDEX programs (Ruti et al. 2015) to represent duration of very long dry spells.

2. Data & Methodology

The E-OBS precipitation gridded dataset v.10 from the the ECA&D are used in this study (Haylock et al., 2008). Obtained by station series interpolation, this high resolution dataset (0.25°) cover Europe, Middle East and North Africa from 1950 to 2013 at a daily time-step. Due to the low coverage in meteorological stations and to missing values in data series in North Africa and Middle East (Brunet et al., 2014), E-OBS dataset was analyzed and many grid points have been removed in these regions. In this study, E-OBS data are used over the 1979-2013 period, from September to April (rainy seasons).

Different steps were carried out to very long dry spells identification. First one was to detect dry days and dry spells: a day is considered as dry when the daily precipitation amount is lower than 1 mm, for each grid point. Second step was to find the unique values of dry spells length for each grid point and get the 80th centile. Dry spells were defined as consecutive dry days. In this study, very long dry spells are events longer than the 80th centile value. A binary matrix, with value “0” for all rainy grid

points or grid points where dry spells are shorter than the 80th centile and “1” for all grid point belonging to dry spells longer than the 80th centile is then used to detect very long dry spells. To avoid isolated VLDS grid points or local events, a sliding scan is performed using a 6°x6° window. If at least 90 percent of the grid point contained in the window are categorized as dry spells longer than the 80th percentile (matrix value “1”), the central point of the square is retained as a very long dry spells point. This method was adapted from a Euro-Mediterranean heatwaves classification by Stefanon et al. (2012).

Daily RCM precipitations simulations data are also used in this study. The RCM simulations were obtained through the HyMeX and MED-CORDEX programs. To assess the ability of the RCMs to reproduce very long dry spells duration, 5 runs from 5 models are analyzed in this study (table 1). Considering the period covered by the models, data series were analyzed for 30 rainy seasons, from 1979 to 2009. The analysis is performed with RCM time series from grid points the closest of the E-OBS grid. The same dry spell detection algorithm is applied to the HyMeX/MED-CORDEX simulations, with 1 mm threshold to detect rainy days on grid points. Evaluation of the 5 runs is based to the capacity of the 5 models to reproduce the 80th centile of dry spells length.

Table 1. HyMeX/MED-CORDEX simulations used in this study.

Platform	Resolution	RCM	Coupled	Period
CNRM	MED-44	ALADINS2	-	1979-2011
ICTP	MED-44	RegCM4 v4	-	1979-2012
CMCC	MED-44	CCLM4	-	1979-2012
LMDZ	MED-44	LMDZ4	-	1979-2009
LMDZ	MED-44	LMDZ4	NEMO MED8	1979-2009

3. Very long dry spells identification

The above procedure apply to the 80th centile E-OBS binary matrix identifies 61 very long dry spells events of 2822 days total duration. Among this 61 events, 12 are classified as multiples events because 2 or more events occurred in the same days but in really different places throughout the Mediterranean basin. The sliding scan reports only one event but in reality there are more than one event. The next step of the VLDS identification is to apply hierarchical clustering methodology to characterize typical VLDS patterns for the Mediterranean region. Multiples events are here grouped in single events to apply hierarchical clustering on the median days of each event. Keeping multiple events occurring at the same time would have create biases on the hierarchical clustering. Clustering analysis was finally applied to 48 events leading to 5 clusters.

Cluster 1 contains 6 VLDS events mainly located over the Iberian Peninsula. Cluster 2 contains 5 VLDS events

mainly located over the Iberian Peninsula, Morocco and Algeria. Cluster 3 contains 19 events spread in different places over the Mediterranean Basin. Cluster 4 contains 5 events mainly located over the Balkan region. The last cluster contains 13 events mainly located over the Middle East. This 5 clusters will be analyzed more precisely in the course of this research project.

4. Multi-model assessment

Figure 1 represents the 80th centile of dry spells lengths for E-OBS and RCMs (biases with respect to E-OBS). The E-OBS value display north/south and west/east gradients of the 80th percentile in the Mediterranean Basin. The lowest values are found in the north part of the basin, i.e. in northern Spain, France, southern Italy and in the Balkans. In these regions, the 80th percentile is about 20 to 35 consecutive dry days. The highest values are found in the south-western Mediterranean (Iberian Peninsula, Morocco and Algeria), in the Alps and in the Middle East. In these regions, the 80th percentile of dry spells length is about 35 and 65 consecutive dry days. Extreme southern part of the Middle East show very high values up to 95 consecutive dry days. These values may be true, because we are dealing here with an arid climate, but the low number of stations data in this sector may also cause biases in the E-OBS data.

All models simulations display positive biases in the extreme south of Middle East, biases values goes from +40 days to +94 days compared to the E-OBS 80th centile value. In the rest of Middle East, 3 models shown positive biases (CCLM4, LMDZ4 and LMDZ4-NEMO; +15 days on average) and 2 display negative biases (ALADIN 52 and RegCM4; -15 days on average). 4 of the 5 models simulations display negative biases on nearly all the studied region. Only CCLM4 model mostly show positive biases. Atmosphere-only model LMDZ4 and ocean-atmosphere coupled model LMDZ4-NEMO display no significant differences.

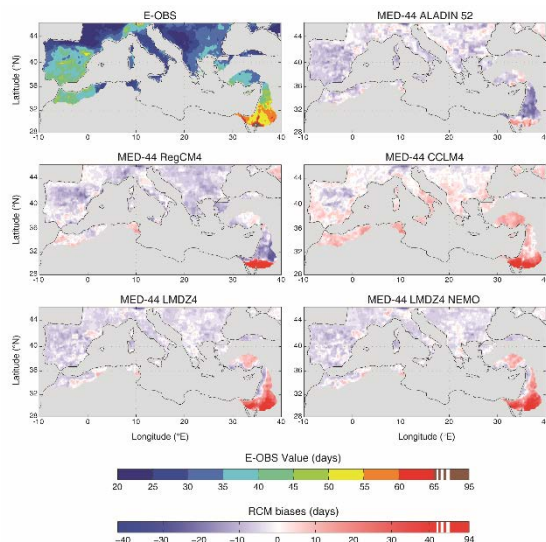


Figure 1. 80th centile value of dry spells length (E-OBS) and biases (RCM simulations with respect to E-OBS) for rainy seasons (September to April) in the 1979 – 2009 period.

5. Conclusion

This study has two main objectives: identify very long dry spells in the Mediterranean basin using E-OBS observation data and analyze the ability of regional climate models to represent VLDS duration. 48 VLDS events are observed during the 1979-2013 rainy seasons (September to April). All this 48 events were classified into 5 clusters using hierarchical clustering method. Concerning the ability of regional climate models to reproduce dry spells length, the 5 models mainly showed negative biases on the 80th percentile length, relative to the E-OBS data observations.

This study is the beginning of a research project based on rainy seasons dry spells analysis in the Mediterranean Basin. Next steps will be to use ERA-Interim reanalysis to identify the large scale atmospheric conditions associated with the various VLDS clusters obtained from the E-OBS data and RCM simulations over 1979-2013 period. A natural follow-up will be to simulate occurrence of VLSD in anthropogenic scenarios over the 21st century.

References

Brunet M., Gilabert A. and Jones P., 2014, A historical surface climate dataset from station observations in Mediterranean North Africa and Middle East areas. *Geoscience Data Journal*, vol. 1, 121–128. DOI : 10.1002/gdj3.12

Drobinski P, Ducrocq V, Alpert P, Anagnostou E, Béranger K, Borga M, Braud I, Chanzy A, Davolio S, Delrieu G, Estournel C, Filali Boubrahmi N, Font J, Grubisic V, Gualdi S, Homar V, Ivancan-Picek B, Kottmeier C, Kotroni V, Lagouvardos K, Lionello P, Llasat M C, Ludwig W, Lutoff C, Mariotti A, Richard E, Romero R, Rotunno R, Roussot O, Ruin I, Somot S, Taupier-Letage I, Tintore J, Uijlenhoet R, Wernli H (2014) HyMeX, a 10-year multidisciplinary program on the Mediterranean water cycle. *Bull. Amer. Meteorol. Soc.* 95:1063-1082

Haylock M. R., Hofstra N., Klein Tank A. M. G., Klok E. J., Jones P. D., New M., 2008, A European daily high-resolution gridded data set of surface temperature and precipitation for 1950–2006. *Journ. of Geoph. Res.*, vol. 113, D20119. doi: 10.1029/2008JD010201

IPCC (2013) *Climate Change 2013: The Physical Science Basis. Contribution of Working Group I to the Fifth Assessment Report of the Intergovernmental Panel on Climate Change.* Stocker, T.F., D. Qin, G.-K. Plattner, M. Tignor, S.K. Allen, J. Boschung, A. Nauels, Y. Xia, V. Bex and P.M. Midgley (eds.), Cambridge University Press, Cambridge, United Kingdom and New York, NY, USA

Stéfanon M, D'Andrea F, Drobinski P (2012) Heatwave classification over Europe and the Mediterranean region. *Env. Res. Lett.* 7:doi:10.1088/1748-9326/7/1/014023

Ruti P, Somot S, Giorgi F, Dubois C, Flaounas E, Obermann A, Dell'Aquila A, Pisacane G, Harzallah A, Lombardi E, Ahrens B, Akhtar N, Alias A, Arsouze T, Raznar R, Bastin S, Bartholy J, Béranger K, Beuvier J, Bouffies-Cloche S, Brauch J, Cabos W, Calmanti S, Calvet J C, Carillo A, Conte D, Coppola E, Djurdjevic V, Drobinski P, Elizalde A, Gaertner M, Galan P, Gallardo C, Gualdi S, Goncalves M, Jorba O, Jorda G, Lheveder B, Lebeaupin-Brossier C, Li L, Liguori G, Lionello P, Macias-Moy D, Onol B, Rajkovic B, Ramage K, Sevault F, Sannino G, Struglia M V, Sanna A, Torma C, Vervatis V (2015) MED-CORDEX initiative for Mediterranean climate studies. *Bull. Amer. Meteorol. Soc.* in revision

Modelling the impacts of atmospheric dust deposition on the biogeochemical cycles in the Mediterranean Sea

C. Richon¹, J.-C. Dutay¹, F. Dulac¹, J. Vincent², B. Laurent², K. Desboeufs², M. Mallet³, P. Nabat⁴, J. Palmiéri^{1*}

¹ Laboratoire des Sciences du Climat et de l'Environnement, CEA CNRS UVSQ, Gif-sur-Yvette, France (camille.richon@lsc.ipsl.fr)* Now at Southampton University – National Oceanography Center (NOC), Waterfront Campus, European Way, Southampton SO14 3ZH, UK

² LISA, UMR CNRS 7583, Universités Paris 7 et 12, 61 Av. du General de Gaulle, 94010 Créteil Cedex, France

³ Laboratoire d'Aérodologie, 16 avenue Edouard Belin, 31400 Toulouse, France

⁴ Météo-France, Centre National de Recherches Météorologiques, CNRM-GAME, URA1357, 42 avenue G. Coriolis, 31057 Toulouse cedex 1, France

1. Objectives

Atmospheric deposition is not included or is misrepresented in regional oceanic biogeochemical models, whereas, along with river inputs, it may represent a significant source of nutrients at the basin scale, like during intense desert dust deposition events over the Mediterranean Sea. Moreover, experiments (e.g. DUNE campaign, Guieu *et al.* 2014a) show that these events significantly modify the biogeochemistry of the oligotrophic Mediterranean Sea.

We first intercompare dust deposition simulations from two atmospheric regional models (ALADIN-Clim and RegCM) Nabat *et al.* (2012, 2015) and evaluate them by confrontation with observations of dust deposition over the Mediterranean basin. Then, we use the 3D coupled model NEMOMED12/PISCES to investigate the effects of high resolution atmospheric dust deposition forcings on the biogeochemistry of the Mediterranean basin. The model represents the evolution of 24 prognostic tracers in the Mediterranean Sea (Palmiéri, 2014). We evaluate the influence of dust deposition on the budget of nutrients in the basin on a decadal simulation (1982-2012) and its impact on the biogeochemistry (primary production, plankton distributions...).

2. Dust model intercomparison

We show that the two atmospheric regional models display comparable amounts of dust deposition for the year 2012 (Fig.1) although we observe some discrepancies in the spatial distribution of deposition.

We calculated the contribution of dust to the total nutrient inputs and evaluate atmospheric deposition as a significant source for the nutrients (Table 1).

Table 1. Contribution of the atmospheric deposition to the total nutrient input (%) simulated with ALADIN-Clim for the year 1983 and 2012. Krom *et al.*'s estimation is for the eastern basin.

Atmospheric contribution to the total nutrient input	2012		1983	Krom <i>et al.</i> Bergametti 2010 <i>et al.</i> 1992	
	2012	1983			
NO3	40-60	25-75	60	/	
PO4	5-40	0.1-15	28	36	

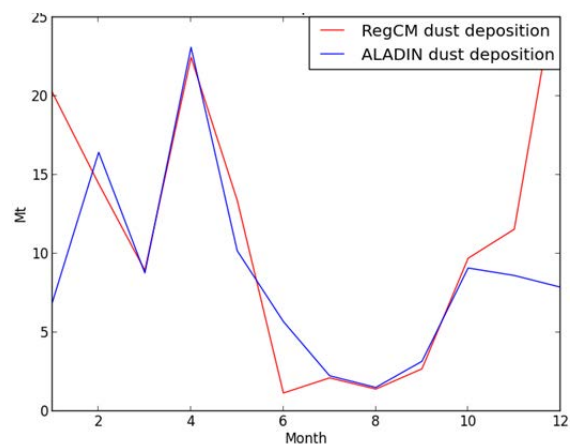


Figure 1. Monthly total dust deposition over the whole Mediterranean basin for the year 2012 simulated with RegCM and ALADIN-Clim.

3. Impacts of dust on primary production

Global ocean simulation has revealed that when high temporal resolution for dust inputs is considered, it generates a very significant effect on the marine biogeochemistry (Guieu *et al.* 2014b). This result is also supported by observations from mesocosm experiments performed during the DUNE project (Guieu *et al.* 2014c). We have investigated this process in the oligotrophic Mediterranean Sea using high resolution regional simulation. Two 30-years simulations were performed: a first one without dust inputs (noDUST) and a second one with 3-hourly natural dust deposition simulated by ALADIN-Clim (DUST). We found that total primary production is increased up to 15% when taking into account the atmospheric input. The primary production is increased in areas corresponding to the maximum deposition for the month, while main differences in nutrients concentrations (phosphate, silica and iron) are not located in the deposition areas.

The PISCES biogeochemical model represents two compartments of phytoplankton and two compartments of zooplankton. Our results show that the primary productivity of the dominant nanophytoplankton is increased by 5-10% after dust fertilization (Figure 2).

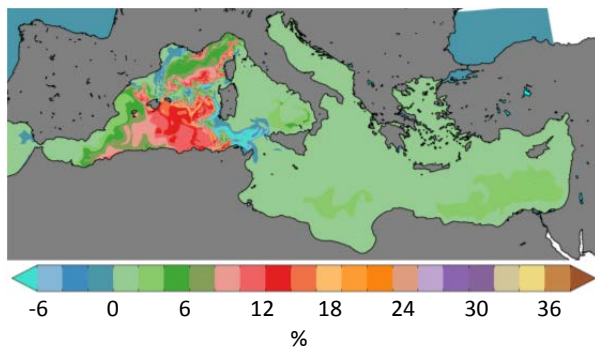


Figure 2. Difference in nanophytoplankton primary production (%) between DUST and noDUST simulations for the month of June of the 21st year of simulation.

4. Impacts of dust on plankton distribution

Dust deposition has different impacts on nanophytoplankton and diatoms primary production. We will also study its impacts on phytoplankton and zooplankton's abundances.

References

- Guieu, C., Dulac, F., Ridame C. and Pondaven, P. (2014a) Introduction to project DUNE, a DUST experiment in a low Nutrient, low chlorophyll Ecosystem, *Biogeosci.*, **11**, 425–442.
- Guieu, C., et al. (2014b) The significance of the episodic nature of atmospheric deposition to Low Nutrient Low Chlorophyll regions, *Global Biogeochem. Cycles*, **28**, 1179–1198.
- Guieu, C., Ridame C., Pulido-Villena, E., Bressac, M., Desboeufs, K. and Dulac, F. (2014c) Impact of dust deposition on carbon budget: a tentative assessment from a mesocosm approach, *Biogeosci.*, **11**, 5621-5635.
- Nabat, P., Solmon, F., Mallet, M., Kok, J.F. and Somot, S. (2012) Dust emission size distribution impact on aerosol budget and radiative forcing over the Mediterranean region: a regional climate model approach, *Atmospheric Chemistry and Physics Discussion*, **12**, pp. 17835–17886
- Nabat, P., Somot, S., Mallet, M., Michou, M., Sevaut, F., Driouech, F., Meloni, D., di Sarra, A., Di Biagio, C., Formenti, P., Sicard, M., Léon, J.-F., and Bouin, M.-N. (2015) Dust aerosol radiative effects during summer 2012 simulated with a coupled regional aerosol–atmosphere–ocean model over the Mediterranean, *Atmospheric Chemistry and physics*, **15**, pp. 3303-3326
- Palmiéri, J., *Modélisation Biogéochimique de la mer Méditerranée avec le modèle régional couplé NEMO-MED12/PISCES (2014)*, thèse de doctorat d'université de Versailles Saint Quentin, 221p

Comparing on centennial time scale the deviation of sea level from the global mean of two marginal seas: Baltic and Adriatic Sea

Luca Scarascia¹, Piero Lionello^{1,2}

¹ CMCC (Centro Euro-Mediterraneo sui Cambiamenti Climatici), Lecce, Italy. (luca.scarascia@cmcc.it)

² University of Salento, DiSTeBa, Lecce, Italy

1. Summary

The aim of this work is to compare the deviation of the sea level of the Baltic and Adriatic Sea from the global mean in the 20th century, both at monthly and annual scale. The variability of the two basins is analyzed taking into account separately different components and estimating the magnitude of their influence on the two basins. The factors involved are: the Inverse Barometer effect due to the local Sea Level Pressure (SLP), the steric effects due to sea temperature and salinity variation under the hypothesis of no mass change in the column water. The residual includes jointly other forcings, whose influence is more difficult to estimate, but has a paramount role in contributing to the annual cycle of the sea level variability, such as the effects of wind, continental ice melting, precipitation and to river-runoff.

2. Baltic and Adriatic Sea Level data.

The first objective is to reconstruct the time series of mean sea level in the Baltic and Adriatic seas from tide gauges data extracted from the Permanent Service of Mean Sea Level (PSMSL). Two seamless time series covering the whole period from 1901 to 2009 are computed using tide records from 13 stations in Baltic Sea and 7 stations in the Adriatic Sea adopting a statistical method based on PCA and Least Square Method (Scarascia and Lionello, 2013). Both for the Baltic and Adriatic Sea the very high spatial coherency of the involved stations implies that the resulting time series can be considered a reliable representation of mean sea level of the whole basin. Note that the Baltic tide gauge records are affected by a strong negative interannual trend due because of the natural isostatic adjustment of the Scandinavian peninsula due to the post glacial rebound. The PSMSL provides the results of a study conducted by R. Peltier (Peltier R. 1998, 2004, 2005) about isostatic movement of all the stations present in the PSMSL dataset whose results have been used to subtract the Glacial Isostatic Adjustment (GIA) to the Baltic sea level records.

The comparison between the reconstructed time series and mean sea level from satellite data (covering the period 1993 to 2009) shows very high correlation both at monthly and annual scale (correlation is 0.97 and 0.87 for the Baltic and Adriatic Sea, respectively).

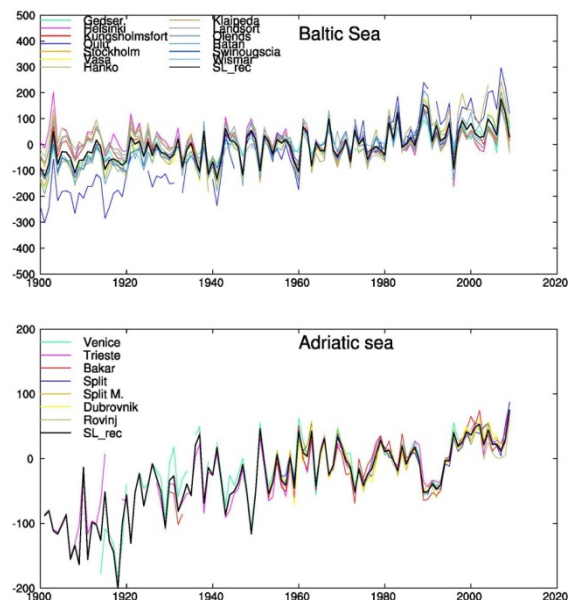


Figure 1. Annual Sea Level time series of the stations considered in the Baltic Sea (top panel) and Adriatic Sea (bottom panel). Bold black line is the Sea Level reconstructed by statistical method and representative for the whole basin from 1901 to 2009. Sea Level is in mm.

3. Global Mean Sea Level.

The Global Mean Sea Level (GMSL) extracted by the PSMSL database, has been computed by Church and White (2006, 2011). The reconstruction of the evolution of GMSL, from 1880 to 2009, is based on in many locations around the world, whose number has progressively grown during the 20th century, until 135 locations (50 in the Southern Hemisphere) and 250 gauges useful on December 2009. The reconstruction is carried out working on monthly data from the PSMSL database (Woodworth and Player, 2003). GMSL presents a trend of +1.65cm/decades in the period 1901-2009. The analysis carried out in this study considers the deviation of the mean sea level in the Baltic and Adriatic basins from the GMSL.

4. Discussion and conclusion.

Barometer effect (IB) is the first factor considered in the analysis of the interannual variability of the two basins. For the computation of IB over Baltic and Adriatic, we used Sea Level Pressure data extracted from ERA_Interim and 20th Century Reanalysis dataset. The steric component of sea level is computed using sea temperature and salinity data obtained by the MEDAR/MEDATLAS 2002 project. Figure 2 shows the time evolution of the sea level anomaly of the Baltic and Adriatic Sea after subtracting the IB correction, in order

to exclude local effects due to the atmospheric pressure. Figure 3 shows the annual cycle of Baltic and Adriatic sea level.

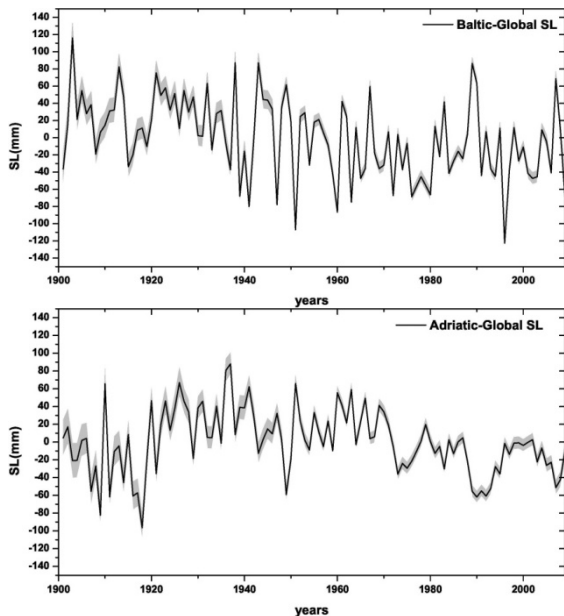


Figure 2. SL anomaly of Baltic (top) and Adriatic (bottom) Sea. Grey area represents the error associated to the computation of the anomaly.

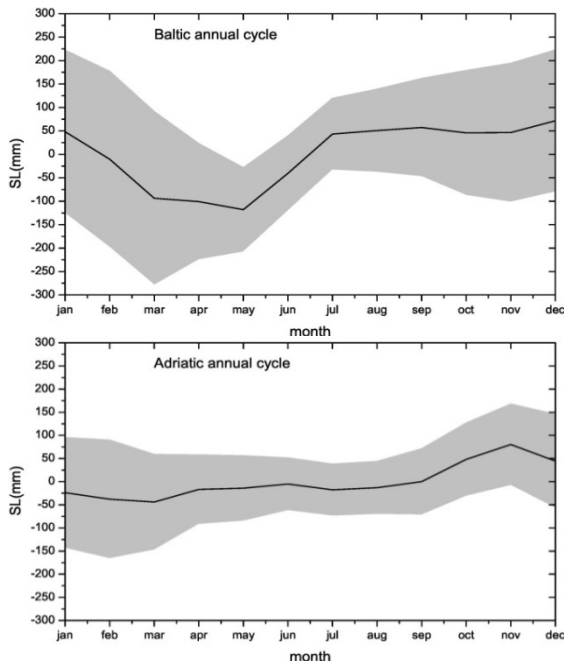


Figure 3. Annual cycle of Baltic (top) and Adriatic (bottom) sea level computed on the period 1901 – 2009. Grey area shows the interannual variability computed as the standard deviation associated to each month.

The Inverse Barometer effect results to play a minor role on the interannual variability, exhibiting a very small annual cycle. Same is true for the steric component, which is particularly small in the Baltic Sea.

The residual sea level appears to be linked mainly to the wind. However correlation between wind and sea level

exhibits a pattern with a substantial interdecadal variability and further it is able to explain only part of the residual sea level variability. Research is in progress and we hope to be able to report new results at the workshop.

References

Church, J. A. and N.J. White (2011), Sea-level rise from the late 19th to the early 21st Century. *Surveys in Geophysics*, doi:10.1007/s10712-011-9119-1.

Church, J. A., and N. J. White (2006), "A 20th century acceleration in global sea-level rise", *Geophys. Res. Lett.*, 33, L01602, doi:10.1029/2005GL024826.

Peltier W.R 1998 Postglacial Variations in the Level of the Sea: Implications for Climate Dynamics and Solid-Earth Geophysics. *Reviews of Geophysics* 1998. 36(4),603-689.

Peltier W.R 2004 Global Glacial Isostasy and the Surface of the Ice-Age Earth: The ICE-5G(VM2) model and GRACE. *Ann. Rev. Earth. Planet. Sci.* 2004. 32,111-149.

Peltier W.R 2005 On the Hemispheric Origins of Meltwater Pulse 1A. *Quat. Sci. Rev.*, 24, 1655-1671.

Permanent Service for Mean Sea Level (PSMSL), 2015, "Tide Gauge Data", Retrieved 09 Feb 2015 from <http://www.psmsl.org/data/obtaining/>.

Scarascia L., Lionello P. (2013), Global and regional factors contributing to the past and future sea level rise in the Northern Adriatic Sea. *Global and Planetary Change*. 07/2013; 106:51-63. DOI: 10.1016/j.gloplacha.2013.03.004

Woodworth and Player (2003): The Permanent Service for Mean Sea Level: An Update to the 21st Century: *Journal of Coastal Research* , Vol. 19, No. 2, Spring, 2003

Low frequency salinity variations in the Baltic Sea

Semjon Schimanke and H.E. Markus Meier

Swedish Meteorological and Hydrological Institute, Norrköping, Sweden (semjon.schimanke@smhi.se)

1. Abstract

A transient multi-century simulation mimicking natural variability has been performed for the Baltic Sea. The simulation is used for investigations of long lasting stagnation periods and long-term variability of the salinity in the Baltic Sea. We find that stagnation periods over ten years appear approximately once per century. On the other hand, considering extended periods of salinity reduction, as observed between 1976-1992, we can not find a similar reduction within the 750 years of our simulation. This might point to an anthropogenic contribution to the event or highlights how unlikely such an event is. The investigation of driving parameters confirms that river discharge, net precipitation and the zonal wind have the most important role for the Baltic Sea salinity. For multi-decadal periods, almost two thirds of the salinity variability can be explained by annual means of river discharge, precipitation, both wind components, temperature and the NAO when multi-linear regression techniques are used. However, the separation of periods for different time slices highlights that this relationship is not constant in time. At least three gaps exist each spanning roughly 50 years where the coherence between salinity and runoff as the common main driver is rather weak. This indicates that the importance of river discharge might be limited for certain periods and drivers as the zonal wind become more important. Finally, the variability of salinity shows increased power on frequencies with 100 years and more. Such periodicity has never been shown for the Baltic Sea but the driving mechanism remains unclear.

2. Introduction

The Baltic Sea is one of the largest brackish sea areas of the world. The sensitive state of the Baltic Sea is sustained by a fresh-water surplus by river discharge and precipitation on one hand and by inflows of highly saline and oxygen-rich water from the North Sea on the other hand. However, since 1976 the number of Major Baltic Inflows (MBIs) is considerably reduced (Fonselius and Valderrama 2003). Reasons for the occurrence of this stagnation period are still debated. Changes in wind speed and direction (Lass and Matthäus 1996) or the corresponding development of sea level pressure (SLP) anomalies (Schimanke et al. 2014) are likely contributors as well as changes in river runoff and precipitation (e.g. Meier and Kauker 2003). Moreover, it might be speculated whether the observed stagnation period is a consequence of beginning anthropogenic climate change. On decadal time scales Baltic Sea salinity variations of about 1 salinity unit are linked inter alia to runoff variations.

The goal of this study is to understand the contribution of different driving factors for the decadal to multi-decadal variability of salinity in the Baltic Sea. Moreover, we will investigate in how far long-lasting stagnation periods are a common feature of the Baltic Sea. Therefore, a transient climate simulation of 850 years (longer than any other reconstruction performed so far) has been carried out with a

regional climate model of the Baltic Sea.

The analysis focuses on the role of variations in river discharge and precipitation, changes in wind speed and direction, fluctuations in temperature and shifts in large scale pressure patterns (e.g. NAO). Hereby, the length of the simulation will allow to identify mechanisms acting on decadal to multi-decadal time scales. Moreover, it will be discussed how likely long stagnation periods are under natural climate variability and if the observed exceptional long stagnation period between 1983-1992 might be related to beginning climate change.

3. Stagnation periods

We will investigate in how far stagnation periods are exceptional in an undisturbed climate. Therefore, we follow the approach of the probability of occurrence of trends greater than in observations. Here, maximum trends found in observations or reconstructions are compared with the likelihood of such trends in free model simulations.

The conclusion we draw from the trend analysis is that a 10 year stagnation period as observed between 1983–1992 is an event which happens every now and then.

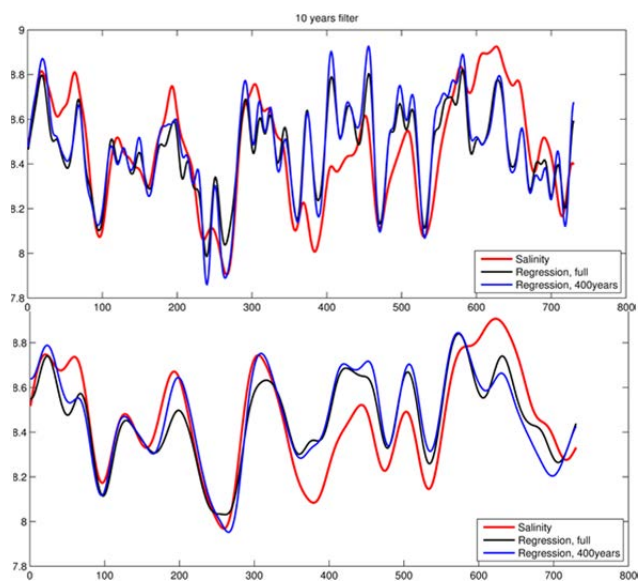


Figure 1. The mean salinity of the Baltic Sea (red) is plotted in combination with the multiple-linear regression based on the entire series (black) and the first 400 years (blue) as training period. The figure includes results for the 10 (top) and 25 years years (bottom) low-pass filtered analyses.

Such an event can be assumed to happen once per century in an undisturbed climate. This fits perfectly into the observed time series though it is too short for such an analysis. However, for the extended stagnation period (1976–1992) that corresponds to a continuously reduction of salinity in the deep Baltic Sea we cannot find similar periods in the control simulation though there are stagnation periods with 20 years and more. This might be due to some special circumstances.

Beside the extraordinary high values during the 1950s, the salinity concentration was very high at the beginning of the reduction period in 1976. Moreover, at the end of the stagnation the lowest concentrations of the entire time series was reached. Whereas it is natural that a long lasting stagnation period leads to very low salinity strong trends can only be reached if the stagnation period starts from very high values as it was the case in 1976. Hence, this might have been a very special situation being so extraordinary that it did not happen during the control simulation. However, on the other hand it can not be ruled out that the stagnation period is related to changing climate and herewith changing weather regimes and changes in the river discharge.

4. Understanding multi-decadal salinity changes in the Baltic Sea

We perform a multiple linear regression (MLR) analysis to investigate combined effects of the driving parameters onto the salinity to perceive the total influence on long time scales. Considering all parameters the correlation becomes 0.72 for the 10 years smoothed series or in other words they explain 51% of the Baltic Sea salinity variance (Fig. 1, top). Using the series filtered with a cutoff-frequency of 25 years the correlation increases to 0.8 when all driving parameters are considered in the MLR (Fig. 1, bottom).

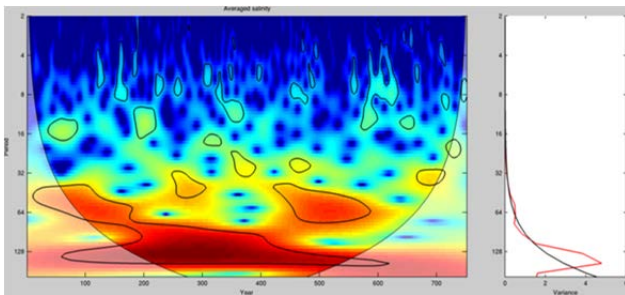


Figure 2. Continuous wavelet power spectrum conducted for the time series of the Baltic Sea salinity. Black lines indicate significant power on the 95%-level compared to red noise based on AR1 coefficient. The cone of influence is shown as a lighter shade. The right part of the figures includes the time averaged variance and the significance level.

The variability of the mean salinity does not show any periodicity for time scales shorter than roughly 30 years (Fig. 2). However, the wavelet analysis indicates that there is significantly enhanced power on longer frequencies and especially for periods of 100 years or longer. The time averaged variance (right part of Fig. 2) is clearly above the significance level for centennial periods. Moreover, river runoff and the zonal wind component have significant power on the same frequency (not shown) supporting this finding. However, one needs to be carefully since large parts of the long-term variability might be affected by artificial behavior close to the edge of the time series as indicated by the cone of influence.

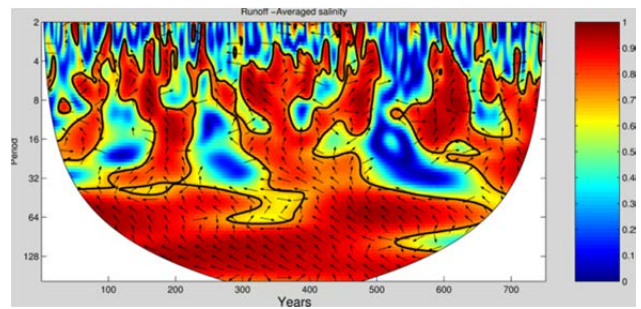


Figure 3. Squared wavelet coherence between the time series of mean salinity and river discharge. Colors represent the coherence and arrows indicate the relative phase relationship between the series (e.g. pointing right: in-phase; left: anti-phase; up: the parameter leads the mean salinity by 90deg (equal to half a period)).

The wavelet coherence analysis confirms basically our results from the MLR and earlier studies that the river discharge has the strongest impact on the Baltic Sea salinity. Fig. 3 shows that the river discharge is strongly coherent with the mean salinity for all periods longer than 3-4 years. The figure highlights also that the time lag between the river discharge and the salinity as indicated by the arrows is mostly 90° (equal to half a period) regardless of the length of the period, i.e. a lag of 10 years for a period of 20 years. It should be noted that also the remaining driving parameters show a lag of 90° (not shown), which indicates that all driving parameters lead the mean salinity. Besides the overall good coherence of salinity and river discharge, gaps exist where the coherence seems not to be valid – especially for decadal to multi-decadal periods (Fig.3). This indicates that there are periods where the river discharge does not play the dominant role for the long-term variability of salinity but other drivers - as zonal wind speed - seems to be in charge.

References

- Fonselius, S., and J. Valderrama, 2003: One hundred years of hydrographic measurements in the Baltic Sea. *JOURNAL OF SEA RESEARCH*, 49 (4), 229–241
- Lass, H. U., and W. Matthäus, 1996: On temporal wind variations forcing salt water inflows into the Baltic Sea. *Tellus A*, 48 (5), 663–671
- Meier, H., and F. Kauker, 2003: Sensitivity of the Baltic Sea salinity to the freshwater supply. *CLIMATE RESEARCH*, 24 (3), 231–242.
- Schimanke, S. et al., 2012: The climate in the Baltic Sea region during the last millennium simulated with a regional climate model. *Climate of the Past*, 8 (5), 1419–1433, doi:10.5194/cp-8-1419-2012

The role of the ocean in the European climate dynamical downscaling

Dmitry Sein¹, William Cabos², Dmitry Sidorenko¹, Qiang Wang¹ and Daniela Jacob³

¹ Alfred Wegener Institute, Bremerhaven, Germany (dmitry.sein@awi.de)

² University of Alcalá, Alcalá, Spain

³ Climate Service Center 2.0, Hamburg, Germany

1. Introduction

Regional climate models are often considered as useful tools that allow us to achieve high-resolution refinement from coarsely resolved global model runs (downscaling). It is considered that they provide a better simulation of mesoscale variability and of the climate in coastal zones and regions with complex orography, with little improvement in the open ocean. This can be the case if a regional atmospheric model with prescribed sea surface temperature is used. For a regional coupled ocean – atmosphere – sea ice model the results of climate simulations can be quite different from those of the driving global model (Sein et al., 2015). The coupling brings to regional modeling an additional degree of uncertainty. This uncertainty is strongly influenced by the extension and location of the model domain (Sein et al., 2014).

For climate simulations over the European continent the inclusion of the cyclogenesis regions in the model domain can play an important role. Besides, the key oceanic regions (for example, deep water production) can be also important, especially for coupled simulations. In our study we try to examine how the inclusion of these regions in the model domain can change or improve the results of climate simulations.

2. ROM setups

A global ocean – sea ice – marine biogeochemistry coupled model (ROM) comprising the REgional atmosphere MOdel (REMO), the Max Planck Institute Ocean Model (MPIOM), the HAMBURG Ocean Carbon Cycle (HAMOCC) model, and the Hydrological Discharge (HD) model was implemented (Sein et al., 2015).

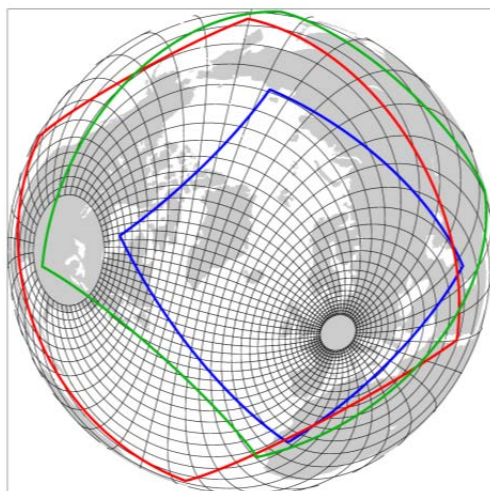


Figure 1. ROM setups. Black lines: MPIOM grid (every 12th grid line). Colored rectangles: REMO domains.

The simulations were performed for the two different coupled domains. The first (SMALL), covers mainly Europe and part of the Arctic Ocean (Fig.1, blue rectangle) and the second (BIG) domain includes the whole of the Arctic and almost all the North Atlantic (Fig.1 red rectangle). Atmospheric forcing was taken from the MPI-ESM CMIP5 simulations, i.e. 20th century run and RCP8.5 climate change scenario.

3. ROM simulation results

The comparison of simulated 2m temperature against the ERA-Interim reanalysis is shown on Fig.2. The most pronounced difference between ROM-SMALL and ROM-BIG occurs in the summer time.

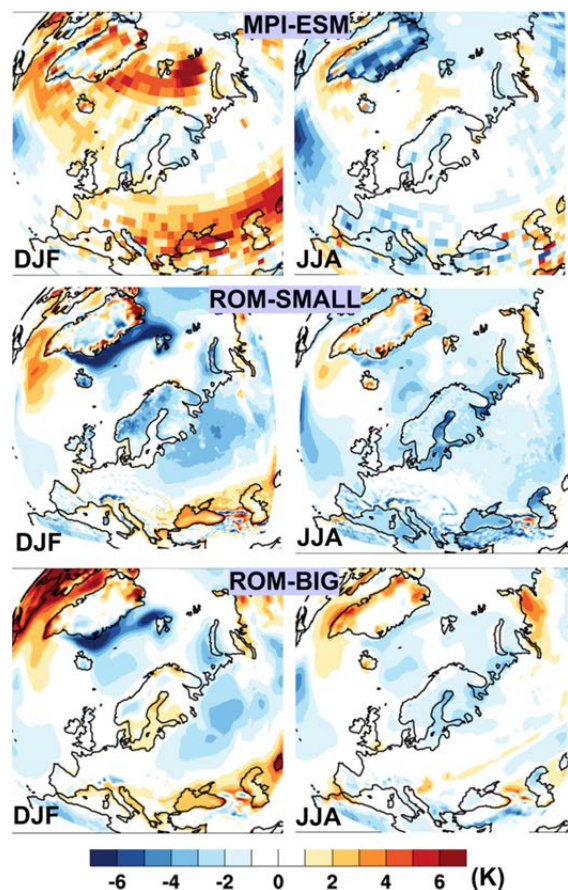


Figure 2. Mean 1980-1999 DJF (left) and JJA (right) 2m Temperature bias (Model-ERA-Interim).

The possible explanation of generally colder summer in ROM-SMALL as well as in the driving MPI-ESM can be the strong cold MPIOM bias (more than 7K) in the Labrador Sea. In ROM-SMALL this bias also influences the temperatures over Western Europe. From the other

hand, by improving the ocean circulation in ROM-BIG and reducing the Labrador Sea cold temperature bias we achieve a much better agreement of the European JJA temperature with observations.

4. RCP85 climate change scenario simulations

The climate change RCP85 scenario simulations were carried out for the period 2006-2099 with two ROM configurations. The differences in the climate change signal between ROM-BIG and ROM-SMALL have been analyzed.

5. Implementation of FESOM

Despite the MPIOM shows relatively good results in reproducing the ocean circulation for the regional climate simulations, it has an important disadvantage which is common to many models based of regular meshes. Namely, the possible grid refinement in MPIOM can be done only near its poles locations. Thus, for example, it is difficult to receive high ocean model resolution in both, the Baltic and Mediterranean Seas.

This is why we employ a next generation Finite-Element Sea ice Ocean Model (FESOM) (Wang et al. 2014) developed at AWI.

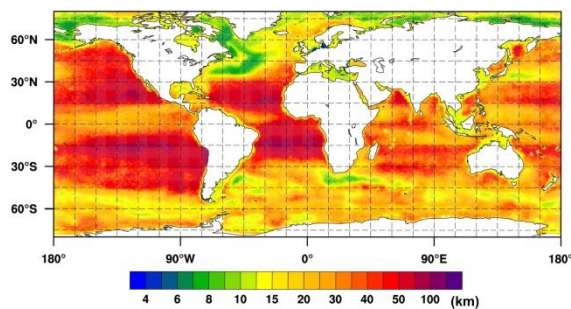


Figure 3. FESOM grid resolution

With FESOM, different grid resolution can be conveniently assigned to different regions in an otherwise global setup. We keep the horizontal resolution relatively coarse (50-75km) in the most parts of the global ocean (Fig.3), and refine it down to 2-3 km in particularly chosen regions. In sensitivity studies we found that the best results are achieved when the degree of grid refinement is determined according to the observed variance of sea surface height (SSH). Physically it means that the larger the SSH variance is, the more vigorous are ocean eddies and the higher grid resolution is required. Thus we increased the model resolution along the pathways of important ocean currents, e.g. Gulf Stream, Antarctic Circumpolar Current (ACC), Kuroshio, etc.

The horizontal resolution is also increased in ocean straits (Fig.4) and deep water production regions. This model setup contains a total of ca. 800000 horizontal nodes and 47 z-coordinate vertical levels.

This configuration with high resolution in many of the dynamically “important” regions shows a very high computational performance allowing to simulate ca. 8 years per day.

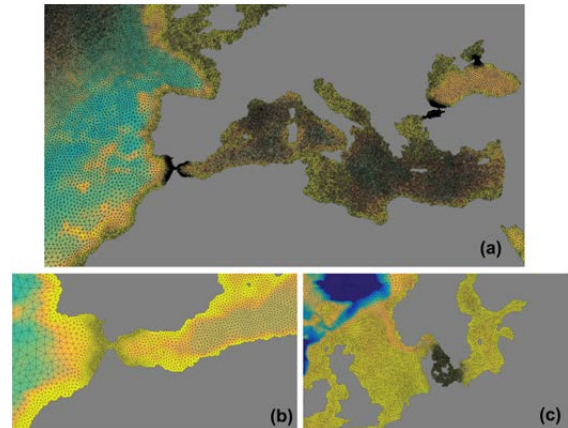


Figure 4 Fragments of the FESOM global setup. Mediterranean Sea (a), Strait of Gibraltar (b), North and Baltic seas (c)

6. Conclusions

The inclusion of the North Atlantic into the regional coupled climate model domain can improve the simulation results, providing additional “added value” due to an improved modeled ocean circulation. These improvements can be due to the higher ocean model resolution, as well as due to the much better resolved regional atmosphere over the key ocean regions.

References

- Sein D.V., Koldunov N.V., Pinto J.G., Cabos W. (2014) Sensitivity of simulated regional Arctic climate to the choice of coupled model domain. *Tellus A* 66:23966. doi:10.3402/tellusa.v66.23966
- Sein D.V., Mikolajewicz U., Gröger M., Fast I., Cabos W., Pinto J.G., Hagemann S., Semmler T., Izquierdo A., Jacob D. (2015) Regionally coupled atmosphere - ocean - sea ice - marine biogeochemistry model ROM: 1. Description and validation. *J Adv Model Earth Syst* 7:268–304 doi:10.1002/2014MS000
- Wang, Q., Danilov, S., Sidorenko, D., Timmermann, R., Wekerle, C., Wang, X., Jung, T., Schröter, J., 2014. The Finite Element Sea Ice-Ocean Model (FESOM) v.1.4: formulation of an ocean general circulation model. *Geosci. Model Dev.* 7, 663–693. doi:10.5194/gmd-7-663-2014

Three ocean scenarios of the 2006-2100 period for the Mediterranean Sea with the regional climate system model CNRM-RCSM4

Florence Sevault, Samuel Somot, Antoinette Alias and Clotilde Dubois

CNRM-GAME, Météo-France, Toulouse, France, (florence.sevault@meteo.fr)

1. Introduction

The study of the future evolution of the Mediterranean Sea requires at the same time a high-resolution representation of the sea itself, of the various forcings (air-sea fluxes, rivers) and the coupling between them in order to take into account the full complexity of the regional climate system.

In this study, we use the fully-coupled Regional Climate System Model (CNRM-RCSM4, Sevault et al. 2014, see Fig 1) dedicated to the Mediterranean region. In the frame of Med-CORDEX, we carried out one historical simulation and 3 future projections under the RCP8.5, RCP4.5 and RCP2.6 scenarios.

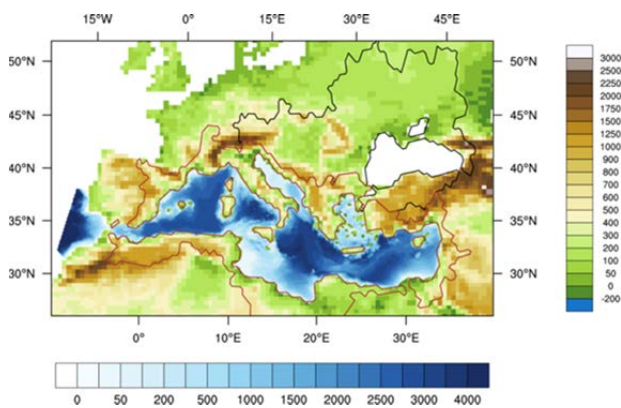


Figure 1. ALADIN-Climate land-sea mask and orography (in m) for the Med-CORDEX domain, and NEMOMED8 bathymetry (in m). The drainage areas of the Black Sea (in black) and of the Mediterranean Sea (in red, cut North of 26°N, without the Nile basin) are contoured.

CNRM-RCSM4 includes the regional representation of the atmosphere at 50 km (ALADIN-Climate model, Colin et al., 2010), the land-surface at 50 km (ISBA model), the river at 50 km (TRIP model, Oki and Sud, 1998, Decharme et al., 2010) and the ocean at 10 km (NEMOMED8 model, Beuvier et al., 2010) with a daily coupling by the OASIS3 coupler (Valcke, 2013). This model aims at reproducing the regional climate system with as few constraints as possible: no surface salinity nor temperature relaxation, the Black Sea budget is parameterized and the river runoffs (except for the Nile) are fully coupled.

The stability and the quality of the historical simulation is first evaluated; then the response of the Mediterranean Sea to global climate change is investigated.

2. Experimental setup

The lateral boundary conditions, atmospheric and oceanic in the near-Atlantic Ocean come from the CNRM-CM5.1 Global Climate Model (Voltaire et al., 2013). A special attention is given to the Atlantic initial condition and evolution, which upper layer forms the Atlantic Waters entering the Mediterranean at the Gibraltar Strait. They are corrected from the small trend of the 152-year control run of the global ocean model and from the mean 1960-2005 bias in temperature and

salinity with the NEMOVAR-COMBINE reanalysis (Balmaseda et al. 2010).

As for the atmospheric fluxes sent by ALADIN-Climate, a first try of the coupled system shows that we need to impose a correction in the heat fluxes, otherwise the ocean will reach a too cold equilibrium.

After 5 years of oceanic spin-up, a 100-year coupled spin-up is performed, with the 1949-1979 boundary conditions in random order inside each 30-year period. After this spin-up period, an historical simulation (1950-2005) is carried out driven at its boundaries by the CNRM-CM5.1 historical run and by observed evolution of the GHG and aerosol concentrations. From 2006, three scenarios are completed (RCP8.5, RCP4.5 and RCP2.6) following the Med-CORDEX protocol. In parallel of the historical and scenario runs, an additional 150-year control run is carried out using the same protocol as in the spin-up (LBC randomly chosen, GHG and aerosol conditions from the 1950s) in order to check the model stability.

3. First results

The historical run is evaluated, and the average 1950-2005 surface circulation is shown in Fig. 2.

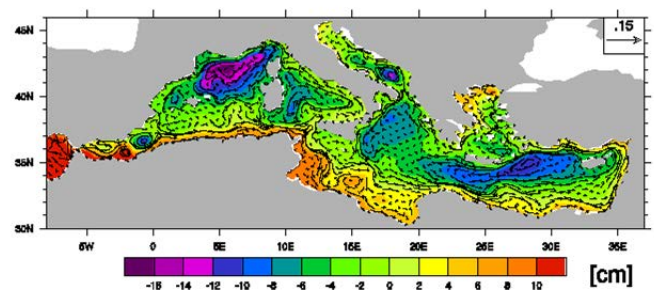


Figure 2. 1950-2005 dynamic SSH (in cm) and currents at 25 m (in m/s) for the historical simulation.

The control run is stable, thus the difference between the end of the scenarios (2070-2100) and the beginning of the historical (1950-1980) can be used to estimate a range of evolution of the Mediterranean basin. The 3 scenarios show a spatial-averaged increase in Sea Surface Temperature on the Mediterranean ranging from 1.2° for RCP2.6 to 2.9° for RCP8.5, and a decrease in Sea Surface Salinity of 0.01 to 0.07. This decrease is to be related to the decrease of salinity of the Atlantic water imposed by the GCM ocean boundary conditions. Indeed the 0-150m average of the Atlantic zone of buffer decreases by -0.22 to -0.53 depending on the scenario. The Mediterranean SSS decrease shown by our simulations is a new finding when compared to previous studies. Adloff et al. (2015), for example, show an increase in salinity of the Atlantic surface layer (from 0.16 to 0.61 depending on the simulation), and an associated increase in Mediterranean SSS (between +0.48 and +0.89).

The surface circulation (Fig. 3 to 5) is strongly modified with the major changes occurring in the RCP8.5 run as awaited. Besides the thermohaline circulation is weakened in the three scenarios, and no strong convection event appears after 2050 (not shown).

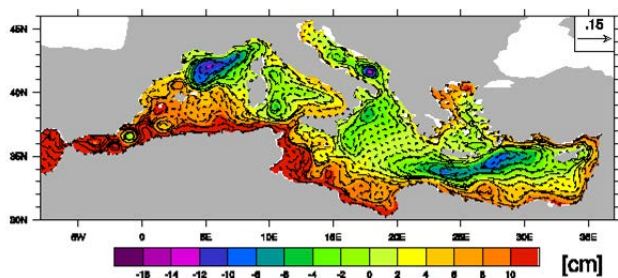


Figure 3. 2070-2100 dynamic SSH (in cm) and currents at 25 m (in m/s) for the RCP8.5 scenario.

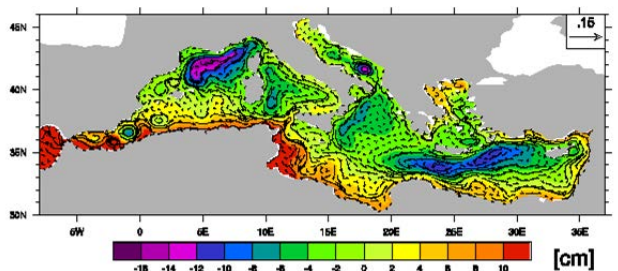


Figure 4. 2070-2100 dynamic SSH (in cm) and currents at 25 m (in m/s) for the RCP4.5 scenario.

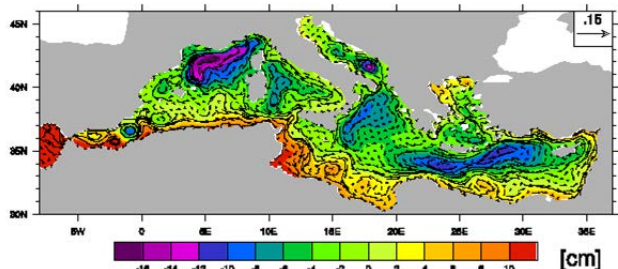


Figure 5. 2070-2100 dynamic SSH (in cm) and currents at 25 m (in m/s) for the RCP2.6 scenario.

3. Conclusion and perspectives

The three coupled scenario simulations performed with the coupled CNRM-RCSM4 model offer a new perspective on the 21st century climate change in the Mediterranean Sea. The crucial role of the Atlantic boundary conditions is confirmed as in Adloff et al. (2015). The range of uncertainties of the responses obtained in this study can be added to the ones given in Somot et al. (2008), using a former version of the CNRM-RCSM model, and in Adloff et al. (2015) using the NEMOMED8 model in a forced mode. The future comparison with the other Med-CORDEX coupled scenarios will widen this knowledge.

R eferences

Adloff F., S. Somot, F. Sevault, G. Jorda, R. Aznar, M. Déqué, M. Herrmann, M. Marcos, C. Dubois, E. Padorno, E. Alvarez-Fanjul, D. Gomis (2015) Mediterranean Sea response to climate change in an ensemble of twenty first century scenarios, *Clim Dyn*, DOI 10.1007/s00382-015-2507-3

Balmaseda, M. A., K. Mogensen, F. Molteni and A. T. Weaver (2010) The NEMOVAR-COMBINE Ocean Re-Analysis. Technical Report 1, COMBINE Technical Report (ISSN 2221-1128).

Beuvier J., Sevault, F., Herrmann, M., Kontoyiannis, H., Ludwig, W. and co-authors (2010) Modeling the Mediterranean Sea interannual variability during 1961-2000: focus on the Eastern Mediterranean Transient. *J. Geophys. Res.* 115, C08017.

Colin J., M. Déqué, R. Radu, and S. Somot (2010) Sensitivity study of heavy precipitation in limited area model climate simulations: influence of the size of the domain and the use of the spectral nudging technique. *Tellus A.* 62, pp. 591-604.

Decharme B., R. Alkama, H. Douville, M. Becker and A. Cazenave (2010) Global evaluation of the ISBA-TRIP Continental Hydrological System. Part II: Uncertainties in river routing simulation related to flow velocity and groundwater storage. *Bull. Am. Meteorol. Soc.* 11, pp. 601-617.

Oki T. and Y. C. Sud (1998) Design of total runoff integrating pathways (TRIP). *A Global River Channel Network*. *Earth Interact.* 2, pp. 1-36.

Sevault F., S. Somot, A. Alias, C. Dubois, C. Lebeaupin-Brossier, P. Nabat, F. Adloff, M. Déqué and B. Decharme (2014) A fully coupled Mediterranean regional climate system model: design and evaluation of the ocean component for the 1980-2012 period, *Tellus A*, 66, 23967.

Somot S., F. Sevault, M. Déqué and M. Crépon (2008) 21st century climate change scenario for the Mediterranean using a coupled atmosphere ocean regional climate model. *Global Planet. Change.* 63, pp. 112-126.

Valcke S. (2013) The OASIS3 coupler: a European climate modelling community software, *Geosci. Model Dev.* 6, pp. 373-388

Voldoire, A., E. Sanchez-Gomez, D. Salas y Méliá, B. Decharme, C. Cassou and co-authors (2013) The CNRM-CM5.1 global climate model: description and basic evaluation. *Clim. Dynam.* 40(910), pp. 2091-2121.

Interannual variability of the deep water formation in the North-West Mediterranean Sea using a fully-coupled regional climate system model

Samuel Somot, Loic Houpert, Florence Sevault, Pierre Testor, Anthony Bosse, Isabelle Taupier-Letage, Marie-Noëlle Bouin, Robin Waldman, Christophe Cassou, Xavier Durrieu de Madron, Fanny Adloff, Marine Herrmann

CNRM-GAME, Météo-France/CNRS, Toulouse, France, (samuel.somot@meteo.fr)

1. Motivations

The North-Western Mediterranean Sea is known as one of the only place in the world where open-sea deep convection occurs (Marshall and Schott 1999) with the formation of the Western Mediterranean Deep Water (WMDW). This phenomena is mostly driven by local preconditioning of the water column and strong buoyancy losses during Winter (Herrmann et al. 2010, L'Heveder et al. 2013). At the event scale, the WMDW formation is characterized by different phases (preconditioning, strong mixing, restratification and spreading), intense air-sea interaction and strong meso-scale activity (Herrmann et al. 2010, Durrieu de Madron et al. 2013) but, on a longer time scale, it also shows a large interannual variability (Béthoux et al. 2002) and may be strongly affected by climate change (Somot et al. 2006, Adloff et al. 2015) with impact on the regional biogeochemistry (Herrmann et al. 2014). Therefore observing, simulating and understanding the long-term temporal variability of the North-Western Mediterranean deep water formation is still today a very challenging task.

2. Methodology

In this study, we try to tackle this challenge thanks to (1) a thorough reanalysis of past in-situ observations (CTD, Argo, surface and deep moorings, gliders) and (2) an ERA-Interim driven hindcast simulation using a recently-developed fully coupled Regional Climate System Model (CNRM-RCSM4, Sevault et al. 2014, Nabat et al. 2015) in the frame of HyMeX/Med-CORDEX. CNRM-RCSM4 includes the regional representation of the atmosphere at 50 km (ALADIN-Climate model), the land-surface at 50 km (ISBA model), the river at 50 km (TRIP model) and the ocean at 10 km (NEMOMED8 model) with a daily coupling by the OASIS3 coupler. The multi-decadal simulation (1979-2013) has been designed to be temporally and spatially homogeneous with a realistic chronology (use of the spectral nudging technique), a high resolution representation of both the regional ocean and atmosphere, specific initial conditions, a long-term spin-up and a full ocean-atmosphere-land-river coupling without constraint at the interfaces.

Besides, the observation reanalysis allows to reconstruct interannual time series of deep water formation (DWF) indicators. Using those observation-based indicators and the model outputs, the Winters of the period 1979-2013 are analysed in terms of weather regimes, related Winter air-sea fluxes, ocean preconditioning, mixed layer depth, surface of the convective area, deep water formation rate and long-term evolution of the deep water hydrology.

3. Results

Observation-based indicators have been built for the yearly-maximum mixed-layer depth over the whole period studied (see Fig. 1), for the yearly-maximum convective surface and the

deep water characteristics over the last years as well as for the deep-water volumes and deep-water formation (DWF) rate over the HyMeX observing period (2012-2013). The strong interannual variability of the phenomena is confirmed as well as the recent warming and saltening trend of the WMDW. The chronology of the last years is now well qualified and quantified. From in-situ observation deep water volume estimates during the year 2012-2013, the possibility to reach a DWF rate equal to 1 Sv is confirmed.

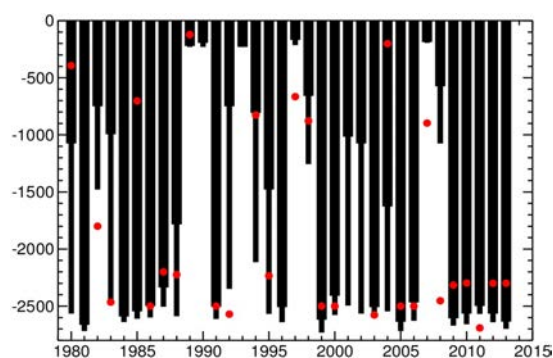


Figure 1. Interannual time series of yearly-maximum mixed layer depth for the period 1989-2013 for the model in black bars (thick bars for the turbocline criteria and thin bars for the pycnocline criteria) and for the observations in red dots.

The model is able to realistically represent the DWF phenomena as it is observed and in particular its mean behaviour, its interannual chronology (see Fig. 1 for the maximal mixed layer depth) and the water mass characteristics. In addition, the model shows a detectable warming and saltening trend of the deep water masses, though underestimated with respect to deep mooring observations.

In addition, the model allows to identify the main drivers of the interannual variability of the DWF phenomena. Two independent factors allow to explain more than 70% of the variance of key convection indicators such as the yearly-maximum mixed layer depth, the convective surface and the DWF rate. Those factors are the Winter (DJFM) cumulative buoyancy loss over the Gulf of Lions and the pre-Winter stratification index on December, the 1st averaged over the Gulf of Lions. This strong relationship is illustrated on Fig. 2: years with a yearly DWF rate above 0.6 Sv (red dots) always occur when the buoyancy loss is stronger than the stratification index over the Gulf of Lions. Years with no or very low DWF rate occur when buoyancy loss is largely weaker than the stratification index.

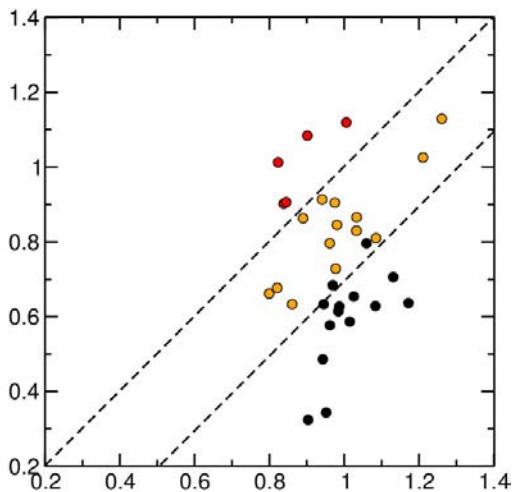


Figure 2. Scatterplot (1 point per year) of the relationship between the stratification index in x-axis (in m^2/s^2) and the buoyancy loss in y-axis (in m^2/s^2). Colors of the point indicate the yearly DWF rate (below 0.05 Sv in Black, above 0.6 Sv in Red and orange in between)

We demonstrated that the interannual variability of the Winter cumulative buoyancy loss is driven by a small number of stormy days with very strong associated buoyancy losses and is also strongly related to daily weather regimes. Indeed, among the four classical North-Atlantic daily weather regimes, two (Atlantic Ridge and negative phase of the NAO) favor the DWF phenomena whereas the positive phase of NAO is detrimental and the last one (Blocking) is neutral.

The interannual variability of the stratification index is mainly driven by the variability of the salt and heat content of the Gulf of Lions surface layer (0-150m).

In addition, we show that, in the model, the warming and saltening trend of the deep water masses is not due to trends in the two main explaining factors. It is mainly due to (i) a saltening of the surface waters related to an increase in the Atlantic Water salinity entering at the Gibraltar Strait and (ii) a warming and saltening trend in the intermediate waters (LIW layer) formed in the Eastern Mediterranean Sea and reaching the North-Western Mediterranean Sea after advection.

4. Conclusion and perspectives

In this study, a thorough reanalysis of past in-situ observations and a long-term hindcast simulation performed with a fully coupled Regional Climate System Model allow to improve the understanding of the interannual variability of the deep-water formation phenomena in the North-Western Mediterranean Sea. It allows to identify the main drivers of this variability as well as possible factors explaining the observed trends in the deep water characteristics.

Only multi-model studies, for example in the frame of Med-CORDEX, and long-term in-situ monitoring of the phenomena could allow to make our conclusions robust.

References

- Adloff F. et al. (2015) Mediterranean Sea response to climate change in an ensemble of twenty first century scenarios, *Clim Dyn*, DOI 10.1007/s00382-015-2507-3
- Béthoux J. P. et al. (2002). Deep water in the western Mediterranean: peculiar 1999 and 2000 characteristics, shelf formation hypothesis, variability since 1970 and geochemical inferences. *Journal of Marine Systems*, 33, 117-131.
- Durrieu de Madron X. et al. (2013) Interaction of deep dense shelf water cascading and open-sea convection in the Northwestern Mediterranean in winter 2012 *Geophysical Research Letters*, 40, 1–7, doi:10.1002/grl.50331
- Herrmann M. et al. (2010) What induced the exceptional 2005 convection event in the Northwestern Mediterranean basin ? Answers from a modeling study. *JGR-O*, 115 (C12), 1978–2012, doi:10.1029/2010JC006162
- Herrmann M. et al. (2014). Impact of climate change on the northwestern Mediterranean Sea pelagic planktonic ecosystem and associated carbon cycle. *Journal of Geophysical Research: Oceans*, 119(9), 5815-5836.
- L'Hévéder B. et al. (2013) Interannual variability of deep convection in the Northwestern Mediterranean simulated with a coupled AORCM. *Climate Dyn.*, 41:937-960. doi: 10.1007/s00382-012-1527-5
- Marshall J. and Schott F. (1999). Open-ocean convection: Observations, theory, and models. *Rev. Geophys*, 37(1), 1-64.
- Nabat P. et al. (2015) Direct and semi-direct aerosol radiative effect on the Mediterranean climate variability using a coupled Regional Climate System Model. *Clim. Dyn.* 44, 1127-1155, DOI:10.1007/s00382-014-2205-6
- Sevault F. et al. (2014) A fully coupled Mediterranean regional climate system model: design and evaluation of the ocean component for the 1980-2012 period, *Tellus A*, 66, 23967.
- Somot S. et al. (2006) Transient climate change scenario simulation of the Mediterranean Sea for the 21st century using a high-resolution ocean circulation model. *Climate Dynamics*, Volume 27, Numbers 7-8, December, 2006, pp. 851-879, DOI :10.1007/s00382-006-0167-z

On the resolution of inter-basin exchanges in numerical models: The example of Black Sea and Baltic Sea straits

E. V. Stanev¹, S. Grashorn¹, S. Grayek¹, and Y.J. Zhang²

¹ Helmholtz-Zentrum Geesthacht, Institut für Küstenforschung, Geesthacht, Germany (emil.stanev@hzg.de)

² Virginia Institute of Marine Science, College of William & Mary, Center for Coastal Resources Management Gloucester Point, VA 23062, USA

1. Motivation

The inter-basin exchange can be considered as a two-layer flow constrained by the physical characteristics of straits. Low-salinity outflows are more pronounced in the surface layers; saltier inflows sink below the cold intermediate layers. The propagation of this water into the basin interiors of two estuarine basins is quite different. While in the Black Sea the continental slope is close to the strait and the shelf is narrow, there is a long way undertaken by the Atlantic water before reaching the Baltic proper. Physical processes controlling the inter-basin exchanges are very sensitive to small scales imposed by the geometry of straits, as well as to complex processes of entrainment and detrainment at the interface between two water masses. This requires both very fine horizontal and vertical resolution and appropriate sub-grid scale parameterizations.

2. The models

In this paper we present two approaches to study the sensitivity of straits exchanges upon horizontal grids. In the first approach the unstructured grid model SCHISM is used (1) for the Black Sea starting from the Azov Sea and ending in the north-western part of Aegean (Fig. 1) and (2) for the North-Sea and Baltic Sea (Fig. 2).

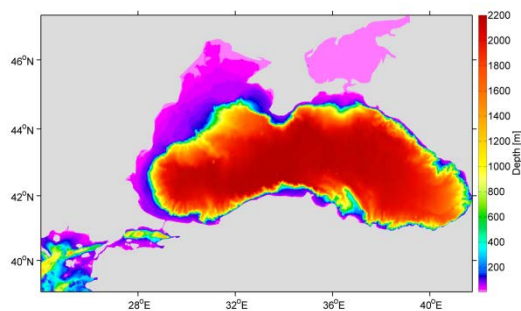


Figure 1. Black Sea model (SCHISM) area and topography.

The second approach describes a two-way nesting method, which is developed for the coupled North-Sea and Baltic Sea model using NEMO (Fig. 1a) where a high-resolution is enabled in the transition zone between two basins (Fig. 1b).

3. Analysis of numerical simulations

The analysis of results is focused on the model validation, model performance to resolve regional hydrodynamics, as well on the temporal variability associated with transition between inflows and outflows.

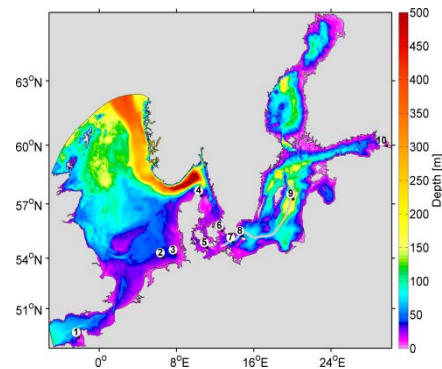


Figure 2. North Sea-Baltic Sea model (SCHISM) area and topography.

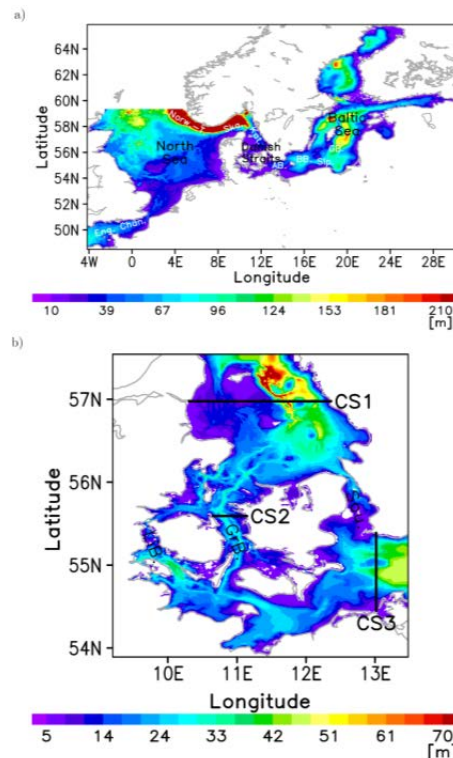


Figure 3. North Sea-Baltic Sea model (NEMO) area and topography (a) with a nested domain where the horizontal resolution is 1 km.

References

Zhang, Y.J., E.V. Stanev, and S. Grashorn (2015) Unstructured-grid model for the North and Baltic Sea: validation against observations, Ocean Modeling (submitted)

Impact of land surface coupling on the Mediterranean continental water cycle

Marc Stéfanon¹, Jan Polcher²

¹ Laboratoire des Sciences du Climat et de l'Environnement (LSCE) - Institut Pierre Simon Laplace, CEA/CNRS/UVSQ, Gif sur Yvette, France (marc.stefanon@lsce.ipsl.fr)

² Laboratoire de Météorologie Dynamique (LMD) - Institut Pierre Simon Laplace, (CNRS/Ecole Polytechnique/ENS/UPMC), Palaiseau, France

Water management is facing major challenges given that the Mediterranean region undergoes fast socio-economic changes and is influenced by environmental changes. Water scarcity, environmental issue, global warming and increasing population question the future sustainability in water resources. Improvement in the modelling of the hydrological continental cycle is a necessary step in order to better predict its future evolution and impacts on water resources. Land-surface-atmosphere interactions play a pivotal role in the availability of water resources by modifying the water fluxes at different timescales, from medium range weather prediction to climate variability and change.

Regional modelling platforms include a growing number of processes related to the continental hydrological cycle, coupling with river routing and vegetation phenology models, thus they represent efficient and powerful tools for understanding water resources variability. In this study, we conduct regional climate simulations to quantify the contribution of coupled processes in the continental water

cycle during the last decades (ERA-Interim period: 1979-2012), using with the WRF atmospheric model coupled with the ORCHIDEE land-surface model. Preliminary findings from these simulations aim to provide impact estimates for land-atmosphere and phenology-atmosphere coupling on several component of the continental water cycle: river discharge, evapotranspiration, rainfall.

References

- Stéfanon, M., P. Drobinski, F. D'Andrea, and N. deNoblet-Ducoudré (2012), Effects of interactive vegetation phenology on the 2003 summer heat waves, *J. Geophys. Res.*, 117, D24103, doi:10.1029/2012JD018187.
- Drobinski, P., Anav, A., Lebeaupin Brossier, C., Samson, G., Stéfanon; M., et al. (2012) Model of the Regional Coupled Earth system (MORCE): Application to process and climate studies in vulnerable regions, *Environmental Modelling & Software* 35, 1-18.

Multi model for sea level forecast by artificial neural networks

Marzenna Sztobryn

Maritime Administration of Poland

The development of teleinformatics, measurements methods and computer infrastructures caused the development of sea level forecast methods. Now, for one localization, the forecast services are able to generate the forecast by the several models or by one model but with different input from meteorological models. The series of predicted sea level by several models are called the multi-model or ensemble forecast. The forecasters should, on the basis of ensemble models and their (forecasters) knowledge and experience, produce the final values of forecast. The aim of the work was the construction of multi-model for management of ensemble dedicated forecasters. The model is based on artificial neural network methodology. The multi-model was prepared and verified for Polish maritime tide gauge Hel working in the IMGW-PIB network (Polish Hydro-Meteorological service). Results done by multi-model shown the significant increase of accuracy of forecast.

Modelling climate change impact on hydroecological conditions of the Tyligulskyi Liman lagoon (north-western coast of the Black Sea)

Yurii Tuchkovenko¹ and Valeriy Khokhlov¹

¹ Hydrometeorological Institute, Odessa State Environmental University, Odessa, Ukraine (tuch2001@ukr.net)

1. Physio-Geographic Description of the Tyligulskyi Liman lagoon

The Tyligulskyi Liman lagoon is located on the Ukrainian coast in the north-western part of the Black Sea (46°39.3'–47°05.3'N, 30°57.3'–31°12.7'E; see Fig. 1), and its basin area is 5420 km². The lagoon used to be a valley of the Tyligul River that was later flooded by seawater. The mean water-surface area and volume of the lagoon are 129 × 10⁶ m² and 693 × 10⁶ m³, respectively. The Tyligul River is the main source (16.9 × 10⁶ m³ y⁻¹, i.e. >90%) of freshwater into Tyligulskyi Liman.

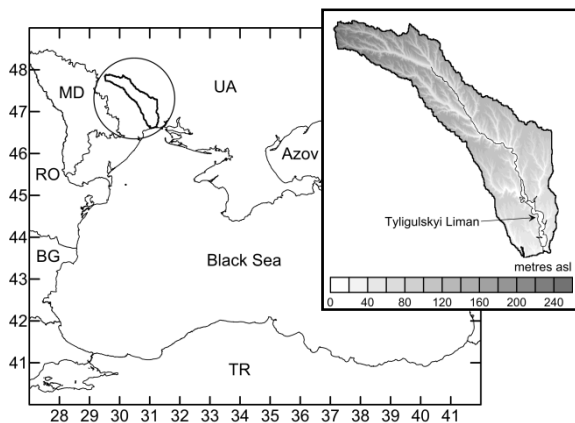


Figure 1. Location and topography of the Tyligulskyi Liman lagoon basin area.

The lagoon is separated from the sea by a natural sand isthmus, which is breached by 3.3 km long artificial channel connecting the lagoon and the sea. Usually, the channel is manually open in April–June. The northern part of the lagoon, where the Tyligul River falls, is shallow, with depths of up to 4 m, while the southern and central parts are deeper (10–16 m) and divided by a shallow-water spit.

During a few last decades there is a negative freshwater balance, which was estimated to be 32 × 10⁶ m³ y⁻¹ in the period of 1991–2012, in response of regional climate change and anthropogenic forcings. This deficit can be only compensated by sea water inflow through the connecting channel.

2. Regional Climate Change Scenario

The outcomes of 15 RCMs from the FP6 ENSEMBLES Project were used in order to select single climate change scenario that can be considered as a most feasible at the Tyligulskyi Liman basin area during the nearest future. The analysis of differences between the observed seasonal temperature and precipitation with the modelled ones by each of 15 models was the basis for this selection (Wörner et al., 2012). It was revealed that the REMO model (Max

Planck Institute for Meteorology, Hamburg, Germany) under A1B scenario provides the results with minimal differences from the observables.

3. Regional Modelling Approaches

The future freshwater inflow and nutrient inputs to the lagoon from the basin area have been simulated by the eco-hydrological model SWIM (Soil and Water Integrated Model; Krysanova and Wechsung, 2000; Hesse et al., 2015).

In order to assess the climate change impact on lagoon's hydroecological conditions we used the 3-D numerical model MECCA-OSENU-EUTRO, which is the modified hydrodynamic model MECCA (Model for Estuarine and Coastal Circulation Assessment) with the original chemical and biological unit of water eutrophication (Hess, 2000; Ivanov and Tuchkovenko, 2008). The 3-D model was run for four 'typical' years within each of the climatic periods, that is, 1971–2000 (p0) – the reference, and 2011–2040 (p1), 2041–2070 (p2), 2071–2098 (p3) for evaluation of climate impact. The typical, with respect to hydrometeorological conditions, years were selected by analyzing three variables – monthly air temperature, precipitation and runoffs from the lagoon's basin area.

The climate scenarios were analysed and evaluated comparing long-term temperature, precipitation and runoffs in three future periods to those in the reference period. By that, so called climate change signals were estimated. The climate change signals for temperature will amount to 2.2°C for period p1, 3.0°C for period p2 and 4.0°C for period p3. Comparing with annual precipitation 482 mm for period p0, that value will decrease to 413 mm for period p1, then will increase to 456 mm for period p2, and will again decrease to 411 mm for period p3. Similarly, the runoff was estimated as 85 × 10⁶ m³ y⁻¹ for period p0, 14 × 10⁶ m³ y⁻¹ for period p1, 110 × 10⁶ m³ y⁻¹ for period p2, and 56 × 10⁶ m³ y⁻¹ for period p4.

4. Results and Discussion

The average long-term results of model calculations testify that the present-day period (p1) is characterized by minor volumes of lateral fresh flow into the lagoon, which results in an increase of water salinity, diminishing concentrations of NH₄-N, the deficit of which leads to limited primary water-weed production in summer months and an overall biomass reduction, and a raise in concentrations of PO₄-P. The deep southern and central parts of lagoon, the volume of waters in which comes up to 80% of the total volume of waters in the lagoon, pose a considerable damping effect as regards the influence of the river flow (2% of the total volume of water in the lagoon). However, even in these parts, a few unit increase

in salinity of water is observed in course of an annual cycle, which in a few decades will result in an increase in salinity of water in the lagoon of some tens of PSU. The most intensive increase of salinity takes place in the shallow northern part of the lagoon. In view of a lack of fresh flow and intensive evaporation in summer months the salinity here could reach 27 PSU by the end of the year. These salt waters get to the central and the southern parts of the lagoon thus contributing to their salinization. The obtained results of hydrodynamic modeling are substantiated by independent calculations with the use of a model of water-salt balance in the lagoon according to which average salinity of waters in the lagoon will rise to reach 30–40 PSU by the end of the period p1.

In the scenario period p2 a considerable increase of lateral fresh water flow into the lagoon is expected. The inflow of mineral compounds of nitrogen will increase together with the flow, which will entail an increase of water-plant biomass in the lagoon as well as intensification of their ‘blooming’ (at the maximum values of the biomass). In spite of an increase of utilization of PO₄-P by the water plants, their concentration will also increase on the average due to additional input through the river flow. Considerable incidental diminishing in the concentration of PO₄-P is however possible in periods of ‘flashes’ of the biomass, especially in the shallow northern part of the lagoon. The mean values of phytoplankton biomass and concentrations of NH₄-N will restore to those of the reference period. The mean concentrations of PO₄-P and especially NO₃-N will rise.

The scenario period p3 is characterized by a lower river flow as compared to p2 and p0, which is, however, higher than p1. In the same period the temperature of water and air and, consequently, evaporation from the water surface in the lagoon will attain the maximum values. To set off the deficit of fresh water balance the inflow of salt waters into the southern part of lagoon through the channel will increase. Spatial distribution of phytoplankton biomass in this period will be characterized by the maximum values in the southern part of lagoon and minimum ones in the northern, where development of the water plants will be restrained by the lack of NH₄-N. The mean values concentrations of NH₄-N will be smaller and PO₄-P and NO₃-N will be greater than those for the period p0.

Parallel to a general tendency of increasing water temperature and phytoplankton biomass in the deep southern and central parts of the lagoon in the 21st century, the oxygen regime will also get worse, and the minima of oxygen in the benthic layer, especially in the central part, turn deeper.

Table 1 summarizes the above mentioned results.

Table 1. Relative changes (in %) of modelled hydroecological characteristics in lagoon for scenario periods p1-p3 comparing with reference period p0

Scenario	C-Phyto	NO ₃ -N	NH ₄ -N	PO ₄ -P	O ₂	Salinity
p1/p0	-26.9	5.8	-32.5	9.9	-9.3	10.1
p2/p0	-1.0	30.6	-1.1	3.4	-11.2	3.9
p3/p0	-10.6	28.0	-12.1	6.0	-13.4	3.4

5. Conclusions

For the Tyligulskyi Liman lagoon, its biodiversity and fish productivity during the period p1 will be endangered by the gradual increase in the water salinity up to the mean values of 30–40 PSU. The increase will arise from the reduction in the freshwater inflow into the lagoon. Nevertheless, the mineral nitrogen will limit the production of organic matter by algae. During the period p2, the increasing freshwater inflow will diminish the problem of water salinity. However the additional input of mineral nitrogen will enlarge the primary production of organic matter; as a result, the eutrophication with all its negative effects, for example, hypoxia and anoxia, will develop. The high evaporation rate will be registered during the period p3. This will result in the inflow of sea water together with the mineral nitrogen that can deteriorate ecological conditions in the southern part of Tyligulskyi Liman.

Acknowledgement

This study was supported by the European Commission, under the 7th Framework Programme, through the collaborative research project LAGOONS (contract n° 283157).

References

- Wörner V., Hesse C., Stefanova A., Krysanova V. (2012) Evaluation of climate scenarios for the lagoons. – Potsdam Institute for Climate Impact Research, 40 p.
- Krysanova V., Wechsung F. (2000) SWIM User Manual, Potsdam Institute for Climate Impact Research
- Hesse C., Stefanova A. and Krysanova V. (2015) Comparison of water flows in four European lagoon catchments under a set
- Hess K.W. (2000) Mecca2 Program Documentation, NOAA Technical Report NOS CS 5, Silver Spring, MD, 49 p.
- Ivanov V.A., Tuchkovenko Yu.S. (2008) Applied mathematical water-quality modeling of shelf marine ecosystems, Sevastopol, Marine Hydrophysical Institute, Odessa State Environmental University, 295 p.

Flood zone modeling for a river system relying on the water spread over a terrain

Alexander Volchek, Dmitriy Kostiuik, Dmitriy Petrov

Brest State Technical University, Brest, Belarus (dmitriykostiuk@bstu.by)

1. Introduction

Flood visualization by means of GIS is a necessary task involved both in planning anti-flood measures and predicting further course of such extreme events. The solution is based on crossing the surfaces of a terrain and a high water mirror, but this geometrical model accuracy highly depends on used mathematical apparatus. Simplest approach is based on assumption that height of the water surface is constant (Volchak et al., 2007). It allows to intersect terrain model with a horizontal plane, and gives acceptable results in some cases, e.g. sea shore flooding models. But it produces huge errors in case of water level difference, e.g. river floods. In such tasks water mirror is described by a ribbon of inclined planes, appropriate to measured water level data (Volchak et al., 2010). Further increase of accuracy may involve triangulated curve-based surface.

These methods are convenient for a single river flow, but not for cases of a river network. So different approaches are to be used in such cases as flood modeling for the river delta. Also width of flooding may substantially vary due to different soil moistening, so simple geometry calculation based on surfaces intersection without including precipitation factor has impaired accuracy.

Approach intended to overcome these disadvantages has to include elements of water spread and precipitation specifics into the flood zone calculation. One of popular techniques of the liquid movement modeling over an underlying surface is the mathematical apparatus of cellular automation, as described by M.V. Avolio et al. (2003), J. Cirbus, M. Podhoranyi (2013) and others.

Here we present an algorithm of flood modeling, which is based on this technique with a set of further discussed specific traits.

2. The algorithm specifics

Presented flood zone calculation approach uses three objects: DEM in the form of a rectangular matrix, a set of georeferenced points of the water level along the river flow (measured or predicted, in case of forecast), and the river axial line, approximated with the polyline.

Modeling includes two parts: the preparatory stage and the computational one.

3. Preparatory stage of the modeling

This stage includes three steps:

1. elements proximate along von Neuman neighborhood of the 1st range, which are crossed by the river axial line segments, are selected in a DEM matrix while moving from headwaters towards the river's offing (fig. 1);
2. as long as selection proceeds, cells are obtaining sequential numbers (fig 2, a) equal to a raster distance along the river axial line;
3. shortest Euclidean distance to a chosen cell is calculated for all non-selected cells of DEM (fig. 2, a), while all selected neighboring cells obtain zero distance and are further supposed to represent the river axial line on the DEM raster.

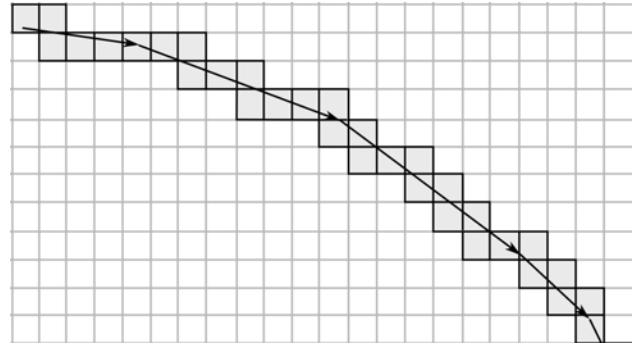


Figure 1. DEM cells covered by the river axial line segments

4. Computational stage of the modeling

Following steps are involved in calculating the flood zone:

1. the Ω set is composed of the axial line cells;
2. the Θ set is composed of cells selected from Ω , which correspond to the control points of the river flow (points with measured water level);
3. all cells from Θ obtain values of the water level;
4. water level is calculated by linear interpolation for all DEM cells which are from the Ω set and are placed at specific distance along the river axial line between pairs of cells belonging to Θ ;
5. when the previous step is over, water level values are assigned to all DEM cells which lay on the river axial line and belong to Ω set;
6. for all elements of Ω their altitude h is taken from DEM matrix and compared with calculated water level h' : in case of $h > h'$, the h value is corrected to make the $h < h'$ inequality true;
7. to determine flood zone a cyclical spread of the calculated water level value is proceeded starting from the axial line cells belonging to Ω towards the neighboring cells, which have positive non-zero value of Euclidean distance from the river axial line.

5. Simulating the spread of a water front

The last step of the computational stage, which simulates the spread of the water front, needs further explanation.

Each cell with already obtained calculated value of the water level copies this value to a set of proximate cells, which are under the following four conditions:

- cell is in von Neuman neighborhood of a 1st range;
- cell is characterized by a higher value of the Euclidean distance to the axial line;
- cell has no calculated value of the water level;
- cell has its altitude h lower than h' value of the emitter cell (i.e. cell acting as a source of the water front spread);

0	0	0	1	1	1,41	2	2	2,23	2,82	3,6	4,12	4,47	5	5,65	6,4
1	1	0	0	0	1	1	1	1,41	2,23	2,82	3,16	3,6	4,24	5	5,65
2	1,41	1	1	0	0	0	0	1	1,41	2	2,23	2,82	3,6	4,24	5
2,82	2,23	2	1,41	1	1	1	0	0	1	1	1,41	2,23	2,82	3,6	4,12
3,6	3,16	2,82	2,23	2	2	1,41	1	0	0	0	1	1,41	2,23	2,82	3,16
4,47	4,12	3,6	3,16	3	2,82	2,23	1,41	1	1	0	0	1	1,41	2	2,23
5,38	5	4,47	4,12	4	3,6	2,82	2,23	2	1,41	1	0	0	1	1	1,41
6,32	5,83	5,38	5,09	5	4,24	3,6	3,16	2,82	2,23	1,41	1	0	0	0	1

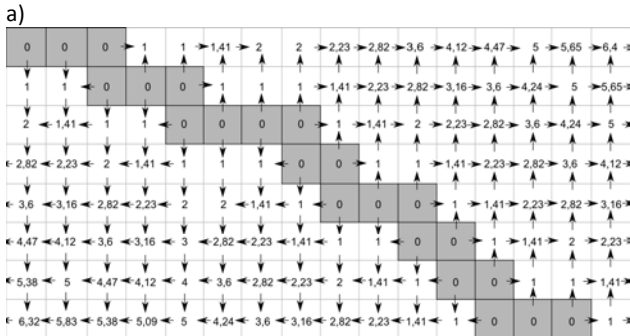


Figure 2. Calculating Euclidean distance to the nearest selected cell (a), and modeling the spread of a water surface front over DEM cells (b).

Each acceptor cell (i.e. cell obtaining the water level value) with only one neighboring emitter cell obtains water level value copied from this emitter cell. If acceptor cell has several neighboring emitter cells, then an arithmetic average of the obtained values is assigned to it. In both situations acceptor cell obtains water level value, and therefore comes inside the limits of a flood zone and adjoins to the set of emitter cells.

Water spread is simulated iteratively. If the set of DEM cells suitable to turn into acceptor becomes empty, flooding zone is finished, otherwise simulation process is repeated from the first step. Figure 2, b shows visual representation of this process.

To take into account the precipitation factors of the DEM elements, cells should obtain a “moisture power” as an additional weight factor. Each acceptor cell with power below threshold decreases summary water level, accepted from the emitter cell, which in its turn decreases the flood width.

6. Model verification

The primary algorithm validity check was based on the monitoring data of floods in Europe caused by strong rains in the end of May – beginning of June of the year 2013. Flooding and destruction took place mainly in East and North Germany, Czech Republic, Austria, Poland, and Hungary. Flood had spread down the Elbe River, the Danube, and touched the basin of their feeders.

The algorithm testing was driven on the data of flood zones of the Elbe River, plotted for their stage on 03.06.2013 near the Torgau, Riesa, and Dresden. These data are opened by the Copernicus EU program of the environment monitoring and security – as in form of the overview maps, so as georeferenced vector images in ESRI Shapefile format. Shuttle Radar Topographic Mission data were used as DEM of the terrain. The flooding zones near Torgau, Riesa, and Dresden were rasterized with resolution relevant to the SRTM DEM.

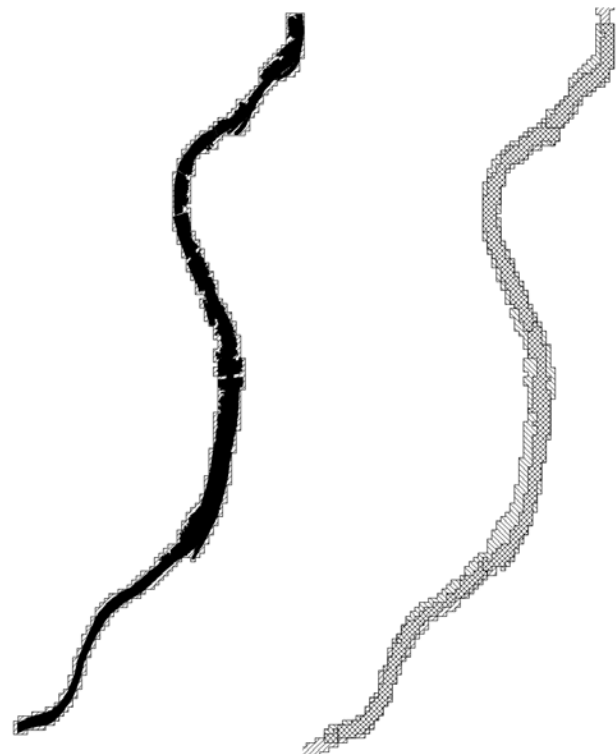


Figure 3. Modeling results for the floodplain near Dresden

Fig.3 shows rasterized contour of the observed flood on the left and modeling results on the right (real and modeled flood zones have different types of diagonal crossing). The simulation demonstrates rather low resolution of DEM data. Modeling have also shown that algorithm tends to depend higher on DEM accuracy for more complex river nets due to error accumulation.

References

- A. Volchek et al. (2007) A distributed automated system of flood registration and prediction. Fifth Study Conference on BALTEX, pp. 189-190.
- A. Volchek et al. (2010) Electronic system of flood monitoring and visualization, XXVI Nordic hydrological conference, P. 66-68.
- M.V. Avolio et al. (2003). An extended notion of Cellular Automata for surface flows modelling. WSEAS Transactions on Computers, No. 2, pp. 1080-1085.
- J. Cirbus, M. Podhoranyi (2013) the flow simulations on the earth surface, optimization computation process, Appl. Math. Inf. Sci., vol. 7, no. 6, pp.2149 -2158.

Seasonality in Intraseasonal and Interannual Variability of Mediterranean SST and its Links to Regional Atmospheric Dynamic

Igor I. Zveryaev

P.P. Shirshov Institute of Oceanology, RAS, Moscow, Russia (igorz@sail.msk.ru)

The Sea surface temperature (SST) data from the NOAA OI SST V2 High Resolution dataset for 1982-2011 are used to investigate intraseasonal and interannual variability of Mediterranean SST, their relationships and links to regional atmospheric dynamics during winter and summer seasons.

Conventional correlation analysis and Empirical Orthogonal Functions [Wilks, 1995; von Storch and Navarra, 1995; Hannachi et al., 2007] analysis are applied.

1. Standard deviations and leading EOFs of SST

An EOF analysis has revealed that both in winter and summer the leading EOFs of the seasonal mean SSTs and the intensities of their intraseasonal fluctuations (expressed by STDs of the daily data) are characterized by the principally different patterns. For example, in winter EOF-1 of SST is characterized by east-west dipole with the largest variability in the western Mediterranean. Wintertime EOF-1 of intraseasonal STD, however, is characterized by the monopole pattern with the largest variability in the eastern Mediterranean. Interannual variability of the leading principal components was also different for SSTs and intraseasonal STDs. Therefore, present analysis did not reveal significant links between interannual variability of Mediterranean SST and that of intensity of intraseasonal fluctuations.

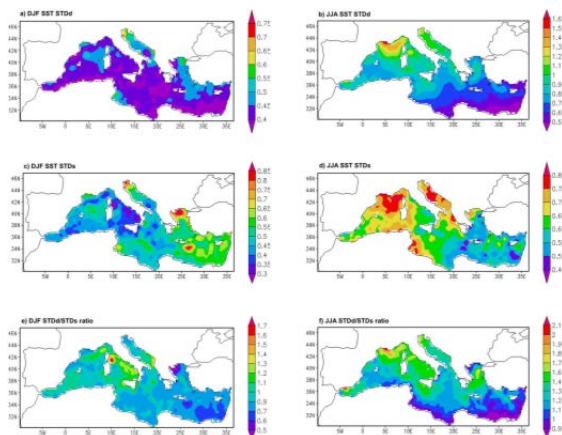


Figure 1. Intraseasonal (STDd, a, b) and interannual (STDs, c, d) standard deviations (b, d) of Mediterranean SST and their ratios (e, f) for winter (a, c, e) and summer (b, d, f) seasons. Standard deviations are presented in °C.

2. Relation to atmospheric dynamics

Analysis of the links to the regional atmospheric dynamics has revealed quite different patterns of correlations between leading PCs and SLP obtained for seasonal mean SSTs and intraseasonal STDs. It was found that during winter EOF-1 and EOF-2 of SST are associated respectively with the East Atlantic and the East

Atlantic/West Russia teleconnections. Wintertime EOF-2 of intraseasonal STDs is linked to the North Atlantic Oscillation. Overall, results of the study suggest that interannual variability of Mediterranean SST is not associated with variations in the intensity of its intraseasonal fluctuations.

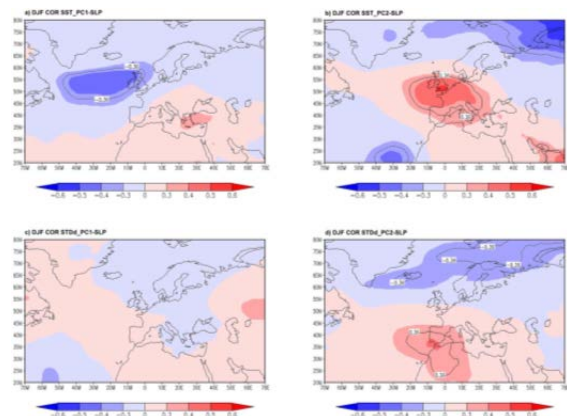


Figure 2. Correlations between PC-1 (a, c) and PC-2 (b, d) of SST (a, b) and its intraseasonal STDd (c, d) and SLP fields estimated for winter season. Red (blue) color indicates positive (negative) correlations. Black solid (dashed) curve indicates areas of significant positive (negative) correlations.

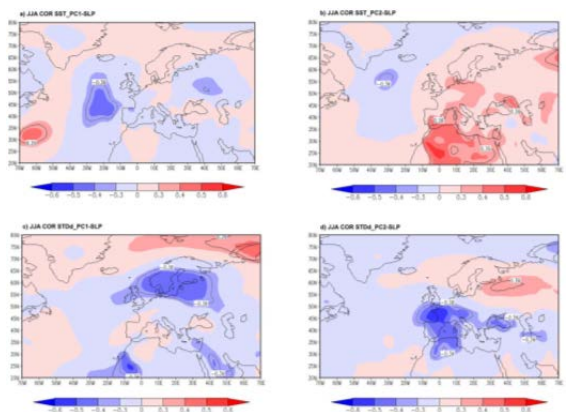


Figure 3. Correlations between PC-1 (a, c) and PC-2 (b, d) of SST (a, b) and its intraseasonal STDd (c, d) and SLP fields estimated for summer season. Red (blue) color indicates positive (negative) correlations. Black solid (dashed) curve indicates areas of significant positive (negative) correlations.

Details of the study are provided in Zveryaev [2015].

References

- Hannachi, A., I.T. Jolliffe, D.B. Stephenson (2007), Empirical orthogonal functions and related techniques in atmospheric science: A review. *Int J Climatol* 27: 1119-1152
- von Storch, H., and A. Navarra (1995), *Analysis of Climate Variability*. Springer-Verlag, New-York, 334 pp
- Wilks, D.S. (1995), *Statistical Methods in the Atmospheric Sciences*. Academic Press, 467 pp
- Zveryaev II (2015) Seasonal differences in intraseasonal and interannual variability of Mediterranean Sea surface temperature. *J. Geophys Res. Oceans*, 120, 2813-2825, doi 10.1002/2014JC010387

Participants

Adloff	Fanny	CNRM / Météo-France	France	fanny.adloff@meteo.fr
Ahrens	Bodo	Goethe University	Germany	Bodo.Ahrens@iau.uni-frankfurt.de
Akhtar	Naveed	IAU, Goethe University Frankfurt	Germany	naveed.akhtar@iau.uni-frankfurt.de
Almowafy	Marwa	International Centre for Theoretical Physics	Italy	malmowaf@ictp.it
Beranger	Karine	LMD	France	karine.beranger@ujf-grenoble.fr
Brauch	Jennifer	Deutscher Wetterdienst (DWD)	Germany	Jennifer.Brauch@dwd.de
Bukantis	Arunas	Vilnius University, Dept. of Hydrology and Climatology	Lithuania	arunas.bukantis@gf.vu.lt
Cabos Narvaez	William	Universidad de Alcala	Spain	william.cabos@uah.es
Calmanti	Sandro	ENEA	Italy	sandro.calmanti@enea.it
Cavicchia	Leone	CMCC	Italy	leone.cavicchia@cmcc.it
Christensen	Ole B	Danish Meteorological Institute	Denmark	obc@dmi.dk
Dell'Aquila	Alessandro	ENEA	Italy	alessandro.dellaquila@enea.it
Di Biagio	Valeria	OGS, Trieste, Italy	Italy	vdibiagio@ogs.trieste.it
Dieterich	Christian	Swedish Meteorological and Hydrological Institute	Sweden	christian.dieterich@smhi.se
Djordjevic	Vladimir	Institute of Meteorology, Faculty of Physics, University of Belgrade	Serbia	vdj@ff.bg.ac.rs

Drews	Martin	Technical University of Denmark	Denmark	Mard@dtu.dk
Drobinski	Philippe	LMD/IPSL, CNRS and Ecole Polytechnique	France	philippe.drobinski@lmd.polytechnique.fr
Dubrovsky	Martin	Institute of Atmospheric Physics, Czech Academy of Sciences	Czech Republic	dub@ufa.cas.cz
Dutay	Jean-Claude	Isce	France	jean-claude.dutay@lsce.ipsl.fr
Farneti	Riccardo	ICTP	Italy	rfarneti@ictp.it
Genovés	Ana	AEMET	Spain	agenovest@aemet.es
Gregoire	Marilaure	Liege University	Belgium	mgregoire@ulg.ac.be
Gröger	Matthias	Swedish Meteorological and Hydrological Institute	Sweden	matthias.groger@smhi.se
Gustafsson	Erik	Baltic Nest Institute, Baltic Sea Centre, Stockholm University	Sweden	erik.gustafsson@su.se
Harzallah	Ali	INSTM	Tunisia	ali.harzallah@instm.rnrt.tn
Jimenez-Guerrero	Pedro	University of Murcia	Spain	pedro.jimenezguerrero@um.es
Khokhlov	Valeriy	Odessa State Environmental University	Ukraine	vkhokhlov@ukr.net
Koldunov	Nikolay	Climate Service Center Germany (GERICS)	Germany	nikolay.koldunov@hzg.de
Kostiuk	Dmitriy	Brest State Technical University	Belarus	mitriykostiuk@bstu.by
Krichak	Simon	Dept. of Geosciences, Tel Aviv University	Israel	shimonk@post.tau.ac.il
Larsen	Morten Andreas Dahl	Technical University of Denmark	Denmark	madla@dtu.dk

Leiding	Tina	Deutscher Wetterdienst	Germany	tina.leiding@dwd.de
Lionello	Piero	University of Salento and CMCC	Italy	piero.lionello@unisalento.it
Llasses	Josep	IMEDEA	Spain	josep.llasses@uib.es
Macias Moy	Diego Manuel	European Commission. Joint Research Centre	Italy	diego.macias-moy@jrc.ec.europa.eu
MacKenzie	Brian	Technical University of Denmark, National Institute for Aquatic Resources (DTU Aqua)	Denmark	brm@aqua.dtu.dk
Maity	Suman	Indian Institute of Tchnology Kharagpur	India	suman.buie@gmail.com
Mallet	Marc	Laboratoire Aerologie	France	malm@aero.obs-mip.fr
Mariotti	Laura	ICTP	Italy	mariotti@ictp.it
Meier	Markus	Swedish Meteorological and Hydrological Institute	Sweden	markus.meier@smhi.se
Mikolajewicz	Uwe	Max-Planck-Institut f. Meteorologie	Germany	uwe.mikolajewicz@mpimet.mpg.de
Nikulin	Grigory	SMHI	Sweden	grigory.nikulin@smhi.se
Omstedt	Anders	Marine Sciences	Sweden	anders.omstedt@marine.gu.se
Orr	James	Lab. des Sciences du Climat et de l'Environnement / IPSL, CEA-CNRS-UVSQ	France	james.orr@lsce.ipsl.fr
Philippenko	Dmitry	Kaliningrad Regional Center for Environment and Tourism / Kaliningrad State Technical University	Russian Federation	dmiphi@gmail.com
Raub	Thomas	Climate Service Center Germany	Germany	thomas.raub@hzg.de

Reckermann	Marcus	Internatinal Baltic Earth Secretariat, Helmholtz-Zentrum Geesthacht	Germany	marcus.reckermann@hzg.de
Richon	Camille	LSCE	France	camille.richon@lsce.ipsl.fr
Sanchez	Enrique	UCLM (University of Castilla-La Mancha)	Spain	e.sanchez@uclm.es
Sannino	Gianmaria	ENEA	Italy	gianmaria.sannino@enea.it
Schimanke	Semjon	Swedish Meteorological and Hydrological Institute	Sweden	semjon.schimanke@smhi.se
Schrum	Corinna	Helmholtz-Zentrum Geesthacht	Germany	corinna.schrum@hzg.de
Sein	Dmitry	AWI	Germany	dmitry.sein@awi.de
Sevault	Florence	METEO-FRANCE	France	florence.sevault@meteo.fr
Shaltout	Mohamed	Alexandria University	EGYPT	Mohamed.shaltout@Alexu.edu.eg
Somot	Samuel	Meteo-France/CNRM	France	samuel.somot@meteo.fr
Stanev	Emil	HZG	Germany	emil.stanev@hzg.de
Stéfanon	Marc	LSCE - IPSL	France	marc.stefanon@lsce.ipsl.fr
Sztobryn	Marzenna	Maritime Office in Gdynia	Poland	marzenna.sztobryn@tlen.pl
Visioni	Daniele	Università degli studi di L'Aquila	Italy	daniele.visioni@gmail.com
Zujev	Mihhail	Marine Systems Institute at Tallinn University of Technology	Estonia	mishazujev87@gmail.com
Zveryaev	Igor	P.P. Shirshov Institute of Oceanology, RAS	Russia	igorz@sail.msk.ru

International Baltic Earth Secretariat Publications

ISSN 2198-4247

- No. 1 Programme, Abstracts, Participants. Baltic Earth Workshop on "Natural hazards and extreme events in the Baltic Sea region". Finnish Meteorological Institute, Dynamicum, Helsinki, 30-31 January 2014. International Baltic Earth Secretariat Publication No. 1, 33 pp, January 2014.
- No. 2 Conference Proceedings of the 2nd International Conference on Climate Change - The environmental and socio-economic response in the Southern Baltic region. Szczecin, Poland, 12-15 May 2014. International Baltic Earth Secretariat Publication No. 2, 110 pp, May 2014.
- No. 3 Workshop Proceedings of the 3rd International Lund Regional-Scale Climate Modelling Workshop "21st Century Challenges in Regional Climate Modelling". Lund, Sweden, 16-19 June 2014. International Baltic Earth Secretariat Publication No. 3, 391 pp, June 2014.
- No. 4 Programme, Abstracts, Participants. Baltic Earth - Gulf of Finland Year 2014 Modelling Workshop "Modelling as a tool to ensure sustainable development of the Gulf of Finland-Baltic Sea ecosystem". Finnish Environment Institute SYKE, Helsinki, 24-25 November 2014. International Baltic Earth Secretariat Publication No. 4, 27 pp, November 2014.
- No. 5 Programme, Abstracts, Participants. A Doctoral Students Conference Challenges for Earth system science in the Baltic Sea region: From measurements to models. University of Tartu and Vilsandi Island, Estonia, 10 - 14 August 2015. International Baltic Earth Secretariat Publication No. 5, 66 pp, August 2015.
- No. 6 Programme, Abstracts, Participants. International advanced PhD course on Impact of climate change on the marine environment with special focus on the role of changing extremes. Askö Laboratory, Trosa, Sweden, 24 - 30 August 2015 International Baltic Earth Secretariat Publication No. 6, 61 pp, August 2015.
- No. 7 Programme, Abstracts, Participants. HyMex-Baltic Earth Workshop "Joint regional climate system modelling for the European sea regions", ENEA, Rome, Italy, 5- 6 November 2015. International advanced PhD course on Impact of climate change on the marine International Baltic Earth Secretariat Publication No. 7, 103 pp, October 2015.

For a list of International BALTEX Secretariat Publications (ISSN 1681-6471), see
www.baltex-research.eu/publications

International Baltic Earth Secretariat Publications
ISSN 2198-4247